Optimization for interaction fluide-structure problems. Application to modelling floating breakwaters.

Ghassan Elchahal

Université de Technologie de Troyes (UTT)

Optimisation pour les problèmes d'interaction fluide structure : Application à la modélisation d'un brise-Lame flottant

Thèse à présenter et soutenir publiquement pour l'obtention du grade de Docteur de l'Université de Technologie de Troyes

Spécialité «Systèmes Mécaniques et Matériaux»
Par

Ghassan ELCHAHAL

Soutenue le 18 Décembre 2007 devant le jury composé de :

C.Sansour	Professeur, Nottingham University- United Kingdom	Rapporteur
S.Huberson	Professeur, LEA, Université de Poitiers	Rapporteur
A. Ouahsine	Professeur, Roberval-Université de Technologie de Compiègne	Président du jury
P.Lafon	Maître de conférences-HDR, Université de Technologie de Troyes	Directeur
R.Younes	Maître de conférences-HDR, Université Libanaise	Co-Directeur
P.Ferrant	Maître de conférences-HDR, LMF- Ecole Central de Nantes	Examinateur

Acknowledgments

I would like to express my sincere appreciation and gratitude to my thesis supervisors for their consistent guidance, constant support, and encouragement all through this work. This thesis would have not been completed without their help.

First, I would like to thank *pascal Lafon* for hosting me in his laboratory where I was able to work on this thesis and providing me with the guidance and assistance which I needed to complete the task. I truly appreciate his patience with me throughout these two years of my research and especially in the last days. He had spent with me a lot of efforts and helped me to optimize my work.

Second, I would like to thank *rafic Younes*, the person then the scientific that I have known since my master. He has been instrumental in allowing me to complete my Phd studies after I finished the master. I have benefited a lot from his enthusiastic, optimistic and critical view to both research and life. I am really grateful for his encouragement and also for the months that he spent with me in Troyes away from his family.

I want to express my deep appreciation for *carlo Sansour,* professor at the university of Nottingham (United kingdom) and *serge Huberson,* professor at 'Université de Poitiers', for reading my thesis and offering valuable reports. Also, special thanks for *abdellatif Ouahsine,* professor at 'Université de Compiègne', and *pierre Ferrant*, associate professor at 'Ecole Centrale de Nantes', for accepting to participate in the thesis committee. I really thank them all for their contributions and assistance.

My parents deserve my highest respect and deepest gratitude for their constant support in all the steps that I have taken over the years. This work would also not have been possible without their personal support. My mother, *Wafa*, and father, *Ahmad*, have provided encouragement and advices over the years than seems possible. My gratitude also goes to my brother, *Basem*, my sister, *Rayan*, and also to my uncle and aunts: *Abedelatif, Hiyam, Ghada*. Finally, special thanks to all my friends here in Troyes and in Lebanon.

Table of Contents

Chapter 1 : Introduction

Chapter 2 : Numerical Tools

Chapter 3 : Modelling of Waves and Floating Breakwaters

Chapter 4 : Optimization of Floating Breakwaters

Conclusions & Further Work

List of Figures

List of Symbols

k	wave number
L	wavelength
ω	angular frequency
g	acceleration of gravity
ρ_e	sea water density
ρ_m	material density
η	wave elevation
H_I	incident wave height
β	phase angle
d	water depth
h	structure height above the still water level
P	wave pressure
b	draft of the floating breakwater
a	width of the floating breakwater
ϕ_I	time independent incident potential
ϕ_S	time independent scattered potential
ϕ_D	time independent diffraction potential
ϕ_j	time independent radiation potential (j = 1, 2, 3 heave, sway and roll)
φ_j	time independent radiation potential per unit body velocity
Φ	time dependant total velocity potential
X_j	floating breakwater displacement vector
$X_j^{'}$	floating breakwater velocity vector
k_r	reflection coefficient of the reflective sidewall
k_m	mooring lines stiffness
M	mass matrix
K	stiffness matrix
F_j^e	exciting forces vector
f_j^e	time independent exciting forces vector
μ_{jk}	added mass coefficient
λ_{jk}	damping coefficient
H_T	transmitted wave height
C_T	transmission coefficient
α	mooring line angle
D	clearance distance between floating breakwater and reflective sidewall
σ	mechanical stresses

Résumé

Les contraintes d'aménagement du territoire, associées à la nécessité de développement économique des sites touristiques et industriels côtiers poussent les industriels à proposer des structures flottantes de plus en plus ambitieuses. Ces structures flottantes sont conçues soit pour protéger des aménagements portuaires, lorsque la configuration des fonds marins ne permet l'usage de structures fixes, soit pour étendre les surfaces utiles en bordures des côtes. Les structures flottantes de protection des effets de la houle offrent de nombreux avantages par rapport aux structures fixes. Elles sont plus économiques à construire et facilement reconfigurables pour s'adapter aux évolutions des activités portuaires.

La thèse que nous venons de présenter fait apparaître le manque de travaux dans le domaine de l'optimisation de la forme et de la topologie de digues flottantes. Quelques travaux se rapportent à l'optimisation des digues fixes, mais ne concernent pas l'optimisation de la forme et ou de topologie de ces structures et encore moins celle des structures flottantes. Le sujet de cette thèse concerne la modélisation et l'optimisation d'une digue flottante ; l'étude du mouvement de la digue et sa réponse à la houle, l'analyse du comportement hydrodynamique de la digue basé sur une analyse paramétrique, et finalement l'amélioration de sa conception et de ses performances en utilisant des techniques d'optimisation. L'objectif principal est de développer une optimisation de brise-lames flottants (forme et la topologie), afin de réduire le poids, ou de chercher une nouvelle forme, conformément aux contraintes physiques et mécaniques.

C'est une problématique complexe, à caractère multidisciplinaire, mêlant des problèmes d'hydrodynamique, d'interaction fluide – structures, et dans une moindre mesure de mécanique des structures. Une procédure basée sur un modèle bidimensionsionnel a été développée pour former un outil général de conception. Il a pour but de déterminer les dimensions optimales d'une digue flottante capable de d'atténuer une houle avec une hauteur donnée. Dans cette première approche du problème, la digue est assimilée à une géométrie de section rectangulaire creuse. Les paramètres géométriques décrivant la section, la masse, l'angle des lignes d'ancrages, et la rigidité des ancrages sont pris en compte dans la formulation du problème d'optimisation.

Nous avons commencé par aborder le problème en étudiant les modèles de propagation d'ondes de surface que sont les vagues et la houle pour formuler un problème d'optimisation de structures avec des conditions limites issues de l'interaction fluide – structures sans prendre en considération le mouvement de la structure. Dans cette étape nous avons pu proposer des formulations originales du problème d'optimisation de forme et de la topologie de digues flottantes. Deux idées originales ont été proposées pour mettre en œuvre cette optimisation. La première est basée sur l'utilisation d'un double maillage l'un plus grossier servant à l'optimisation de topologie, tandis qu'un second maillage plus fin est utilisé pour le calcul des

contraintes mécaniques, celui-ci n'affectant pas la taille de problème d'optimisation. La seconde idée utilise une description géométrique avec un polygone dont le nombre de côtés varie et augmente au fur et à mesure des calculs d'optimisation. Cette méthode donne de très haut degré de flexibilité dans le processus d'optimisation car les coordonnées des points constituent les variables du problème conduisant à des formes sans aucune restriction.

Afin d'évaluer les performances d'une digue flottante nous avons ensuite élaboré un modèle de comportement dynamique (Newmann 1994, 1997). Ce modèle prend en compte les effets de diffraction – radiation de la houle, le couplage fluide – structure grâce aux concepts de masses additionnelles et de coefficients d'amortissement spécifiques, et les conditions limites imposées par la géographie d'un port. Afin de rendre compte plus précisemment des effets du port, ce modèle prendre en compte les murs comme des éléments réfléchissant associés à un coefficient de réflexion spécifique. Cette particularité permet d'appliquer ce modèle à différents sites portuaires. Afin de déterminer le coefficient de transmission, une modéle analytique du comportement dynamique de la structure est développé en utilisant le modèle lagrangien. Les équations des mouvements sont résolues pour évaluer les réponses de la digue dans les trois degrés de liberté. A partir de ce modèle, une étude paramétrique nous a permis de mettre en évidence le domaine d'utilisation de ces digues flottantes amarrées et d'identifier l'influence des paramètres structuraux sur ses performances.

Les résultats de l'analyse paramétrique montrent l'intérêt d'une optimisation de forme de la digue avec ce modèle de comportement dynamique, ils mettent en évidence que certaines valeurs des paramètres géométriques maximisent les performances de la digue. Cette analyse montrent aussi l'existence, de pics de résonance répétitifs et corrélés avec certains paramètres structurel. Cette particularité montre la nécessité d'envisager une modélisation tridimensionnelle pour vérifier la corrélation de ces pics de résonance avec ces paramètres structuraux.

Finalement, en utilisant ce modèle dynamique nous avons formulé un problème d'optimisation de forme nous permettant de déterminer les dimensions optimales de la digue en fonction des performances (coefficient d'atténuation de la houle) à atteindre. En fait, il constitue un problème d'optimisation multidisciplinaire où, pour chaque itération du processus d'optimisation, un problème de mécanique des fluides couplé à un problème de dynamique du solide et un calcul de structure élastique sont résolus séparément puis assemblés pour former les contraintes du problèmes d'optimisation.

Abstract

The subject of this thesis concerns modelling and optimizing floating breakwaters, i.e., the study of the motion of a floating breakwater and its response to surface water waves, the analysis of the hydrodynamic behaviour of the floating breakwater through a comprehensive parametrical analysis, and finally to improve the performance and design of the floating breakwater through an optimization problem. It is an interdisciplinary problem, where it addresses the fluid mechanics, mechanical resistance, and structural optimization. A two dimensional modelling and optimisation process has to be developed to serve as a general design tool to determine the dimensions of an optimal floating breakwater capable of surviving in a significant wave height. A rectangular floating body with varying width, draft, mass, internal geometrical section, mooring line angle, and mooring stiffness constitutes the optimization problem.

The hydrodynamic analysis was studied using the diffraction-radiation numerical model and extended so as to include the reflective sidewall characterizing the port terminal and assimilating a real practical problem for port sites. So it is different to the problems of structures oscillation on water surface with unbounded domain. In order to proceed forward and determine the transmission coefficient, an analytical modelling for the vibrating structure is developed using the Lagrangian mechanics. The equations of motions are solved to evaluate structure responses in the three modes of motion, and hence vibrational effects are determined and discussed. Finally, a parametrical analysis is developed to identify the influence of the structural parameters on the wave attenuating capacity of the moored floating breakwater.

The complexity of the floating breakwater design due to repetitive resonance bands and the interference between the structural parameters makes an analytical optimal design somehow difficult if not impossible. This forces us to orient the problem towards an optimization approach. The main idea in this work is to address the optimization of floating breakwaters (shape and topology) in order to reduce its weight, or to represent a new resistive form, in accordance to the physical and mechanical constraints using various optimization methods.

It starts with a simple approach summarized by optimizing a predefined geometry using its geometrical parameters or dimensions. Then, continues towards topology optimization, where we have elaborated a new contribution in this field. Two types of triangular meshes were used. One for indicating the number of variables in the optimization problem, and another refined mesh used for Finite element computations. Thus, we can use very fine meshes without affecting the scale of the optimization problem. Also, we have elaborated another idea in the domain of shape optimization based on arbitrary geometrical shape composed by introducing n variable points constituting a valid structure. This method yields to high flexibility in the optimization process since the points coordinates constitute the variables of the problem leading to unrestricted shapes. All these previously mentioned methods are applied for a simplified model for the wave structure interaction. Where we considered that to some extent, we can disregard or omit the dynamical vibration of

the floating breakwater itself. This has permitted us to go thoroughly in structural optimization methods and their developments, where it was very hard to start the optimization problem with the complete dynamical model. It consumes an enormous computational time and especially for the topology problem.

Finally, the optimisation problem of a real floating breakwater model is treated with the predefined geometrical shape method. In fact, it constitutes a multidisciplinary optimization problem, where in each iteration a problem of fluid mechanics, dynamic motion, and mechanical resistance are to be solved separately and then assembled through the imposed constraints. This yields to realistic results adaptable with the practical data and experience used in their construction, since it concerns the fluid flow propagation (diffraction-radiation), dynamic motion, mooring lines, and the structural demands.

RESUME ETENDU

Ⅰ-Introduction

Les contraintes d'aménagement du territoire, associées à la nécessité de développement économique des sites touristiques et industriels côtiers poussent les industriels à proposer des structures flottantes de plus en plus ambitieuses. Ces structures flottantes peuvent être conçues soit pour protéger des aménagements portuaires, lorsque la configuration des fonds marins ne permet l'usage de structures fixes, soit pour étendre les surfaces utiles en bordures des côtes.

Les digues à talus et les digues verticales sont des structures maritimes destinées à la protection des ports. Elles réfléchissent et/.ou dissipent l'énergie des vagues et mettent ainsi à l'abri des effets de la houle les installations portuaires. Ces structures assurent une protection très efficace pour une large gamme de condition maritime. Cependant pour des conditions géographique et bathymétrique spécifiques les structures flottantes de protection peuvent offrir de nombreux avantages par rapport aux structures fixes. Elles se révèlent plus économiques à construire et facilement reconfigurables pour s'adapter aux évolutions des activités portuaires.

Ces digues flottantes réfléchissent une partie de l'énergie des vagues et absorbent partiellement l'autre partie de cette énergie. La partie absorbée met en mouvement la structure créant ainsi des « anti-vagues », d'où leur capacité à atténuer la hauteur de la houle sans toutefois pourvoir l'annihiler. Plusieurs types des digues flottantes ont été développés, comme décrit par McCartney (1985), mais les plus utilisées sont les digues rectangulaires, amarrées au fond de mer par des câbles ou des chaînes. Ce sera la configuration retenue comme sujet de ce travail de thèse.

La difficulté d'établir des similitudes acceptables avec des maquettes à échelle réduite ($1/100^{ième}$), pour concevoir au mieux ces structures de grande dimension, rend indispensable l'usage de modèle numérique permettant de prévoir les performances de ces structures (Bougis 1996). C'est une problématique complexe, à caractère multidisciplinaire, mêlant des problèmes d'hydrodynamique, le couplage fluide – structures, et dans une moindre mesure de mécanique des structures.

La compréhension de la physique et le calcul de l'interaction houle-structure est l'un des plus importants processus hydrodynamiques dans l'ingénierie côtière et offshore. Il est crucial pour estimer l'impact de houle sur les structures et la réponse structurelle sous l'effet de la houle.

Dans le domaine de l'interaction fluide-structure et plus précisément pour celui de l'interaction houle-structure l'estimation des effets de la houle sur la structure peut être obtenue de deux manières : par une approche empirique (ex: Morison equation Sainflou, Hiroi, Goda, Svendson…) ou par une approche numérique (G. Gruhan, 2005). Les formules empiriques sont simples mais ne peuvent pas fournir des informations détaillées et précises sur la distribution de la pression sur la structure. L'approche numérique peut être scindées entre deux types :

- La résolution de l'équation de Laplace pour le potentiel de vitesse de la houle (D.Jeng, 2005).
- La résolution de l'équation de Navier Stockes pour un fluide visqueux, où cette dernière est utilisée pour la simulation de l'interaction houle-structure, où les phénomènes de turbulence et de vortex peuvent apparaître.

La résolution de l'équation de Laplace en imposant les conditions aux limites sera la base de la modélisation de la houle dans notre étude.

Les concepts de modélisation pouvant s'appliquer à ces structures flottantes sont issus des modèles d'interaction fluide structure développés pour l'étude des navires et des plateformes offshores (Newman 1977). Les phénomènes de diffraction de la houle (houle réfléchie par la structure), de radiation (houle créée par les oscillations de la structure) et les particularités induites par les dimensions finies du domaine, ont été abordés dans ces travaux. Des modèles de comportement dynamique de la structure (corps rigide, oscillations harmoniques de petite amplitude) ont été proposés. Afin de rendre compte des effets de l'eau lors des oscillations, ces modèles utilisent des « masses additionnelles » et des coefficients d'amortissement spécifiques.

L'optimisation des digues flottantes n'a pas encore été abordée dans la littérature. Quelques travaux se rapportent à l'optimisation des digues fixes (Ryu 2005, Castillo 2006) mais ne concernent pas l'optimisation de la forme et ou de topologie de ces structures et encore moins celle des structures flottantes. Cette absence de travaux d'optimisation de digues flottantes motive donc en grande partie cette étude.

Dans ce travail nous avons commencé par aborder le problème en étudiant les modèles de propagation d'ondes de surface que sont les vagues et la houle pour formuler un problème d'optimisation de structures avec des conditions limites issues de le couplage fluide – structures indépendantes du temps. Dans cette étape nous avons pu proposer des formulations originales du problème d'optimisation de forme et de la topologie de digues flottantes.

Pour évaluer les performances d'une digue flottante nous avons ensuite élaboré un modèle de comportement dynamique. Ce modèle prend en compte:

- Les effets de diffraction – radiation de la houle.
- Le couplage fluide – structure grâce aux concepts de masses additionnelles et de coefficients d'amortissement spécifiques.
- Les conditions limites imposées par la géographie d'un port.

A partir de ce modèle dynamique, une étude paramétrique nous a permis de mettre en évidence le domaine d'utilisation de ces digues. En utilisant ce modèle dynamique, nous avons formulé un problème d'optimisation de forme nous permettant de déterminer les dimensions optimales de la digue en fonction des performances (coefficient d'atténuation de la houle) à atteindre.

Finalement, la méthodologie suivie dans cette thèse est premièrement identifiée par une modélisation de la houle (analytique et numérique) et leurs pressions induites exercées sur la digue verticale et puis la modélisation du comportement de la digue flottante due à l'interaction houle-structure. Il est intéressant de considérer le cas d'une digue verticale qui apparaît dans la construction des ports loin de la cote, à une profondeur constante, et à un point fixe. Alors, les problèmes des propagations des houles sur un bathymétrie et les conséquences de l'eau de faible profondeur sont éliminés. Et puis, nous établissons le problème d'optimisation qui résoudre un problème non linéaire pour minimiser le poids en respectant tous les contraintes physiques et mécaniques (flottaison, stabilité, hauteur minimum de la houle dans le port, comportement mécanique de la structure).

Ⅱ-Modélisation de la houle

Nous avons développé des modèles analytiques et numériques pour décrire la propagation de la houle. Dans le première cas, les oscillations de la structure sont considérées faibles où ils peuvent être négliges. Cette simplification nous donne la possibilité d'étendre la partie d'optimisation pour explorer et appliquer différentes méthodes de forme et de topologie. Où nous avons inclus dans le modèle numérique le comportement de la digue et les effets de diffraction – radiation de la houle pour bien approcher le cas réel.

1- Modèle Analytique

Considérons le cas d'une onde se propageant dans un volume de fluide dont une dimension est infinie. Dans le système de coordonnée cartésienne Oxy de la figure 1 on considère l'onde incidente se propageant dans une direction parallèle à l'axe Ox. Dans ce cas l'onde frappe perpendiculairement la digue et on obtient ainsi la pression maximale appliquée par les ondes sur la digue, le cas le plus dangereux.

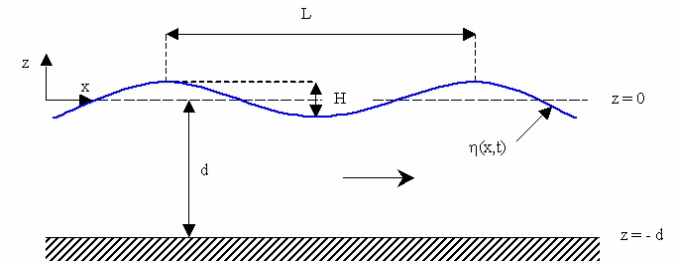

Figure 1 Notations de la houle

Le mouvement du fluide est défini comme suit: soit t le temps, x et z les coordonnées horizontale et verticale respectivement, et η l'élévation de la surface libre au-dessus du niveau de l'eau calme. Les valeurs élevées de la densité et de la vitesse du son dans l'eau rendent les effets de la compressibilité négligeables dans l'eau de mer, donc on la considère incompressible. Le fluide sera également considéré irrotationnel, on peut alors caractériser le mouvement du fluide par un potentiel de vitesse, Φ , reliée a sa vitesse $\vec{U}(u,w)$.

Une fois que les paramètres caractérisant les ondes de mer sont connus (longueur de l'onde L, période T, hauteur H), un modèle est nécessaire pour étudier les propagations des ondes et en déduire les charges exercées sur la digue. C'est une étude basée sur le principe physique fondamental de la conservation de la quantité de mouvement et de la masse. La combinaison entre l'équation de la conservation de la force et celle de la conservation de la masse, conduit à une équation bien connue, dite de Bernoulli-Lagrange, qui constitue l'équation fondamentale pour déterminer le champ de la pression dans le fluide.

$$\frac{\partial \Phi}{\partial t} + \frac{1}{2}(grad\Phi)^2 + \frac{P(x,z,t)}{\rho} + gz = Q(t)$$

Si Φ est connue partout dans le fluide, les quantités physiques (pression et vitesse) peuvent être déterminées ou obtenues à partir de l'équation de Bernoulli. Le problème aux limites vérifié par le potentiel Φ s'écrit

$\nabla^2\Phi = \Delta\Phi = 0$ l'équation de Laplace dans le domaine du fluide.

$\left(\frac{\partial\Phi}{\partial z}\right)_{z=-d} = 0$ condition sur le fond de la mer.

$\left(\frac{\partial\Phi}{\partial n}\right)_{x=0} = 0$ condition cinétique sur le frontière solide.

$\left(\frac{\partial\eta}{\partial t} + \frac{\partial\Phi}{\partial x}\frac{\partial\eta}{\partial x} - \frac{\partial\Phi}{\partial z}\right)_{z=\eta} = 0$ condition cinétique sur la surface libre.

$\left(\frac{\partial\Phi}{\partial t} + \frac{1}{2}\left(\left(\frac{\partial\Phi}{\partial x}\right)^2 + \left(\frac{\partial\Phi}{\partial z}\right)^2\right) + g\eta\right)_{z=\eta} = Q(t)$ L'équation dynamique sur la surface libre.

L'équation de Laplace exprime la conservation de la masse, la condition écrite au fond de la mer exprime l'imperméabilité du fond où la composante normal de la vitesse est nulle. La condition cinétique sur le frontière solide (brise-lame, x=0), exprime la condition statique du brise-lame (réflexion de l'onde) ou $\vec{n}$ est la direction normal à la frontière solide dirigée vers l'extérieur; la condition cinétique sur la surface, $z = \eta$, exprime qu'une particule du fluide sur la surface doit conserver sa place tout le temps, alors que la condition dynamique exprime que la pression sur la surface libre est nulle.

En utilisant un modèle classique de houle de Stockes, modèle non linéaire du second ordre nous avons déterminé l'expression analytique de la pression dynamique due à la houle. Finalement, la pression exercé par le fluide sur la digue s'exprime avec la relation :

$$P(x,z,t) = -\rho g z + \mathrm{Re}\left\{\frac{1}{2}\rho g H \frac{ch[k(z+d)]}{ch(kd)}\left[\exp i(kx-\omega t) + r\exp i(-kx-\omega t+\beta)\right]\right\} + \mathrm{Re}\left\{\frac{3}{4}\rho g H \frac{\pi H}{L}\frac{1}{sh(2kd)}\left[\frac{ch2k(z+d)}{sh^2 kd} - \frac{1}{3}\right]\left[\exp 2i(kx-\omega t) + (r^2+r)\exp 2i(-kx-\omega t+\beta)\right]\right\}$$

$$+ \mathrm{Re}\left\{r\rho H^2\omega^2 \exp i(-2\omega t+\beta)\right\} - \frac{1}{4}\rho g H \frac{\pi H}{L}\frac{(r+1)}{sh(2kd)}\left[ch2k(z+d) - 1\right]$$

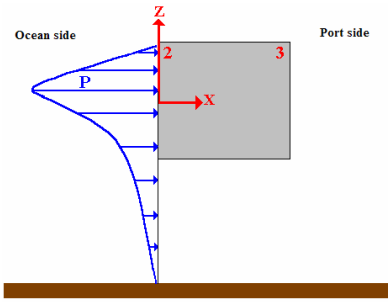

Figure 2 Distribution de la pression hydrodynamique sur la digue

La figure 2 montre une répartition typique de cette pression et nous permet de conclure sur l'intérêt d'une digue flottante puisque le pic de pression est situé dans le tiers supérieur de la hauteur d'eau. La pression hydrodynamique (Fig. 2) est exercée sur la surface extérieure de la digue est du à l'hypothèse que toutes les ondes se propageant de l'océan sont totalement réfléchies vers l'extérieur du port (pas de transmission); On peut également en déduire qu'il n'existe pas de pression dynamique

exercée sur la surface intérieure de la digue en supposant l'absence de propagation d'ondes a l'intérieur du port (cas simplifié). Cette pression dynamique peut être exprimée comme suit:

$$P = a\cosh k(z+d) + b\cosh 2k(z+d) + f$$

$$a = \frac{\rho g H}{2}\frac{(r+1)}{chkd}\cos(\omega t),\ b = \frac{\rho g \pi H^2}{4Lsh2kd}\left[\frac{(3r^2+3r+3)\cos(2\omega t)}{sh^2 kd} - r - 1\right]$$

$$f = \frac{\rho g \pi H^2}{4Lsh2kd}\left[\left(-r^2 - r - 1\right)\cos(2\omega t) + r + 1\right] + \rho H^2 \omega^2 r\cos(2\omega t)$$

Elle est réduite en une équation avec une fonction hyperbolique de z (altitude), où les autres variables indépendantes de l'altitude sont regroupées ensemble suivant les termes $a,\ b,$ et f .

2- Modélisation numérique

Dans cette partie, la modélisation de la houle est réalisée numériquement en se basant sur une approche linéaire. Seule une modélisation du comportement dynamique de la digue permet d'évaluer la performance de cette dernière, c'est-à-dire le coefficient d'atténuation de la houle (rapport entre la hauteur de la houle coté port et la hauteur de la houle coté mer). Le modèle que nous avons développé prendre en compte :

- Les effets de diffraction (houle réfléchie par la digue) et de radiation (houle créée par les mouvements de digue).
- Des conditions limites traduisant les limites du domaine fluide (profondeur et limite du port).
- Les effets de l'eau sur le mouvement d'oscillation de la digue au travers des coefficients de masse et de frottement additionnels calculés à partir des efforts hydrodynamiques du potentiel de radiation du champ de vitesse.

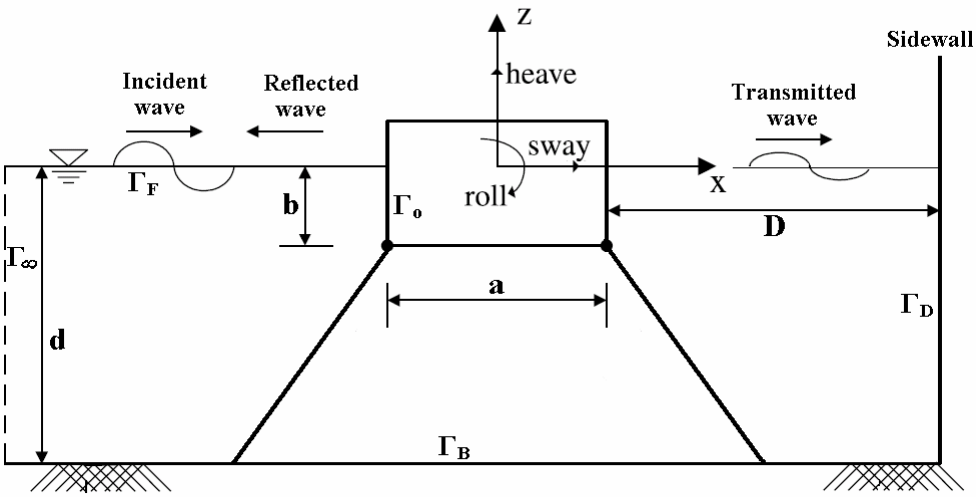

Figure 3 Notations d'un modèle numérique

Cette linéarisation nous permet de séparer la potentiel total en potentiel incident réfléchi, et un potentiel de radiation qui est relie a la dynamique de la digue. Pour résoudre le problème d'interaction on découpler le problème de diffraction et radiation, car la diffraction ne dépend pas de la dynamique de la digue. Pour chaque potentiel, on résout l'équation de Laplace avec 5 conditions aux limites linéaires

correspondante aux surfaces libres, au corps de digue, au fond, aux frontières de radiation et au mur du port.

Problème de Diffraction

Le potentiel de diffraction ϕ_D peut être exprimer en fonction du potentiel incident ϕ_I et du potentiel de réflexion ϕ_S. Le problème aux limites qui vérifie le potentiel ϕ_D s'écrit:

$\phi_D = \phi_I + \phi_S$

$\nabla^2 \phi_D = 0$ dans le domaine fluide Ω

$\frac{\partial \phi_D}{\partial z} - \frac{\omega^2}{g}\phi_D = 0$ à la surface libre, Γ_F, $z = 0$

$\frac{\partial \phi_D}{\partial z} = 0$ sur le fond marin, Γ_B, $z = -d$

$\frac{\partial \phi_D}{\partial x} + ik\phi_D = 0$ sur la frontière de radiation, Γ_∞, $x \to -\infty$

$\frac{\partial \phi_D}{\partial z} = 0$ sur la digue, Γ_0, $z = -b$, $-a/2 \le x \le a/2$

$\frac{\partial \phi_D}{\partial x} = 0$ sue la digue, Γ_0, $x = \pm a/2$, $-b \le z \le 0$

$\frac{\partial \phi_D}{\partial z} = ik\frac{k_r - 1}{k_r + 1}\phi_D$ sur le mur vertical, Γ_D, $x = a/2 + D$, $-d \le z \le 0$

où k_r caractérise le coefficient de réflexion du mur

Problème de Radiation

Le potentiel de radiation, φ_j, vérifie les conditions aux limites suivantes :

$\nabla^2 \varphi_j = 0$ dans le domaine fluide Ω

$\frac{\partial \varphi_j}{\partial z} - \frac{\omega^2}{g}\varphi_j = 0$ à la surface libre, Γ_F, $z = 0$

$\frac{\partial \varphi_j}{\partial z} = 0$ sur le fond marin, Γ_B, $z = -d$

$\frac{\partial \varphi_j}{\partial x} + ik\varphi_j = 0$ sur la frontière de radiation, Γ_∞, $x \to -\infty$

Pour le potentiel de radiation, φ_j, $j = 1,2,3$, les conditions de couplage fluide – structure peut être écrit comme :

$\frac{\partial \varphi_j}{\partial x} = ik\frac{k_r - 1}{k_r + 1}\varphi_j$ sur le mur vertical , Γ_D, $x = D + a/2$

$\frac{\partial \varphi_j}{\partial n} = n_j$ sur la digue, Γ_0

Où n_1 et n_2 sont les composantes de la normale à la digue, et $n_3 = (x - x_c)n_2 - (z - z_c)n_1$, où (x_c, z_c) sont les coordonnées de la centre de rotation de la digue flotttante.

Le problème diffraction - radiation est résolu numériquement par éléments finis sous en utilisant la boite à outils « PDE : équation aux dérivées partielles » (PDE) de MATLAB™, Dans ce cas, l'équation de Laplace est vue comme une forme particulière d'une l'équation elliptique. Il faut alors écrire tous les conditions aux limites précédentes suivant dans la forme de Newman ou de Dirichlet, créer un maillage du domaine de calcul pour pouvoir résoudre le potentiel de radiation et diffraction. (Figure 4)

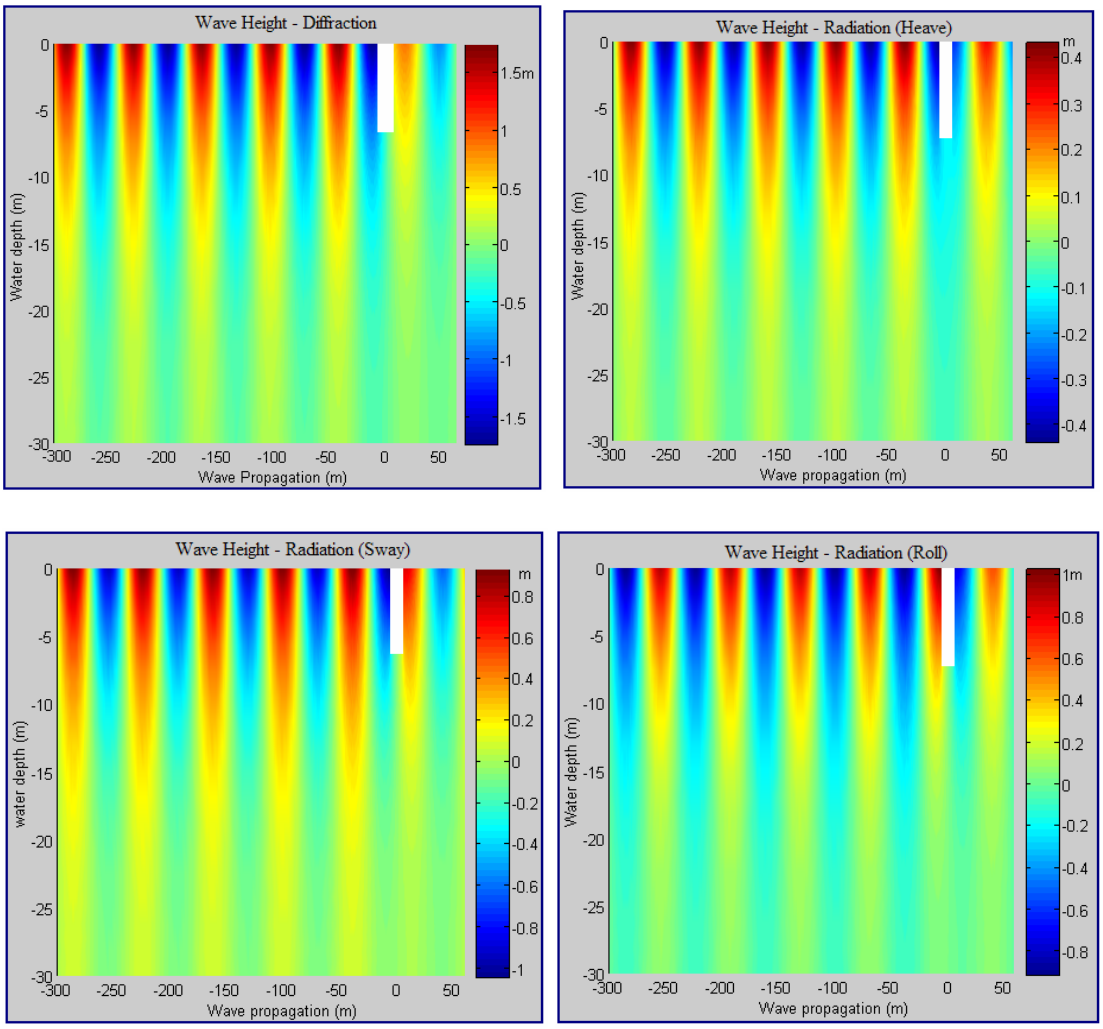

Figure4 Houle de diffraction et de radiation crées par le mouvement de la digue
De gauche a droite: Diffraction - Heave – Sway – Roll

Dans la deuxième étape, il faut résoudre l'équation de mouvement pour étudier le comportement dynamique de la digue. Cette dernière est mise en oscillation par les forces d'excitation venant de la houle incidente $\left(F_j^e\right)$. Bien que la digue flottante puisse être assimilée à un système mécanique masse ressort, et donc avoir les mêmes caractéristiques dynamiques, il y a une différence importante qui affecte son comportement dynamique. L'eau entourant la structure joue le rôle « d'amortisseur hydrodynamique ». Cette particularité est gérée avec le concept de masse additionnelle (μ) et de coefficients d'amortissement spécifiques (λ). D'après le

théorème de Lagrange, on peut déterminer les matrices de masse (M) et de raideur (K). L'équation de mouvement dans la forme des matrices s'exprime comme :

$$[M+\mu]X^{"}+\lambda X^{'}+KX=F_j^e(t)$$

Il faut résoudre l'équation de mouvement pour déterminer le vecteur du mouvement (X) de la digue qui donne le potentiel de radiation et pour déterminer le potentiel total et sa dérivée, l'élévation de la surface.

Les coordonnées Langrangienne (q_1,q_2,q_3) représentent les trois degré de liberté de la structure $x_c, y_c,$ et θ (et décrivent le mouvement du centre de gravité de la digue flottante). Le comportement du système digue flottante avec les lignes d'ancrages est modélisé par un système de trois équations différentielles du deuxième ordre.

$$\frac{d}{dt}\left(\frac{\partial L}{\partial q_i^{\cdot}}\right)-\frac{\partial L}{\partial q_i}=0 \qquad \text{pour } i=1,2,3$$

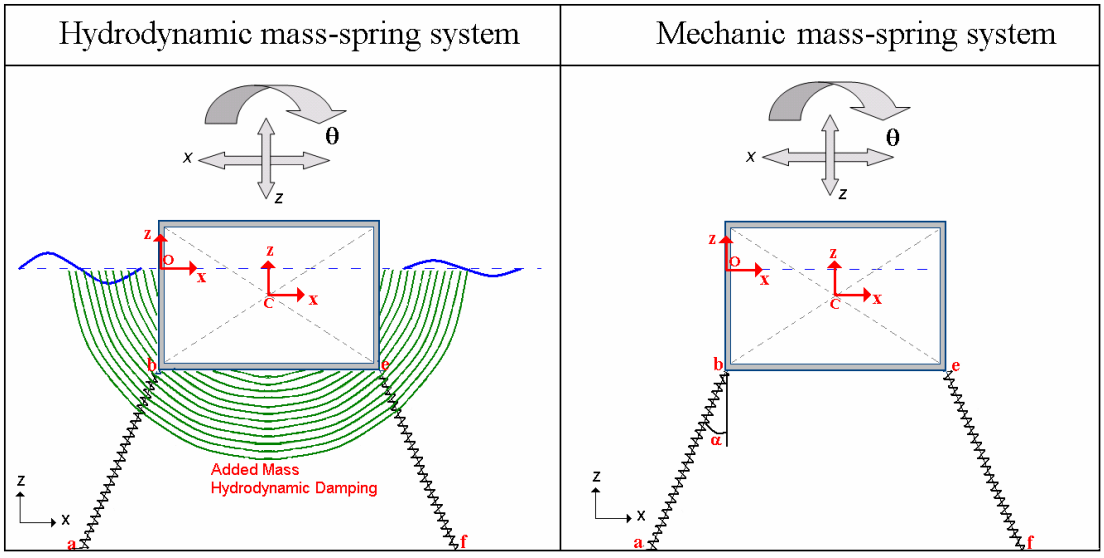

Figure 5 Représentation hydrodynamique et mécanique d'un système mass-ressort

L'équation du mouvement de la digue est formulée après linéarisation autour de la position d'équilibre sous l'hypothèse d'oscillations de petites amplitudes. A cause de la type des forces d'excitation que supposerons de forme sinusoïdale $(F_j^e = f_j^e e^{-i\omega t})$, nous pouvons écrire l'équation de mouvement dans la forme suivante :

$$[-\omega^2(M+\mu)-i\omega\lambda+K]\delta_j=f_j^e \qquad (3.35)$$

Où δ_j est l'amplitude complexe de la réponse de mouvement, $X_j=\delta_j e^{-i\omega t}$

La Figure 6 présente le synoptique de résolution du modèle pour déterminer le paramètre indicateur de la performance de la digue, le coefficient d'atténuation de la houle. Cette figure met en évidence les paramètres d'entrée suivant :

- Les paramètres structuraux définissant la masse et la forme de la digue ainsi que ceux des lignes d'ancrages
- Les paramètres relatifs à la houle à atténuer.

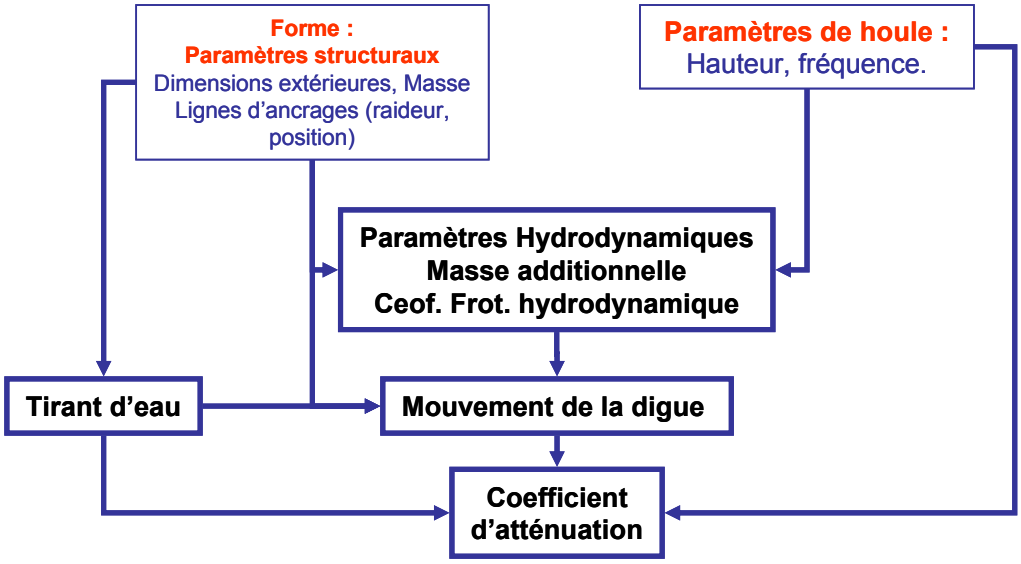

Figure 6 **Synoptique du calcul du coefficient d'atténuation.**

A partir de ce modèle de comportement dynamique, une étude paramétrique nous a permis de déterminer l'influence des paramètres d'entrée du modèle sur le coefficient d'atténuation. Cette analyse montre aussi l'existence, de pics de résonance répétitifs et corrélés avec certains paramètres structurels. Les conclusions essentielles que nous en tirons sont :

- Pour une géométrie donnée il existe, pour les lignes d'ancrage, un intervalle de valeur d'angle (10° - 20°) qui produit un pic de résonnance et donc une très mauvaise valeur du coefficient d'atténuation. En effet dans cette situation la digue n'attenue pas la hauteur des vagues mais l'amplifie par effet de résonnance.

- La largeur de la digue joue un rôle important, il existe une plage de valeurs permettant d'obtenir les meilleures performances d'atténuation.

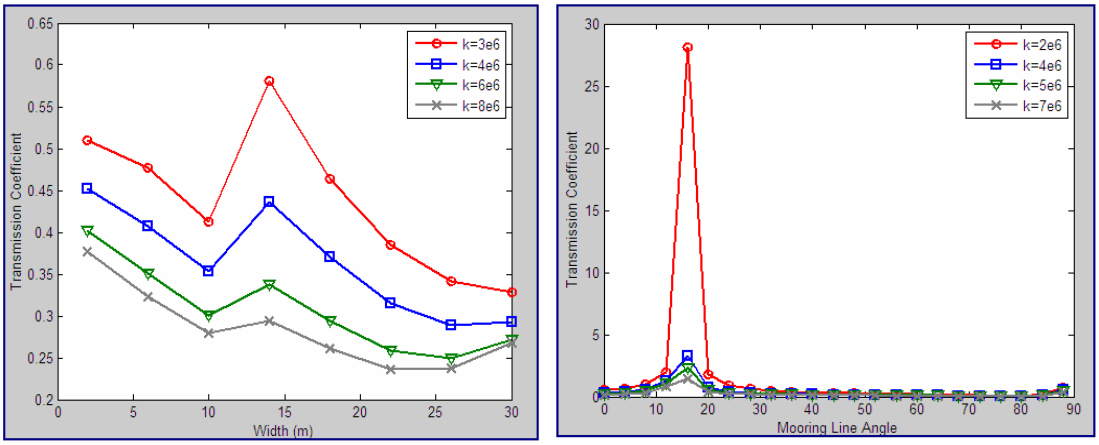

Figure 7 : Etude paramétrique, influence de la rigidité et de l'angle des lignes d'ancrage sur le coefficient d'atténuation.

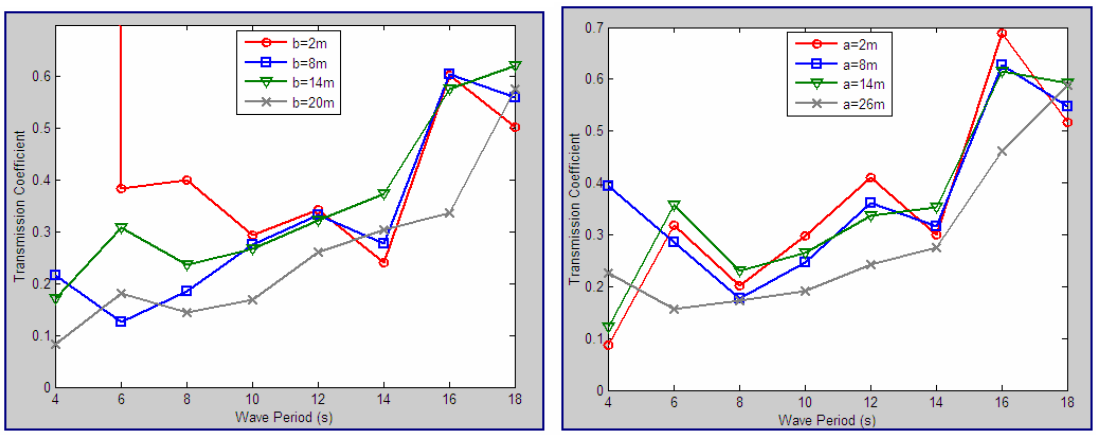

Figure 8 : Etude paramétrique, influence de la profondeur et de la largeur de la digue sur le coefficient d'atténuation.

Ⅲ-Optimisation d'un Digue Flottante

L'objectif principal est de développer une optimisation de brise-lames flottants (forme et la topologie), afin de réduire le poids, ou de chercher une nouvelle forme, conformément aux contraintes physiques et mécaniques. Une digue flottante doit être bien conçue pour assurer :

- La réduction effective de l'énergie transmise, garantissant une protection adéquate pour la zone située en arrière du système flottant.
- La non détérioration de la digue flottante elle-même.
- La tenue des lignes d'ancrages, qui maintiennent en place la digue.

La satisfaction de ces trois conditions traduit la performance totale attende. La non détérioration des lignes d'ancrages a été discutée et amplement étudiée (Loukogeorgaki and Angelides -2005) , par conséquent nos efforts dans cette étude se porteront vers les deux premières conditions.

Etant donné les densités des matériaux de constructions usuels (béton armé), il est évident que de bonnes capacités de flottaison pour une digue s'obtiennent pour des structures creuses, de type caisson par exemple. Cette particularité complique l'écriture du problème d'optimisation. Les paramètres géométriques décrivant la section, la masse, l'angle des lignes d'ancrages, et la rigidité des ancrages sont pris en compte dans la formulation du problème d'optimisation.

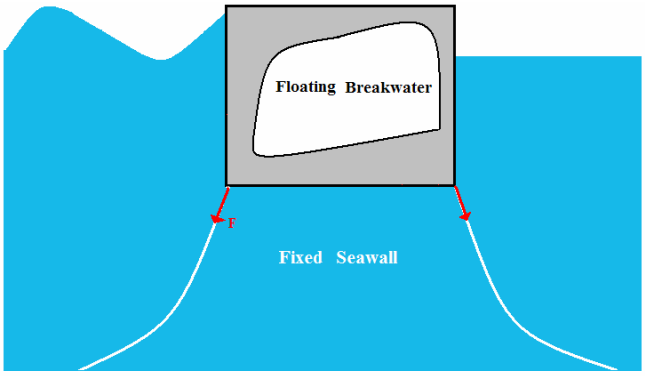

Figure 10 Caractéristique de la digue flottante

L'amélioration de la performance d'une digue flottante, de façon qu'elle peut supporter plus des charges et encore fournir une protection peu adéquat, ouvre plusieurs possibilités parce que la digue flottante, contrairement à la digue fixe, possède plusieurs paramètres caractérisant sa géométrie et définit sa forme. Le problème d'optimisation est posé comme un problème de minimisation de dimension finies avec contraintes, il est symboliquement écrit comme:

Trouver un vecteur variable x ;
Pour minimiser le fonction de poids $f_{ob}(x)$
Soumis à n contraintes $f_i(x) < 0$

1- Optimisation avec un modèle de comportement statique

Le problème d'optimisation s'exprime sous la forme d'un problème d'optimisation non linéaire avec fonctions contraintes.

a- Fonction objectif :, le but est ici de minimiser le poids de la digue, tout en respectant les contraintes du problème d'optimisation.

$f_{ob}(x_i) = Min(poids)$

b- Contrainte de Pression Dynamique:

Le concept du mur fixe d'eau permet de déterminer la hauteur de la digue en accordance avec une faible pression dynamique agissante sur le mur. La figure 11 montre une répartition typique de cette pression et nous permet de conclure sur l'intérêt d'une digue flottante puisque le pic de pression est situé dans le tiers supérieur de la hauteur d'eau. Donc, la hauteur de la digue peut être limitée jusqu'à ce que la pression soit approximativement invariable correspondant à une valeur approximative de $P - 0.05P\max = 0$, où $P\max = P(z = 0)$.

Finalement, la hauteur peut être considérée $L = 8m$, où cette hauteur est vraiment suffisante pour une houle forte, où il constitue environ $2H$ (H est la hauteur de la houle).

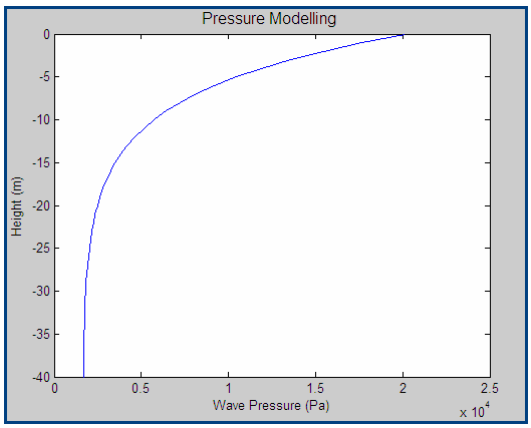

Figure 11 Modélisation de la pression de la houle

Cette contrainte est indépendante des autres contraintes, et alors la hauteur de la digue est seulement déterminée a partir de celle la, et puis on n'a pas besoin de considérer la hauteur comme une variable pour la partie restante dans le processus d'optimisation

c- Contrainte de Flottaison:

Cette contrainte est une application directe du théorème d'Archimède. Alors, la contrainte de flottaison s'écrit comme suit:

$C_1(x_i) = -\rho_m V_m g + \rho_e V_T g \le 0$

ρ_m et ρ_e désigne les masses volumiques du matériau de la digue et l'eau de la mer respectivement,

V_m désigne le volume de la matière à l'intérieur de la digue

V_T désigne le volume de la partie immerge de la digue

d- Contrainte de stabilité:
Dans le cas des objets flottants, on définit ici la stabilité par la capacité de retour à une position d'équilibre stable de la digue après perturbation de cet équilibre par les effets de la houle sur la structure de la digue. Le retour à l'équilibre est assuré par le moment du poids de la digue par rapport au centre de poussée de la digue.

Il y a plusieurs paramètres qui déterminent ensemble la stabilité de digue flottante :
1-Equilibre horizontale initiale, 2- Angle d'inclinaison ,3-Tension des lignes d'ancrages.

La digue flottante peut avoir une forme non symétrique, alors initialement (avant toute perturbation) il est nécessaire pour maintenir une position d'équilibre horizontale. Il est nécessaire de calculer la nouvelle position du centre de gravite en fonction des variables et en l'alignant avec le centre de flottabilité (centre de pression) de la digue flottante (figure 12) qui repose sur le centre géométrique du volume d'eau déplacée ($Tw/2$).

$$C_{eq}(x_i) = x_G - \frac{T_w}{2} = 0$$

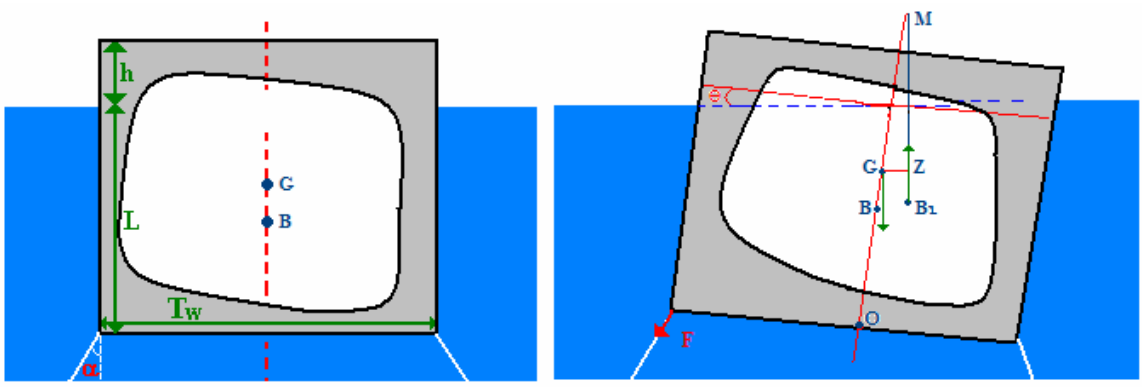

Figure 12 Stabilité d'une digue flottante

Quand la digue est perturbée par une houle, le centre de pression bouge de B à B1 (figure 12) car la forme du volume immergé a changée ; donc le poids et la force de pression (force de flottaison) crée une couple pour retenir la digue à sa position initiale. En plus, la distance GM, bien connue comme la hauteur métacentrique, illustre le principe fondamental de stabilité, où il doit être toujours positif pour créer un couple redresseur et maintenir la stabilité.

L'équation de mouvement est écrit comme suit: $\sum M = I\ddot{\theta} \Rightarrow$ à l'équilibre $Mp - M_F - M_B = 0$, où Mp est le moment de perturbation provenant de la houle, M_F est le moment de la tension dans les lignes d'ancrages, M_B est le moment de la force de flottabilité (couple de redressement), la contrainte de stabilité est finalement écrit comme suit:

$$C_2(x_i) = -W\left(\frac{T_w^2}{12L} - y_G + \frac{L}{2}\right)\sin\theta - F\cos(\alpha-\theta)x_G + F\sin(\alpha-\theta)y_G$$

$$+\left|\int_{-L+y_g}^{0}(a\cosh k(z+d-y_G)+b\cosh 2k(z+d-y_G)+f)zdz\right.$$

$$\left.+\int_{0}^{h-yg}(a\cosh k(z+d-y_G)+b\cosh 2k(z+d+y_G)+f)zdz\right| \le 0$$

α est l'angle entre les lignes d'ancrages et la verticale (α=*20*°), et θ l'angle de perturbation (angle de virage) ; réellement il est fixé par le (designer) et puisque la digue doit être rigide et stable pour protéger les ports, il est considéré comme *1.2*°.(pente 2%)

e- Contraintes structurelle: Ces contraintes constituent une analyse structurelle pur de la digue flottante, où une étude structurelle compréhensive est demandée pour déterminer les contraintes mécaniques qui doivent être restreintes à une certaine limites.

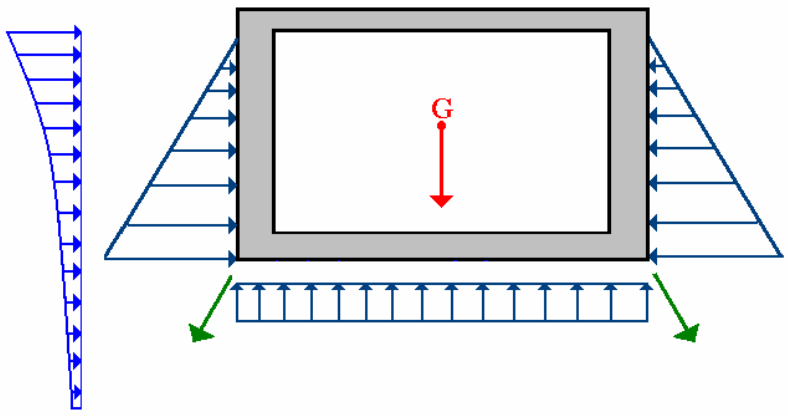

Figure 13 Digue flottante soumis a des pressions hydrostatiques et hydrodynamiques

Lorsque le béton est caractérisé par différent limites de traction et compression, il faut appliquer un critère spécifique appelle Critère Parabolique, (Garrigues.J, 2001) au lieu de la critère de Von Mises.

$$C_3(x_i) = (\sigma_1 - \sigma_2)^2 - (\sigma_t + \sigma_c)(\sigma_1 + \sigma_2) - \sigma_t\sigma_c \le 0$$

σ_1, σ_2 représentant les contraintes principales de la structure, et σ_t, σ_c représentant les contraintes limites des matériaux utilisées.

1.1 – Optimisation topologique

L'optimisation de structures mécaniques est un domaine très important du point de vue des applications qui a connu récemment de nombreux progrès. A coté des méthodes classiques de variation de frontière est apparue une autre méthode d'optimisation, dite topologique, basée sur la théorie de 'bittarray' en utilisant l'algorithme évolutionnaire (Algorithme génétique). Ces algorithmes d'optimisation stochastiques inspirés – grossièrement – de l'évolution naturelle des populations. Méthodes globales d'ordre zéro, leur robustesse et leur souplesse leur permettent d'attaquer la résolution numérique de problèmes difficiles à résoudre autrement. Mais c'est leur capacité à travailler sur des espaces de recherche non standard qui leur offre les perspectives les plus originales.

Normalement, la représentation 'bittarray' est associée à un maillage particulier du domaine – celui qui est utilisé pour calculer le comportement mécanique de la structure et déterminer la performance. A chaque élément du maillage on attribue une valeur 1 si il contient de la matière, et 0 sinon. Malgré son succès dans la résolution de problèmes d'optimisation topologique de formes, la représentation "bitarray" souffre d'un profonde limitation liée à la dépendance de la complexité de l'algorithme avec celle du maillage associe. En effet, la taille d'un individu (le nombre de bits nécessaires pour décrire un individu) est égale à la taille du maillage. Malheureusement, les résultats théoriques comme les constatations empiriques indiquent que la taille critique de population nécessaire pour atteindre la convergence augmente au moins linéairement avec la taille de chaque individu. De plus, les populations plus nombreuses nécessitent souvent un plus grand nombre de générations pour converger. Il est donc clair que cette approche doit restreindre son domaine d'application à de grossiers maillages bidimensionnels, alors que les ingénieurs ont besoin de fins maillages tridimensionnels. Ces considérations conduisent à la recherche de représentations plus compactes, dont la complexité ne dépend pas de celle de la discrétisation.

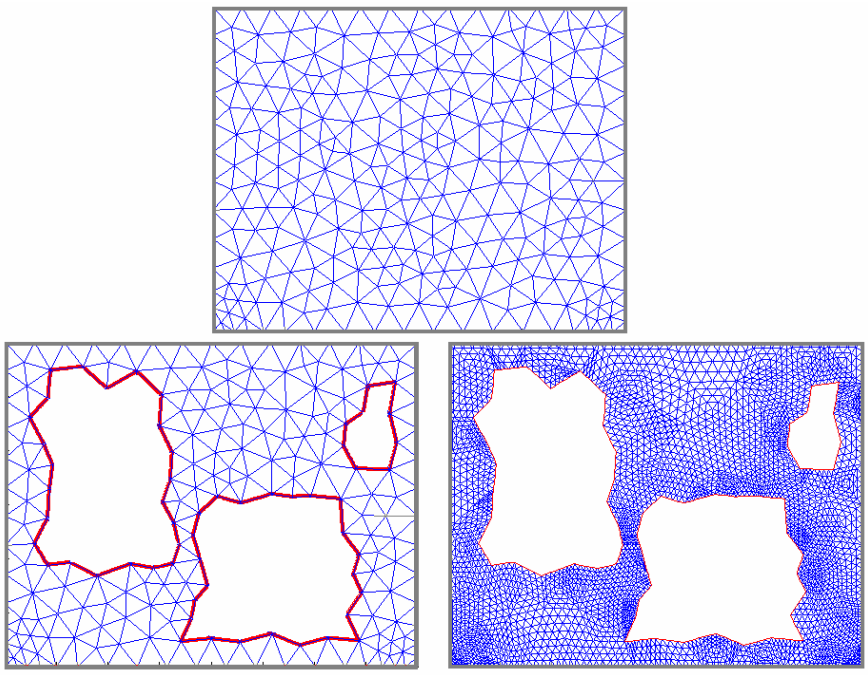

Figure 14: Optimisation topologique : principe du double maillage.

Nous avons proposé d'utiliser un maillage relativement grossier pour décrire la distribution de matériau dans la digue. Chaque élément de ce maillage est associé à une variable binaire déterminant la densité de matériau affectée à chaque élément. On notera sur la l'utilisation d'un second maillage, plus fin, pour le calcul du champ des contraintes mécaniques dans le matériau et pour résoudre le problème de liaison entre le maillage de partitions de domaine et le maillage de calcul mécanique (Fig 14 et 15). Aussi, nous avons résolu le problème d'extraction des frontières par la modification du vecteur de densité pour les éléments correspondantes aux frontières.

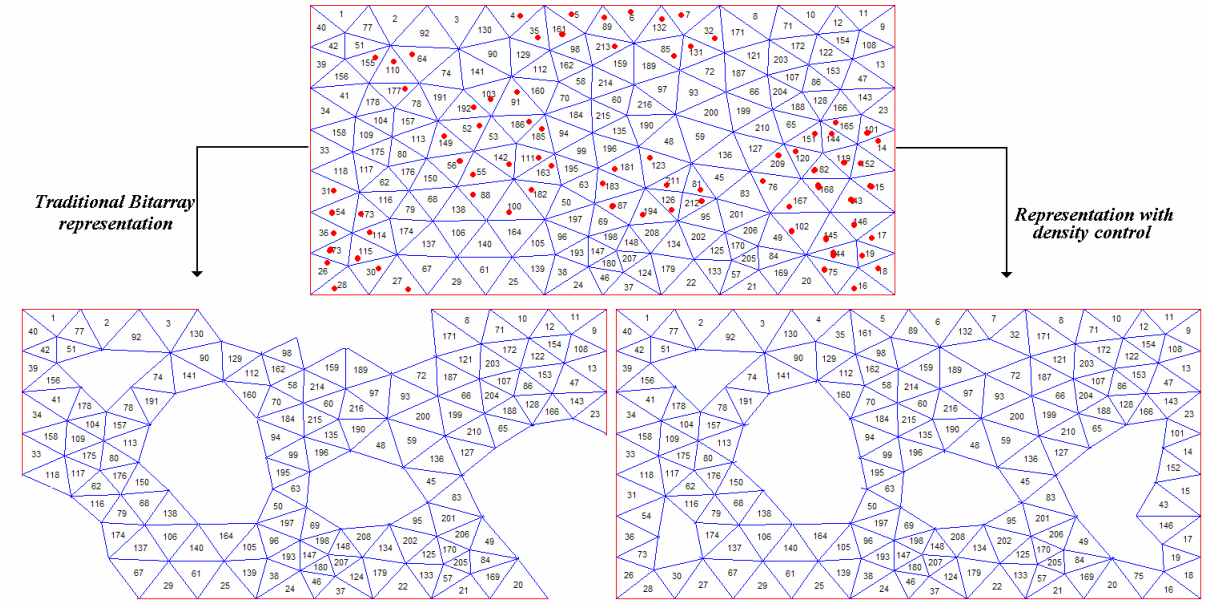

Figure 15 **Contrôle des frontières**

Comme présentée précédemment, le problème d'optimisation topologique se formule de la manière suivante :

- Minimiser le poids de la digue

Sous les contraintes :

- Assurer la flottaison
- Assurer la condition de stabilité statique (position du centre de poussée par rapport au centre de gravité)
- Assurer la résistance statique du matériau de la digue.
- Assurer le non basculement sous l'effet de la pression due à la houle.

Ce problème d'optimisation non linéaire en nombre entier, avec 4 fonctions contraintes et comportant autant de variables que d'éléments de maillage (quelques centaines) est résolu efficacement avec un algorithme génétique (résultats dans la figure 16).

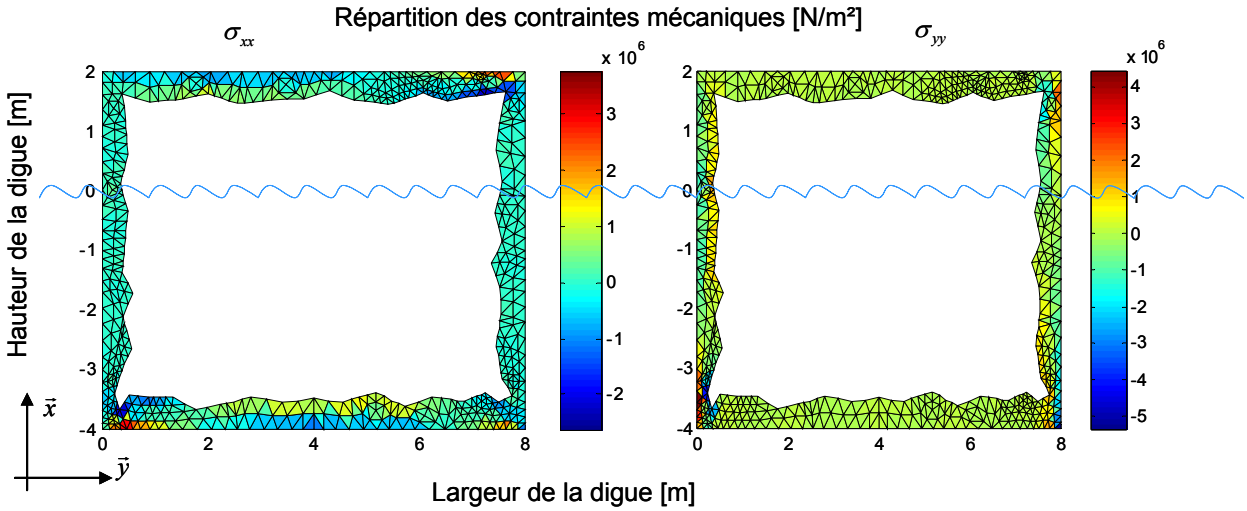

Figure 16 Exemple de topologie optimale avec le maillage de calcul mécaniques

1.2 – Optimisation de forme avec des points variables

Le problème d'optimisation de forme est traité à partir d'une description particulière de la géométrie de la digue, utilisant un polygone dont le nombre de cotés est variable. Le problème d'optimisation se formule de la même manière que précédemment, sauf pour les variables d'optimisation en nombre plus restreint, puisqu'il s'agit des coordonnées (x, y) des sommets du polygone. Les contraintes mécaniques dans le matériau sont calculées par éléments finis comme précédemment. La Figure 17 montre l'évolution de la solution optimale obtenue par un algorithme déterministe de type « SQP » lorsque le nombre de sommets du polygone augmente.

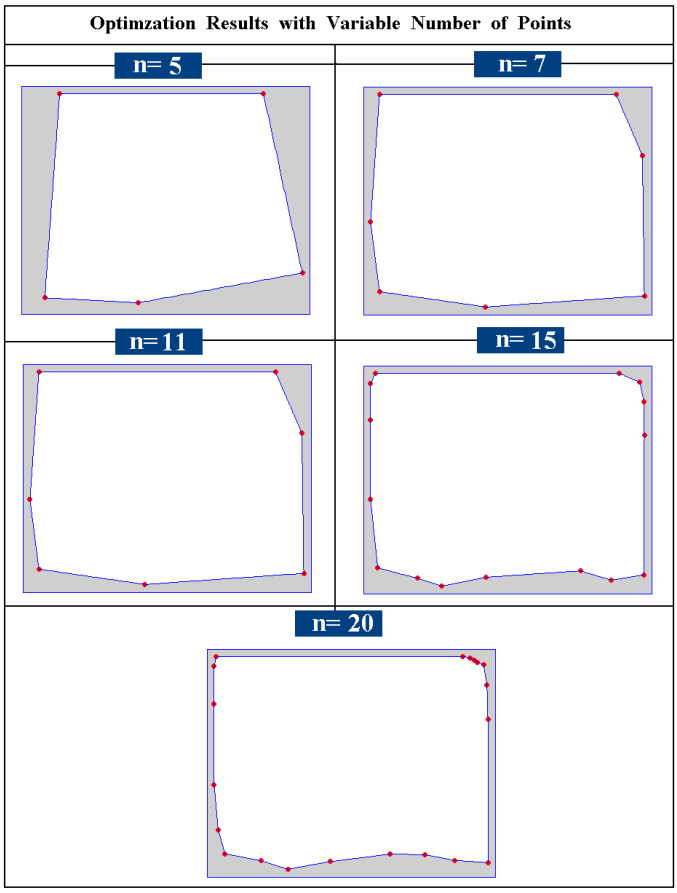

Evolution du nombre de points de description

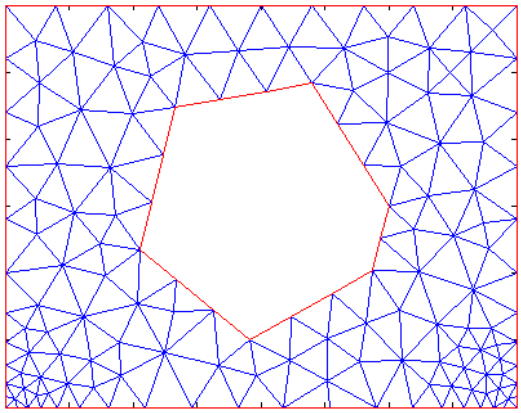

Configuration initiale et maillage

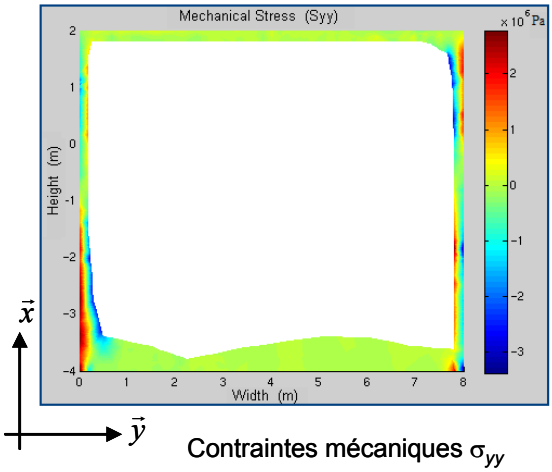

Contraintes mécaniques σ_{yy}

Figure 17: Optimisation de forme avec description évolutive de la géométrie.

2- Optimisation avec un modèle de comportement dynamique

Les résultats de l'analyse paramétrique montrent l'intérêt d'une optimisation de forme de la digue avec un modèle de comportement dynamique. Dans cette première approche nous avons envisagé une optimisation de forme s'appuyant sur une description géométrique simple définie par la Figure 18. Par conséquent le problème d'optimisation s'écrira avec les 6 variables $x = \{x_1,....,x_6\}^T$ de la Figure 18.

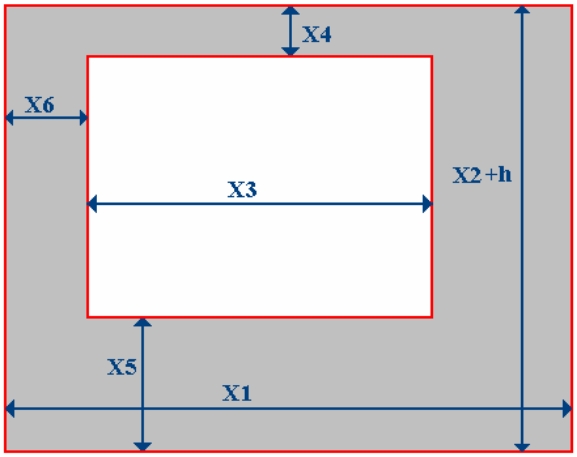

Figure 18 Définitions des variables d'optimisation

Pour chaque « évaluation » du problème deux analyses éléments finis sont requises, l'une pour déterminer le potentiel de vitesse dans le fluide et l'autre pour déterminer les contraintes mécaniques dans la structure de la digue.
Le problème d'optimisation que nous avons formulé consiste à :

- Minimiser la masse de la digue sous les contraintes suivantes :

Sous les fonctions contraintes :

- Limite sur la hauteur maximale de la houle côté port (résolution de modèle dynamique).
- Condition de flottaison de la digue.
- Condition d'équilibre (position du centre de poussée par rapport au centre de gravité).
- Limite sur les contraintes maximales du matériau de la digue.

En fait, il constitue un problème d'optimisation multidisciplinaire où, pour chaque itération du processus d'optimisation, un problème de mécanique des fluides couplé à un problème de dynamique du solide et un calcul de structure élastique sont résolus séparément puis assemblés pour former les contraintes du problèmes d'optimisation. (Figure 19)

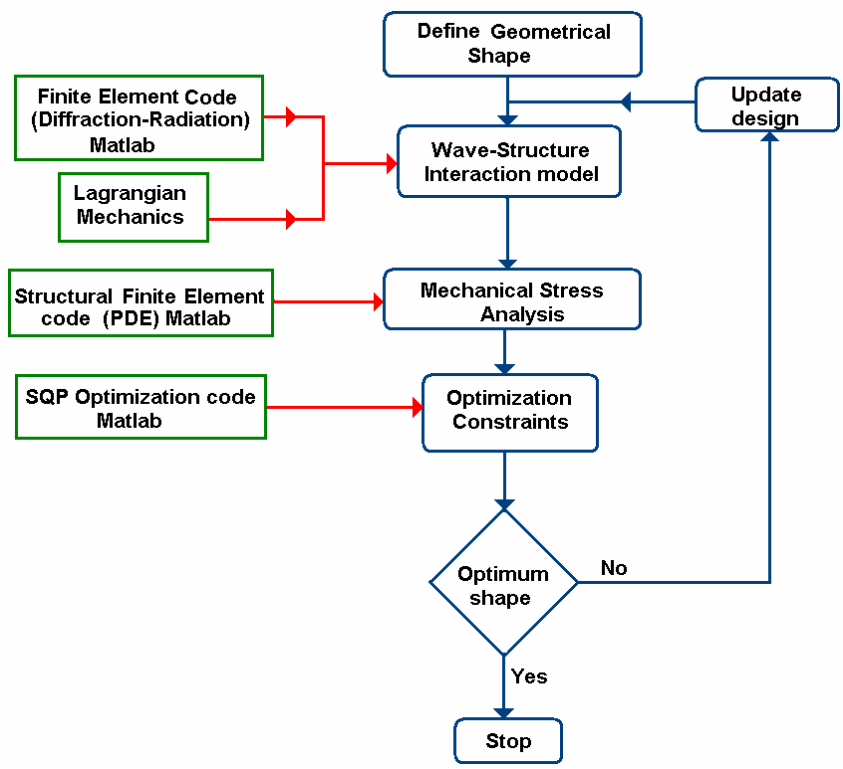

Figure 19 Organigramme pour l'optimisation avec un modèle dynamique

Comme nous l'avons vu dans l'étude paramétrique, la largeur de la digue joue un rôle important, plus celle-ci est importante meilleur sera le coefficient d'atténuation. Pour des hauteurs de houle importante (> 2m), l'obtention d'un bon coefficient d'atténuation (<0.1) nécessite des largeurs importantes. Dans ce cas de figure le problème d'optimisation n'admet pas de solution car la limite de résistance du matériau est atteinte avant que la limite sur la hauteur maximale de la houle ne soit satisfaite. Il faut alors envisager un autre matériau pour la digue, comme par exemple les matériaux composites époxy / fibre de verre qui offrent une meilleure résistance mécanique que le béton, mais sont plus onéreux.

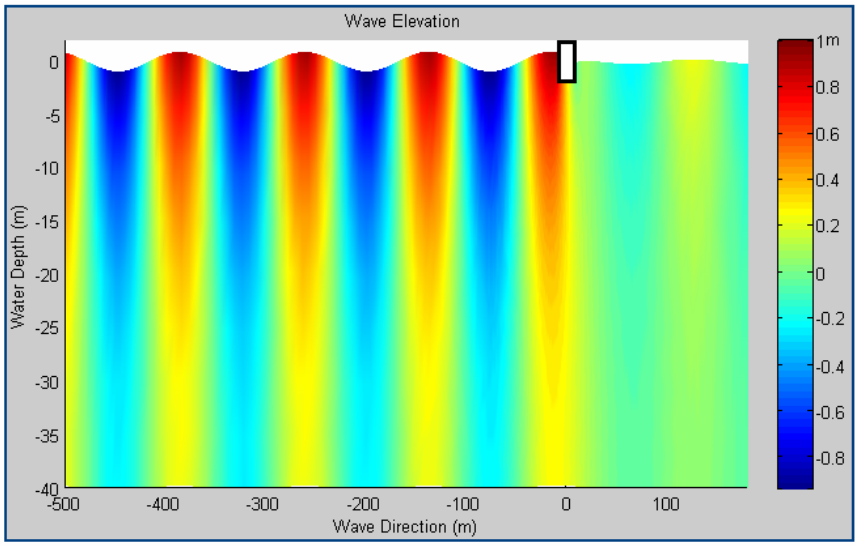

Figure 20 Modélisation de la houle pour une digue optimale

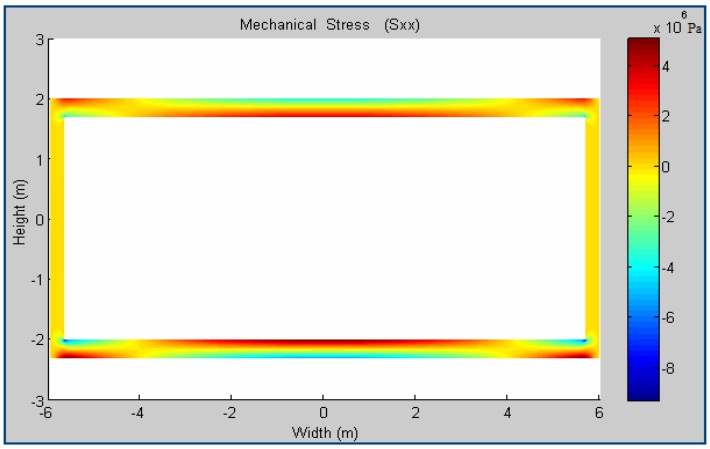

Figure 21 Optimisation de forme à partir du modèle de comportement dynamique : description géométrique et solution optimale (pour le béton et une hauteur de houle de 2m).

Ⅳ-Conclusions et principaux apports

A partir d'un modèle de houle de Stockes nous avons établi l'expression analytique de la pression dynamique. Nous avons ensuite utilisé cette pression dynamique comme condition limite dans un problème d'optimisation de forme et de topologie. Deux idées originales ont été proposées pour mettre en œuvre cette optimisation, l'une basée sur un double maillage avec un maillage plus grossier servant à l'optimisation, tandis qu'un second maillage plus fin est utilisé pour le calcul des contraintes mécaniques. La seconde idée utilise une description géométrique avec un polygone dont le nombre de côtés varie et augmente au fur et à mesure des calculs d'optimisation.
Bien qu'intéressant, les résultats obtenus ne sont pas satisfaisants car un modèle de comportement statique ne permet pas de traduire le phénomène d'atténuation de la houle. Seul un modèle dynamique est capable d'en rendre compte. Le modèle dynamique que nous avons proposé représente une avancée car c'est le premier qui prend en compte les effets de diffraction, dans un domaine fluide de dimension finie et des effets de l'eau sur le mouvement de la digue. Ce modèle est résolu par éléments finis en utilisant la boîte à outil « PDE Tools » de MATLAB™. Nous avons ensuite conduit une étude paramétrique pour identifier l'opportunité d'optimiser la géométrie. Le modèle dynamique que nous avons développé constitue sans doute l'apport scientifique le plus significatif de ce travail.

Perspectives

A court terme les perspectives de ce travail concernent :

- L'optimisation de forme et/ou de topologie avec le modèle dynamique. Cette optimisation pourra s'envisager dans un premier dans le cas d'un modèle bidimensionnel. Il faudra toutefois considérer un modèle tridimensionnel afin de rendre compte plus précisément de l'interaction avec le port. Ces modèles devront limiter la forme de la digue au cas des formes parallélépipédiques car cela simplifie grandement les calculs du potentiel de vitesse (pas d'interaction due aux formes complexes, des vagues diffractés entre elles).
- L'optimisation du positionnement de la digue dans l'espace du port. En utilisant le modèle dynamique que nous avons développé nous avons fait quelques essais qui montrent qu'il serait intéressant de rechercher le meilleur emplacement de la digue compte tenu d'une géométrie du port.

Chapter 1

Introduction

This thesis considers modelling and optimizing floating breakwaters, one of numerous types of floating structures. This involves a fluid-structure interaction problem, and a comprehensive study of dynamical and mechanical behaviour of the floating breakwater itself. In this chapter the general introduction, literature survey and problem definition and objectives of thesis are given. First, a general overview of various floating structures and their worldwide applications are presented. Then, the floating breakwaters background, their concept and development, and their various possible applications are described. A literature survey then gives the information about problems studied by researchers and engineers, methods developed, and results derived. Next, the general problem, theories used, the main objectives, and the methodology of our study are given.

1.1-The need for space

Seen from space, the Earth looks like a blue coloured planet with constantly moving swirls of clouds of Earth's ever changing weather. The Earth is mostly blue because the main part of its surface is covered by oceans, seas, lakes, rivers, etc. The Earth's land surface measures 148,300,000 square kilometers, while the total area of the Earth's surface is 510,083,000 square kilometers. Thus the water surface area takes up 70 percent of the Earth's total surface area; the land only 30 percent, less than one third of the entire surface. We have only a very small part of the Earth to live on.

In the twentieth century, humanity ran into a new problem: lack of land. Now, in the beginning of the third millennium, this problem is becoming serious, with the fast growth of the Earth's population and corresponding expansion of industrial development and urban agglomeration. Countries such as Japan, China, Korea, the Netherlands, and Belgium have a very high population density. Many other countries in Europe and Asia are approaching the same density.

Many developed island countries and countries with long coastlines in need of land have for some time now been successfully reclaiming land from the sea to create

new space and, correspondingly, to ease the pressure on their heavily-used land space. The Netherlands, Japan, Singapore and other countries have expanded their areas significantly through the land reclamation works. Such works are, however, subject to constraints, such as the negative environmental impact on the coastlines of the country and neighbouring countries and marine ecological system, as well as huge economic costs in reclaiming land from deep coastal waters, especially when the sand for reclamation has to be bought from other countries [143 Watanabe et al 2004]. Also, land reclamation is a good solution only for rather shallow waters with a depth of no more than 20 m.

In response to the aforementioned needs and problems, researchers and engineers have proposed an interesting and attractive solution: the construction of floating structures. These offshore structures can be located near the shore as well as rather far into the open sea. They have the following advantages over traditional land reclamation:

- They are easy and fast to construct (components may be made at shipyards and then be transported to and assembled at the site), thus, the sea space can be quickly exploited;
- They can easily be relocated (transported), removed, or expanded;
- They are cost effective when the water depth is large;
- Their construction is not greatly affected by the depth of the water, sea bed profile, etc.;
- Their position with respect to the water surface is constant; hence they can be used for airports, piers, etc.;
- They are environmentally friendly as they do not damage the marine ecological system, or silt up deep harbours or disrupt the ocean/sea currents;
- The structures and people on VLFSs are protected from seismic shocks since the energy is dissipated by the sea.
- The lifetime of floating structures of the proposed concepts is about 100 years (at least 50 years), so the structure can be used for a very long time (with maintenance if any is needed).

Consequently, developing floating structures for all kind of purposes has become more interesting in the past decade since the demand fur such structures increased significantly. They can be constructed to create floating airports, bridges, piers and docks, storage facilities (for instance for oil), wind and solar power plants, for military purposes, to create industrial space, emergency bases, entertainment facilities, recreation parks, mobile offshore structures and even for habitation. Actually, the last could become reality sooner than one may expect: already different concepts have been proposed for building floating cities or huge living complexes. The largest offshore structure built so far is the Mega-Float, a floating runway prototype constructed in Tokyo Bay in the end of year 1999 (Figure 1.1) with the following characteristics: length 1000 m, breadth 60 m (121 m maximum), depth 3 m, draft 1 m, deck area 84,000 m^2, weight of steel materials used 40,000 t, deck strength 6 t in distributed load. It is the world's largest floating object ever built, in particular the largest artificial floating island. Another interesting floating structure is the Yumemai floating bridge, Osaka, Japan, which is shown in figure 1.1. The bridge is a movable floating arch bridge standing on two floating pontoons, which can swing around the pivot with the assistance of tugboats. It has a total length of 940 meters with a floating part length of 410 meters and a width of 38.8 meters for six traffic lanes.

Figure 1.1: floating airport (left), Yumemai floating bridge (right)

Certainly, floating structures can also be used for floating entertainment facilities. Large floating structures (LFS) of different dimensions and design are and can be used for hotels, restaurants, shopping centres, amusement and recreation parks, exhibition centres, theatres, cinemas, fishing piers, etc (Figures 1.2 and 1.3). LFSs having been or being constructed are for example the Aquapolis exhibition centre in Okinawa (1975, already removed), the Floating Island near Onomichi, and another one resembling the Parthenon near Hiroshima, all in Japan, and floating hotels in Australia, Vietnam and North Korea, floating restaurants in Japan, Hong Kong, Russia, Ukraine and other countries. An attractive panoramic view is one of the advantages floating entertainment facilities offer.

Figure 1.2 Floating homes and hotels

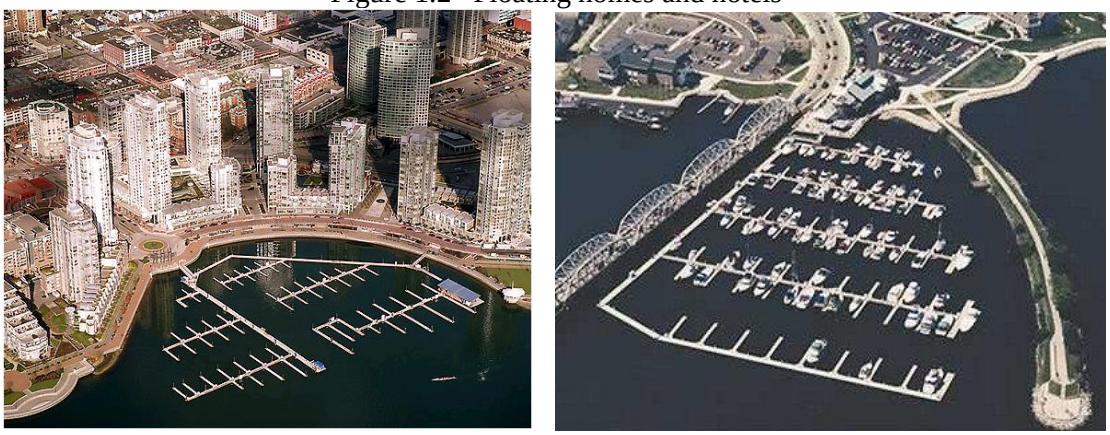

Figure 1.3 Floating marinas and docks

Also, offshore petroleum platforms have been widely spread in the last 30 years, yielding to new applied technologies in such huge floating structures. (Figure 1.4)

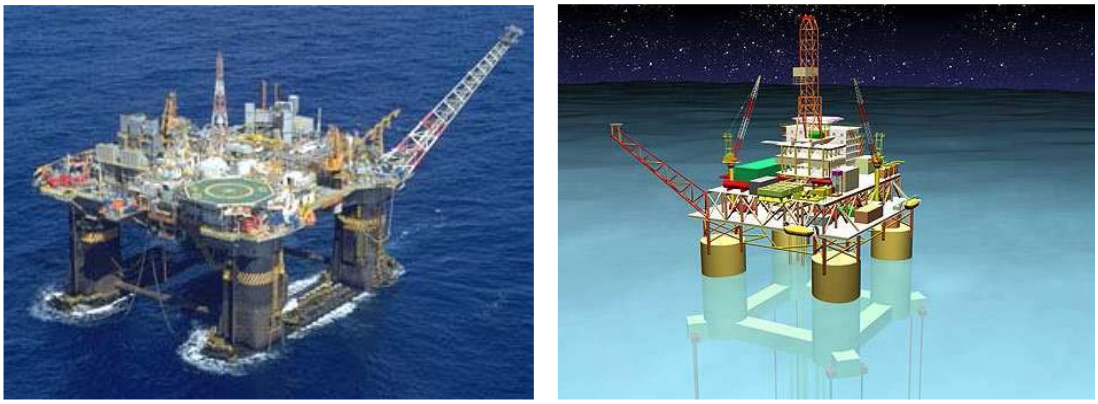

Figure 1.4 Floating Oil Platform, Gulf of Mexico

Another application for floating structures with a military type is the rapidly installed breakwaters (RIB), specifically designed to address problems associated with the efforts of U.S. armed forces to offload ships during Logistics. The RIB system consists of a V-shaped structure in plan view, with rigid vertical curtains extending from the surface of the water toward the bottom for a distance sufficient to preclude excessive wave energy from penetrating beneath the structure. When deployed, the tip of the V is oriented into approaching waves, and works by spreading and reflecting incoming waves. Incident waves are 'trained' away from the interior of the V, providing a sheltered area inside the V and in the lee of the structure. Ships and lighterage are moored in the lee of the V for offloading. (Figure 1.5)

Figure 1.5 RIB used in logistics, US armed forces

In addition to the cited types, an important and viable application of floating structures is floating breakwaters installed in ports to shelter the port area form sea waves. Floating piers have been constructed in Hiroshima, Japan, and Vancouver, Canada. In Valdez, Alaska, a floating pier was designed for berthing the 50000-ton container ships. The main advantage of a floating pier is its constant position with respect to the waterline. Thus, floating piers allow smooth loading and unloading of cargo. Floating docks have been constructed in the USA and other countries. In case of rather deep water, floating structures are a good alternative to traditional harbour facilities. Research on floating harbour facilities, their design and analysis is going on in many countries [Watanabe et al (2004)]. It is an interesting structure in this business from a practical as well as an economical point of view:

- Due to the size of the modern container vessels, it is important to create harbours deep and wide enough able to serve these kinds of vessels.

- The number of harbour calls can be reduced when container terminals can be placed at strategic locations.

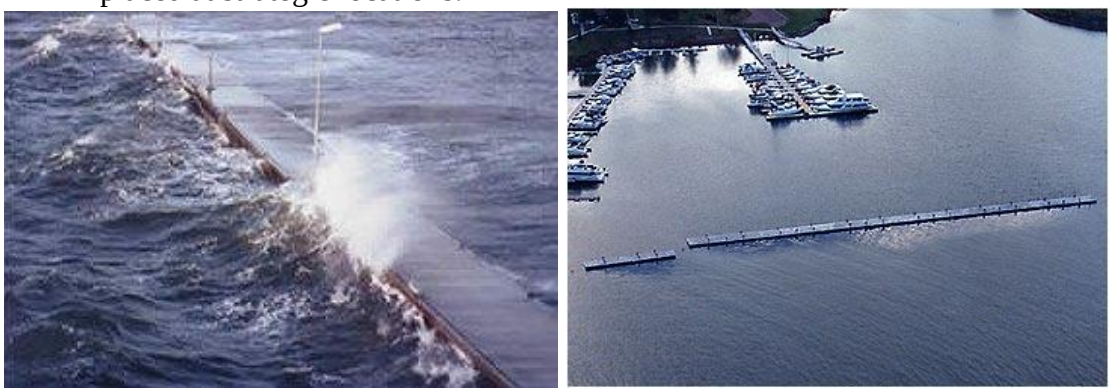

Figure 1.6 Floating breakwaters

From previous studies it appeared that the efficiency of floating harbours is affected by wave attack. A floating breakwater is necessary to increase the efficiency rate and to create a safe haven for vessels when the weather conditions become bad. Thus, we can conclude from the different applications of floating structures, that the floating breakwater is an essential structure mainly used to protect the ports that are increasing their numbers and also their areas due to the developing business and commerce between the countries. Also, it is used as a secondary structure in the projects of floating airports, floating homes, floating hotels, floating oil storage tanks, military logistics, ……etc. Finally, this particular type of floating structures, the floating breakwater, constitutes the topic of this thesis.

1.2- Floating breakwaters

Ever since progressive engineers came up with the idea of creating floating structures into the sea, many studies and model tests were performed to develop a floating breakwater. Although the first engineers used the trial-and-error approach to test their creations (Mr.Thuillard-Froideville in 1884 to protect the harbour of Le Havre), research on this topic professionalized soon after the Second World War. A lot of designs were laboratory tested and checked with numerical calculations. In this section, a short review will be given of the floating breakwaters that have been built and the possibilities for future floating breakwaters. Past model testing will be discussed in this section in order to describe the problems that have been encountered in the past.

1.2.1- Breakwaters in a nutshell

Many coastal activities require protection from waves, and breakwaters are widely used in order to provide such protection. The oldest and most common breakwaters are the bottom founded structures. These generally provide excellent protection from waves. However, they may become uneconomical for large water depths, and limited water circulation behind such breakwaters may lead to problems associated with sedimentation and increased pollutant concentrations within protected areas. Floating breakwaters have proven to be an attractive and economical alternative at locations where water depths are relatively large and the wave climate is not too

severe. They have also been used at locations where temporary or seasonal protection is required.

Since time immemorial, harbours played a deciding role in the extent of prosperity for entire populations. In the early history, naturally sheltered locations (like bays and estuaries) were used as a haven for ships. Soon these sheltered locations, where little wave attack was encountered, became the centres of trade. When the economical importance of harbours increased further more, these harbours became the centres of society as well. Nowadays, space has become very scarce in coastal zones and around harbour areas in particular. However, technological developments made it possible to extend the harbours into the ocean. Often, artificial breakwaters are used to create the sheltered area where harbour activities take place. The primary function of a breakwater is to attenuate waves to an acceptable level or eliminate their effects altogether. It creates a sheltered region in order to prevent damage to shorelines, harbours, and other natural or man-made structures. Although there are several types of breakwater structures, one can roughly distinguish three main types of breakwaters (Figure 1.7), which are:

Conventional (mound) type of breakwaters

Mound types of breakwaters are actually no more than large heaps of loose elements, such as gravel and quarry stone or concrete blocks.

Monolithic type of breakwaters

Monolithic types of breakwaters have a cross section designed in such a way that the structure acts as one solid block. In practice, one may think of a caisson, a block wall, or a masonry structure. Generally this kind of structure is used when space is scarce and local water depths are relatively large.

Composite type of breakwaters

A composite type of breakwater is a combination of the conventional and monolithic type of breakwater. When water depths get larger, this kind of structures is often preferred from an economical point of view.

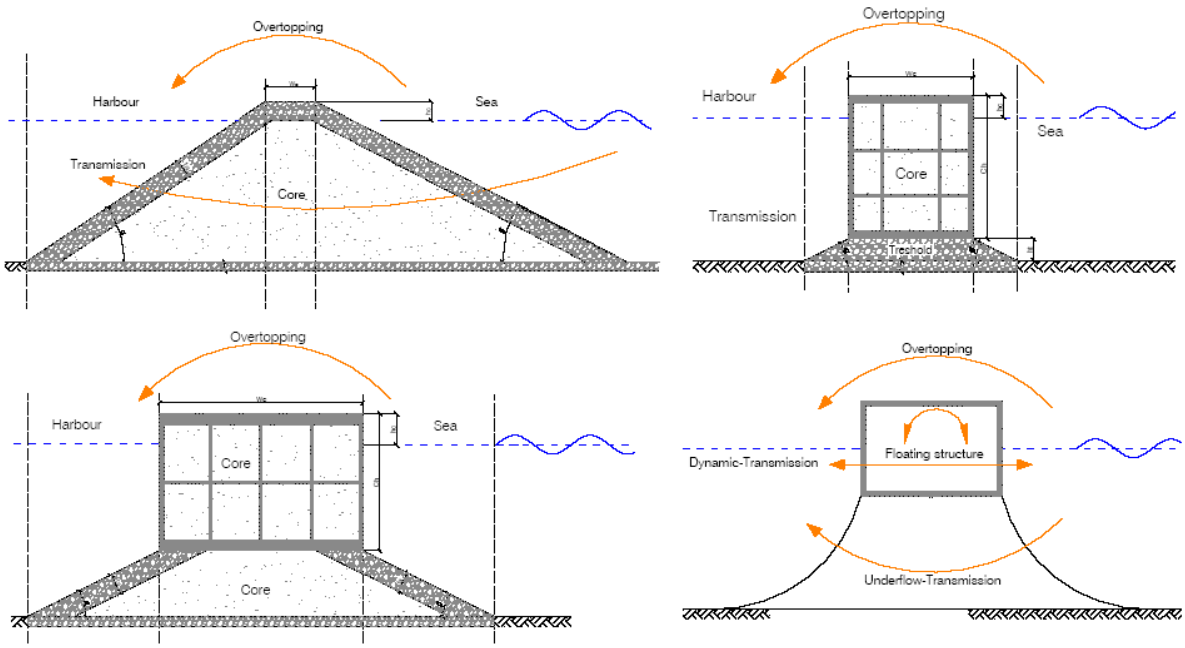

Figure 1.7: Several breakwater structures.
From left to right, top to bottom: Rubble mound breakwater, Caisson breakwater, Composite breakwater, Floating breakwater.

Although the designs of the breakwaters (Figure 1.7) differ form one another, a lot of similarities can be distinguished. They are all built to block the incoming waves and to dissipate or reflect the wave energy. They are all fixed structures, designed for a specific location. Bottom-founded structures are limited to a certain maximum water depth since these structures are impossible in deep water environments from a technical as well as an economical point of view. From a military, a humanitarian, a technical and an economical point of view, a new type of breakwater is needed to overcome the restrictions that are associated with fixed breakwaters. This new type of breakwater has to be rapidly installed, transportable, (re-) usable at several locations with different wave conditions and applicable in deep water areas. Several types of unconventional breakwaters have been developed in the past in order to meet these demands, including the floating breakwater.

Even though a lot of (theoretical and practical) research has been done on a wide variety of floating breakwater concepts, the appliance of floating breakwaters in real situations is very limited. The complex contribution of the dynamic response to the total wave transmission is the main reason for this. This dynamic response makes a floating breakwater only suitable for a small frequency range. Figure 1.7 shows the phenomena that contribute to the two-dimensional wave transmission for several types of breakwaters. In contrast to a normal harbour, where only ship motions occur, a floating harbour will be completely influenced by the wave conditions. Lots of structural and hydraulic factors influence the hydrodynamic behaviour of the different elements in a floating harbour. Determining the relations and the influence of these factors on the wave attenuating capacity of the floating breakwater is thoroughly discussed in this thesis.

1.2.2-Technical and economical arguments

The main reasons to apply unconventional types of breakwaters, and floating breakwaters in particular, are the technical and economic restrictions related to the monolithic and conventional types of breakwaters. Besides these restrictions, there are other arguments that are encouraging the development of floating breakwaters such as the spatial availability, structural limits, and reliability.

Technical arguments
Costs are not the only reason why conventional breakwaters are not preferable when water gets too deep. Local soil conditions and structural stability do also influence the limits of design. A huge structure will result in tremendous pressures on the subsoil as well as stability problems when the slopes become too steep. A floating breakwater can be more feasible in poor soil conditions than a heavy fixed breakwater since the subsoil pressure is virtually non-existent, however, the floating breakwater does have to be anchored to the sea bottom. Floating breakwaters can be easily moved and rearranged due to their transportability, reusability and flexibility in design. Due to this quality, a floating harbour can be adapted and rearranged easily when needed.

Economic arguments
The advantages and disadvantages of the use of floating breakwaters have a common origin: economics. To illustrate this assumption, a construction cost calculation was made to determine the optimal breakwater construction for several water depths. This primary study only involves the construction costs. These constructional costs of the

conventional, the caisson and the composite breakwater are based on the studies done by [Schepers 1998] and [Lenting 2003]. Figure 1.8 shows the relation between construction costs and water depth. In previous reports [d'Angremond 1998], it was already stated that the conventional breakwater, from an economic point of view, will only be preferable until a water depth of around 8m. In depths ranging from 8m to 20m, a caisson breakwater will be the best solution. And after that, up to a depth of 30m, the composite type of breakwater is preferable, which shows agreeable results with Figure 1.8. At this stage, the cost of the floating breakwater is unknown. Since the construction costs of a floating breakwater will hardly increase with increasing depths, the line in the figure will be an almost horizontal line.

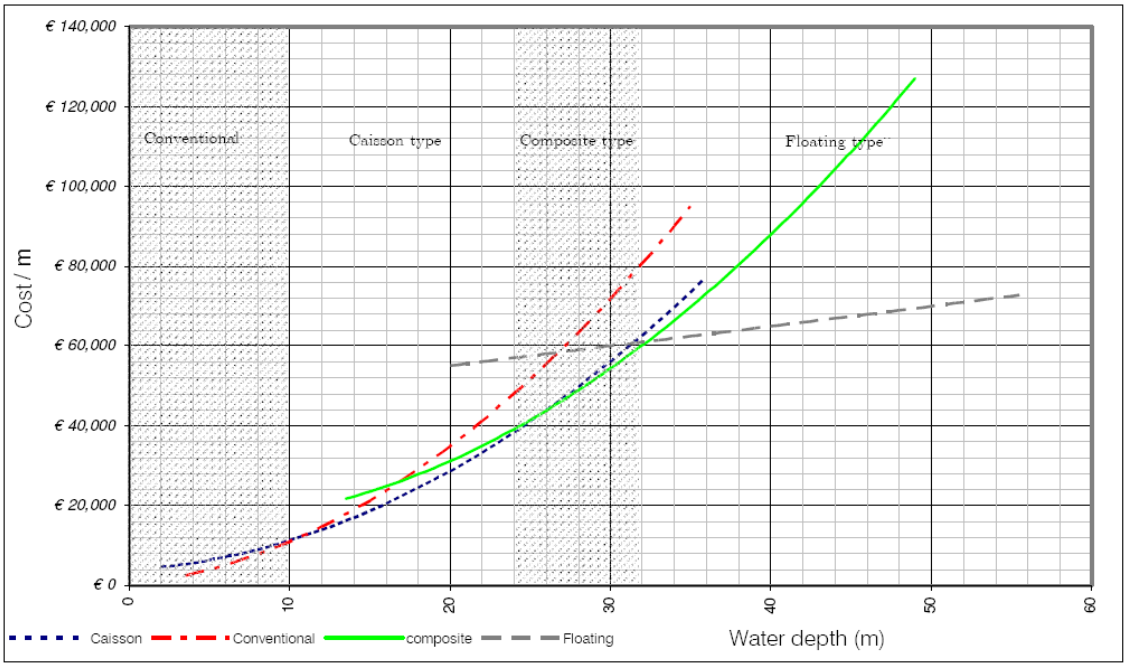

Figure 1.8 Comparison of construction cost /m depending on the water depth.

For real situations, specific site conditions may alter the results drastically. Construction costs depend on the rate of downtime due to wave climate and tidal height conditions. Construction costs are largely depending on the available weather window determined by wave and tidal conditions. Moreover, the feasibility of a caisson solution depends largely on the stability of the foundation and, in particular, the sensitivity of the subsoil to liquefaction.

1.2.3 Past Performance

The development of floating, transportable breakwaters got a real boost when the necessity arose to land men and materials during the Normandy invasion of Wold War II. Two types of breakwaters were used for that purpose. The first types were concrete barges, transported from Great Britain. These barges were positioned just off-shore and were sunken down in order to create a bottom-founded breakwater. The second types of breakwaters were floating structures with a cruciform cross section. These 'Bombardon' floating breakwaters were steel structures arranged in lines along the Normandy coast. The 'Bombardon' floating breakwaters served their purpose during the invasion but failed after 9 days during a storm which created stresses eight times higher than what they were designed for. After this experience, the faith in the reliability of the floating breakwater was gone for many years. In the 1950's, the US

navy saw the potential of these structures to protect small craft and marine structures against open-ocean waves. A manageable, transportable, reusable floating breakwater was investigated that would provide a sheltered environment during several military or humanitarian operations. Serious development of this type of floating breakwater lasted until the 1980's, when several rapidly installed floating breakwaters (RIBS) were tested at full scale. These breakwaters, developed for military purposes were designed to attenuate wave heights in a certain part of the wave spectrum to an acceptable level. Besides the military-orientated floating breakwaters, some commercial breakwaters have been developed as well. Small-structured floating breakwaters, designed to protect small scale marinas against short crested waves, are already in wide use. These kinds of structures are used all around the world in relatively moderate wave conditions. Although these structures are quite successful, the appliance of large-scale floating breakwaters is not yet that common. One of the few interesting examples, designed to defend a large harbour, is the pier extension of Port Hercule in Monaco. In 2002 'La digue semi-flottante' was installed as a pier extension in Monaco, in approximately 55 m of deep water. An enormous caisson, 352 meters long, with a main body 28 m wide, a total depth of 19 m and a draft of 16 m was installed. It is multifunctional and, as a permanent structure, it has to withstand design storm conditions during its expected lifetime of 100 years. The importance of the immerged or the hollow volume appears in constructing 360 parking places over 4 stages and 25 000 m^3 stock capacity over 2 stages (Figure 1.9).

Figure 1.9 Pier extension at Port Hercule, Monaco, France.

Floating breakwaters, as they have been applied in real situations, can be split into three categories:

- Light-weight floating breakwaters which are easy to reuse and to transport. Service times vary from several hours to a couple of days. Example: Rapidly Installed Breakwater System (RIBS) as it is used by the US Navy to load and unload troops into small landing vessels.

- Light-weight floating breakwaters with a semi-permanent character. Service time can take up to 30 years. This type of floating breakwater is very common in small-scale marinas. Example: U-block, which is used to defend several marinas in Greece. The U-block floating breakwater consists of concrete caissons, filled with polystyrene, that are connected to one another by cables. This type of floating breakwater can be transported very easily if wave conditions exceed the design conditions or when it has to be reused at another location.

- Heavy-weight floating breakwaters with a permanent character. Service time can take up to 100 years. This type of floating breakwater is only applied if water depth or soil conditions do not allow a fixed breakwater and the wave conditions are moderate. Example: Monaco semi-floating breakwater. The structural dimensions of this pier extension are of such a level that the structure can cope with the Mediterranean wave spectrum very easily. However, the structure becomes less transportable and reusable due to these structural dimensions.

1.2.4 Possible applications in the near future

In the previous section it became clear that there is a wide range of sources with a maritime origin that emphasize the need to develop a floating breakwater. International container shipping is one of the most dynamic economic sectors of the past few years. Between 1990 and 2005 the container trade at the world's ports expanded by less than 10% on average (Heymann 2006). The expected annual growth of the international container shipping will be around 9% up to 2015. The reason for this growth is twofold. On the demand side, the increasing division of welfare in the world gives a rise in importance of goods, eminently suited to transport by container. Higher efficiency of the loading and unloading processes and the increase in size of container vessels contributed to the growth at the supply side.

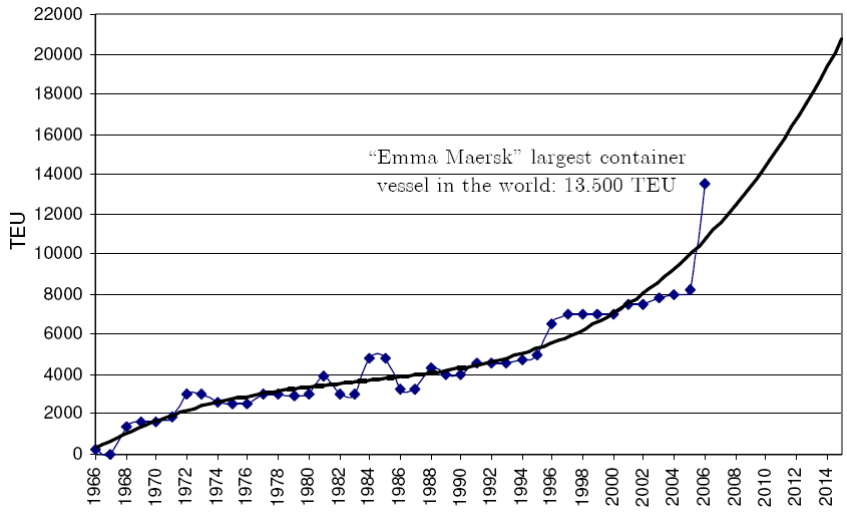

Figure 1.10 Maximum ship size by year of construction (until October 2006).

The increase of container handling in the world makes the development of container terminals necessary. Existing harbours already increased their container handling capacity or transferred their general cargo terminals into container terminals. The introduction of the mega vessel as well as the increasing efficiency of shipping lines demands for deep water container terminals. An increase of efficiency is gained

when container vessels are able to reduce their number of port calls. This is achieved with the 'terminal-feeder' system.

Feeder vessels are container ships with an average capacity of carrying 300-500 TEU (The abbreviation TEU stands for Twenty feet Equivalent Unit. 1 TEU is a 20 ft container). Feeders collect containers from different ports and transport them to central (deep-water) container terminals where they are loaded to bigger vessels. On the way back, the feeders are loaded with other containers that have to be transported to a certain port. Throughout the years so-called feeder lines were created on which ship-owners are transporting containers over a predefined route on a regular basis.

An example of such a terminal-feeder system, and the feeder routes involved with it, is shown in figure 1.11 (European Container Terminals ECT, www.ect.nl). In this case, the terminal is the port of Rotterdam. From Rotterdam, feeder vessels transport the containers to ports all over Europe. The necessity of deep water container terminals, combined with the technical and economical limitations as they were mentioned in the previous section, gave rise to the development of the Floating breakwaters.

Figure 1.11 Container feeder transport system for the port of Rotterdam[9]

1.3-Literature survey

This survey covers books, papers, reports and abstracts that both give the basic theory for wave propagation, diffraction, radiation; and study the interaction between water waves and floating breakwater and the influence of the mooring lines in addition to the structural optimisation. Also, we review what has been done already, what is currently being investigated and the future directions to study for the problem of interaction between the water waves and floating breakwaters.

The numerous publications reported in the offshore structures' conference proceedings, journals, books and websites confirm the interest in and importance of these structures to engineers and scientists. Many papers on the analysis of floating structures were published in the following international journals: Applied Ocean Research, Engineering Structures, Journal of Engineering Mathematics, Journal of

Fluid Mechanics, Journal of Fluids and Structures, Marine Structures, Ocean Engineering, Wave Motion; in the Proceedings of the International Workshops on Water Waves and Floating Bodies (IWWWFB), International Offshore and Polar Engineering Conferences (ISOPE), International Offshore Mechanics and Arctic Engineering Conference (OMAE) and other conferences, workshops and seminars. Also, many publications have been published in non-scientific or scientific-popular journals and newspapers and on the internet. Thus, the attention to and interest in the problems of the behaviour of floating breakwaters in waves has recently increased.

1.3.1 Fluid structure interaction

Fluid-structure interaction is not a new problem of hydrodynamics. In fact, there are two categories of this problem: the interaction between floating structures and water waves, and the interaction between large ice fields and surface waves. Ice-water interaction problems can be solved with the use of the approaches applied for floating structures analysis, using the physical properties of ice instead of those of the structure. The physical understanding and computation of wave–structure interaction, one of the most important hydrodynamic processes in both coastal and offshore engineering, are crucial to assess wave impacts on structures as well as structural responses to wave attacks. Traditionally, the estimation of wave loads on a structure is often done by either empirical approach (ex: Morison equation Sainflou, Hiroi, Goda, Svendson…) or a computational approach. The empirical formulas are simple but crude and will not be able to provide detailed and accurate information about pressure distribution on a structure. The computational approach can be further divided into two types: the Laplace equation solver for potential flows and the Navier–Stokes Equations (NSE) solver for viscous flows, where the latter is used for simulation of wave–structure interaction during which both vortices and turbulence may be present. Solving the Laplace equation by imposing the boundary conditions constitutes the wave modelling part in this study for both analytical and numerical approaches.

Surveys of the design of floating breakwaters include those by Jones (1971), McLaren (198l), McCartney (1985), Werner (1988), and lsaacson (1993a). Comprehensive bibliographies related to analytical formulations and experiences with particular designs have been compiled by Western Canada Hydraulics Laboratory (1981) and Cammaert *et al.* (1994). General design criteria and related considerations relevant to floating docks and small craft harbour facilities have been summarized by Cox (1989), Gaythwaite (1990), the ASCE Ports and Harbours Task Committee (1994), and Tsinker (1995).

1.3.2 Hydrodynamic Analysis

Numerical models of floating breakwater response to waves have originated largely from ship hydrodynamics and reference may be made to Wehausen (1971) and Newman (1977) for the theoretical approaches generally used. In a linear analysis, the structure is assumed rigid and to oscillate harmonically in six degrees of freedom, corresponding to three translational (surge, sway and heave) and three rotational (roll, pitch and yaw) motions. The fluid is assumed incompressible and inviscid and the flow irrotational so that potential theory is used to solve for the fluid flow associated with a specified incident wave motion. The velocity potential relating to the flow is

considered to be made up of components due to the incident waves, scattered waves associated with the structure in its equilibrium position, and forced waves associated with each mode of motion of the floating structure. If the floating breakwater is reasonably long, a two-dimensional analysis may be carried out in place of a three-dimensional analysis. General discussions of potential theory and the hydrodynamics of floating breakwaters are presented in the texts by Sarpkaya and Isaacson (1981), Chakrabarti (1987), Faltinsen (1990) and Rahman (1994).

The hydrodynamic analysis is generally carried out numerically by a wave source method. In a linear analysis, the wave diffraction problem (wave interactions with a fixed structure) and the wave radiation problem (waves generated by an oscillating structure) are uncoupled and may be solved separately. The resulting hydrodynamic forces may then be applied to equations of motion of the structure to determine its motion. As examples of this general approach, Adee (1975) developed a two-dimensional, linear, theoretical model to predict the performance of catamaran type FBWs in deep water and compared the results with measurements in a model tank and from a prototype installation in the field. Yamamoto et al. (1980) solved the problems of wave transformation and motions of elastically moored floating objects by direct use of Green's identity formula, and validated their solutions with experimental investigations. Isaacson and Byres (1988) reported the development of a numerical model, based on linear diffraction theory, to investigate FBW motions, transmission coefficients and mooring forces, in obliquely incident waves. Drimer et al. (1992) presented a simplified analytical model for a floating rectangular breakwater in water of finite depth. Williams (1994) analyzed the Froude–Krylov force coefficients for the case when a rectangular body is located close to the free surface or sea bed based on the linear diffraction theory. Lee (1995) presented an analytical solution to the heave radiation problem of a rectangular structure, and by use of the solution, he calculated the generated waves, added mass, damping coefficients and the hydrodynamic effect of the submergence, width of the structure. Wu et al. (1995) used the eigen function expansion-matching method to analyze the wave-induced responses of an elastic floating plate. Cheong et al. (1996) extended the eigen function expansion method to analyze a submerged platform breakwater.

Hsu and Wu (1997) developed the boundary element method and applied it to study the heave and sway problem in a bounded domain (floating breakwater with a sidewall in the leeward side), which describes the real problem of breakwaters appearing in ports. Williams and Abul-azm (1997) studied the case of a dual pontoon floating breakwater and investigated the effects of the various wave and structural parameters on the efficiency of a dual breakwater. Sannasiraj et al. (1998) adopted a two-dimensional finite element model to study the behaviour of pontoon-type floating breakwaters in beam waves. Also Sannasiraj et al. (2000) used again the finite element method to study the diffraction– radiation of multiple floating structures in directional waves. Williams et al. (2000) investigated the hydrodynamic properties of a pair of long floating pontoon breakwaters of rectangular section. Lee and cho (2003) developed a numerical analysis using the element free Galerkin method and mainly concerning the influence of mooring line condition on the performance of FBWs. Zheng et al (2004) continued the problem of Hsu and Wu, by considering the three modes of radiation and also the diffraction problem. Shen et al (2004) studied the effects of the bottom sill or simply changing the topography on the hydrodynamic and transmission coefficients by a semi analytical method. Loukogeorgaki and Angelides

(2005) focused on a three dimensional modelling of the floating body coupled with a static and dynamic model of the mooring lines. Gesraha (2006) investigated the reflection and transmission of incident waves interacting with long rectangular floating breakwater with two thin sideboards protruding vertically downward, having the shape of the Greek letter ∏.

1.3.3 Mooring Analysis

Apart from a hydrodynamic analysis, the design of moored floating breakwaters also requires a mooring analysis in order to determine motion responses and mooring system loads. Mooring systems are generally made up of uniform cables with or without concentrated loads at various points along each cable. The behaviour of most cables tends to be planar (two dimensional) because of the predominance of dead weight loading on flexible cable segments. A mooring analysis is generally comprised of three steps: (a) the calculation of initial line configuration and equilibrium, (b) a static analysis, and (c) a dynamic analysis. Leonard (1988) has presented the elastic catenary equations and describes a procedure to arrive at principal loads in the initial equilibrium configuration due to the self weight of the line. A static analysis is carried out to obtain the steady offset of the floating breakwater due to wave current and wind loads. This involves the development of a stiffness model of the mooring system about the initial configuration. Various approximate expressions for stiffness are given in Faltinsen (1990). The dynamic response of the breakwater system about its steady displaced position is computed to provide the extreme displacements of the mooring line attachment points, maximum anchor forces, and mooring line tensions. A detailed review of the dynamics of mooring lines with an emphasis on the mechanism of dynamic amplification is given by Triantafyllou (1994).

Several studies have reported on different analysis procedures to obtain the dynamic response of a breakwater. Yamamoto and Takahashi (1974) carried out an experimental study to investigate the influence of various design parameters such as cross-sectional area, moment of inertia, and mooring arrangements on the performance of a floating breakwater. Carver (1979) reported that uncrossing the anchor chains had a negligible effect and adding a vertical barrier-plate has little effect on wave-attenuation characteristics. Yamamoto et al. (1982) developed a two-dimensional model of a floating body with linear elastic springs. They found that if the mooring system is properly arranged, the wave attenuation by a small draft breakwater can be improved several times compared to the same FBW conventionally moored. Yamamato (1982) then applied this model to study floating breakwater response to regular and irregular waves. Skop (1988) solved for the dynamic response of the system by assuming the mooring lines as inertialess springs. Patel (1989) reported that the effects of wave and current loading on mooring lines may be negligible for situations relating to floating breakwaters for which dynamic amplification in the mooring line is small.

1.3.4 Optimisation

Structural optimization is a subject which has attracted the interest of the researches for many years. It refers to the optimal design of the structure under certain loadings, in order to have minimum weight, or uniformly distributed equivalent

stresses or even to control the deflections of the structural components; and is of great importance in structural and mechanical engineering. The optimization procedure is an iterative process in which repeated improvements are carried out over successive designs until the optimal design is acceptable. It is divided into shape and topology optimization. The usual shape optimization procedures start from the given initial design, where the inward or (and) outward boundary of the structure is described and parameterized using a set of simple segments such as straight lines, splines, or nodal coordinates, and the boundary is varied iteratively using the information from the shape design sensitivity to achieve the optimal shape of the structure for a given purpose. On the other side, some of the methods used in determining optimal topology search the optimal values of the densities of finite elements, in which a fixed feasible domain is meshed (homogenisation approaches); in other methods elements are removed from design domain or added to this one, depending on stress values and on the basis of rules. In fact, in many cases it is opportune to perform a shape optimisation just after the topology one (Cappello and Mancuso(2002)), in order to smooth out the rough boundaries obtained in the first step, due to the coincidence of the latter with the discontinuous edges of the elements.

In the analysis procedures of a reliable and effective optimization approach, a problem can be divided into three main tasks. The first step is to represent the changeable geometry of the model during the optimization process. Zienkiewicz and Campbell (1973) defined nodal coordinates of the discrete finite element model as design variables. Yang et al (1992), Chang and Choi (1992), Tortorelli et al (1993) used a set of key points or master nodes to define the geometry entities. Belengundu and Rajan (1988) introduced the natural design method. The geometric modeling can, alternatively, be carried out by using predefined shapes (rectangle, polygon, circle,..), straight lines, Splines: Herskovits et al (2000), Annicchiarico et al (1999), Cerrolaza et al (2000), etc. Secondly, it is necessary to provide a structural analysis technique, which can give sufficiently accurate displacement and stress solutions for the continuous changing boundaries during the optimization process. As well known, great efforts have been devoted to use FEM (Finite Element Method) and BEM (Boundary Element Method) in the structural optimization fields for a long history and these two methods have been applied in various engineering fields: Herskovits and Dias (2000), Holzleitner and Mahmoud (1999), Schleupen et al (2000), Woon & Querin (2001). Mackerle (2003) presented a detailed list of papers on the application of FEM and BEM to topology and shape optimizations from 1999 to 2001. Finally, we must select an appropriate optimization algorithm to achieve the whole optimization process in an effective and reliable way.

There are two types of optimization algorithms mainly, i.e., traditional gradient- based method and stochastic zero-order search method. As demonstrated by the previous investigations the conventional gradient-based optimization techniques are reliable and effective, such as Sequential Quadratic Programming (SQP) (Holzleitner (1999)) and Interior Point Non-linear Programming (Herskovits (2000)). The SQP method, one of numerous methods used in non linear programming (NLP), provides a tool to find the minimum of an objective function which depends on a set of optional free variables and is subjected to arbitrary constraints. In fact, nonlinear programming has many applications in todays engineering practice; particularly in structural design, NLP is successfully used reducing steel weight and cost of marine structures. Among the stochastic zero-order search methods, Genetic Algorithms

(GAs), as a kind of Evolutionary Algorithm represented by Holland, have attracted great attentions from the scientific community as a powerful optimization tool during recent decades. GAs have been successfully used in the structural optimization problems combined with FEM and BEM, and some of the recent works can be found in Cerrolazaa et al (2000), Kovacs and Szabo (2001), Woon et al (2001), Wang and Tai (2005), where they are really recommended to be used especially in topology optimization where there are no available data on the possible solution. The main interest of stochastic methods in engineering sciences is to break the limits of the standard deterministic methods in many optimization problems: when the search space involves both discrete and continuous domains; when the objective function or the constraints lack regularity; or when the objective function admits a huge number of local optima. Therefore, GA is able not only to improve the solution close to a local optimum, but also to explore a larger extension of the design space and to direct the search toward relatively prospective regions in the search space.

1.4-Problem definition & objectives

1.4.1 General

A floating breakwater is not a real breakwater. In fact, this simple but on the other hand complex statement contains the whole floating breakwater problem. A conventional, fixed breakwater reflects and absorbs the wave energy in order to create a sheltered area behind it. A floating breakwater on the other hand, reflects and generates wave energy in order to obtain the same results as the fixed breakwater. In other words: the fixed breakwater tries to diminish the energy of the incoming wave, while the floating breakwater uses this same incoming wave to generate anti-waves. The main problem of this whole thesis is how to create an area where harbour activities can take place in deep, unprotected water conditions. The problems that have to be solved, the objectives of this research, and the methodology of modelling and optimising the floating breakwater, are discussed in this chapter.

1.4.2 Objectives

A floating structure has to be developed that is capable of attenuating the incoming waves to such a level that a floating harbour can become an efficient alternative. The dynamic behaviour of floating structures in waves depends on a lot of factors. It is important to understand the effect of the hydrodynamic as well as the structural factors that are involved. With this knowledge, a model can be created to state the optimal structural dimensions at severe wave conditions. The model can be used as a design tool to determine a theoretical-based design. The main objective of this thesis is therefore twofold:

- Determine the influence of the several structural elements on the dynamic behaviour of the floating breakwater and create a model that proves the influence of these elements.
- Create an optimal constructional design, based on this model to prove that a floating breakwater is possible from a constructive point of view.

Although many studies were performed to determine the performance of floating breakwaters with various designs and with mild wave environment conditions, yet

none of these studies have been discussing their structural design or more even optimizing its shape and topology. On the other hand, optimization of fixed breakwaters has been previously discussed by Ryu et al (2005) but focused on minimizing the cost function imposed to structural failure constraints, and also by Castillo et al (2006) for composite breakwater types and similarly concerning the minimization of initial/construction costs subjected to yearly failure rate bounds for failure modes. Therefore, in this thesis the study is directed towards optimization of floating breakwaters to reduce its weight, or to represent a new resistive form capable of attenuating strong waves and surviving in difficult environmental conditions, in accordance to the physical and mechanical constraints to satisfy the port demands.

It is noticed that applications related to hydrodynamic aspects of marine structures are rarely reported. This may result from several severe problems related to the hydrodynamic analysis and evaluation of such structures and mainly summarized in the difficulty of hydrodynamic analysis for their arbitrarily shapes. Nevertheless, there is some work spent on shape optimization in ocean field but for offshore structures only. For example, Akagi & Ito (1984) optimized the heave motion of a hydrodynamic transparent semi submersible using a quadratic programming technique, Kagemoto (1992) optimized the arrangement of vertical floating cylinders in waves, Clauss & Birk (1996) focused on hydrodynamic shape optimization for large offshore structures (oil platforms) based on non linear programming algorithms.

Another novelty in our work appears in the fluid domain definition that approaches the reality in ports. From the researches of the scholars above, we find most of them focus attention on floating structures oscillation with periodic motion on water surface of deep water with unbounded domain, and almost very few researches attempt to study the problem of floating structures oscillation on water surface of finite deep water and one side of the boundary with vertical sidewall; which assimilates a real practical model for port sites. When a ship is parked in the port, the waves are reflected due to a vertical sidewall. So it is different to the problems of structures oscillation on water surface with unbounded domain. In fact, this constitutes advanced steps for the previous studies, where Zheng et al (2004) have developed only an analytical solution for a freely floating breakwater, and did not continue their study to compromise the effect of the diffraction problem, neither the effect of the mooring lines stiffness and their angle of inclination. But, they limited their study on the influence of structural parameters on the hydrodynamic coefficients only; where the diffraction seems to play an important factor in magnifying the resonant peaks beside the wave's radiation in the bounded domain. Moreover, neither Zheng et al (2004) nor Hsu and Wu (1997) have analyzed the dynamic motion of the breakwater.

1.4.3 Problem Methodology

In order to take into account wave interaction with floating breakwaters we formulate a multidisciplinary problem, where a combination of fluid mechanics, dynamic behaviour of mechanical systems, the vibration theory, and the structural mechanics (mechanical resistance) are introduced to perform a complete analysis capable to develop a representative design of the structure. The interference of these phenomena together with resonance bands occurring in the port side due to the reflective sidewall, and the influence of the structural parameters on the performance

of breakwaters causing mass variation and hence affecting the natural frequencies; demonstrate the complexity of a floating breakwater design, and yields to orient the problem towards an optimization approach that can consider all the relevant consequences together. Therefore, due to the complexity and the interference of these phenomena, the problem is carried out on two stages. The first one eliminates the dynamic behaviour of the floating structure by considering small or negligible oscillations; while the second part develops a complete and thorough formulation of the floating breakwater.

The methodology followed in the fist part is identified by an analytical modelling of waves and their induced pressures on the floating breakwater. After this, physical and mechanical constraints concerning the floating breakwater are imposed to be introduced in the optimization problem. Concerning the optimization procedure, three different methods are elaborated considering the shape and topology. The first method concerns the optimization with a predefined rectangular geometrical shape based on the SQP method, which constitutes a direct approach in the optimization world. This can be done only if the type of the problem permits to create a prospective image for the final shape. The second, concerns topology optimization based on element extraction using genetic algorithms; where topology generates the optimal shape of a mechanical structure by representing a new mass distribution. We built this method on the density distribution process of the discretized domain, and then each element is reserved or removed due to its relative value in the density vector that represents the design variable vector in the GA. We have elaborated a new contribution in this field, where two types of triangular meshes were used. One for indicating the number of variables in the optimization problem, and another refined mesh used for Finite element computations. Thus, we can use very fine meshes without affecting the scale of the general problem.

The third method constitutes a new idea in this field mainly relating topology and shape optimization under a single algorithm by using a variable number of points which create an arbitrary initial valid domain. The coordinates of these points represent the variables for the optimization problem, by this way it is possible to enlarge or extend the expected solution due the achieved shape by connecting multiple points without any restriction to their motion. In other words, a limited number of points (4,7,..) yields the topological representation of the problem, while increasing the number of these points (10,15,20….) will surely yields to smooth the rough surfaces and donates an optimal shape design. This work compose a new evolution in two subjects: the first by combining the shape and topology optimization in one algorithm and the other by widening the usage of points coordinates in the optimization domain; where previous methods (Zienkiewicz and Campbell (1973), Cappello et al (2002)) select key points from existing geometries or some nodal points deduced from the meshing procedure of this existing geometry to constitute the design variables of the optimization. Finally, a comparison between these methods is performed to demonstrate the capability of this approach in optimization among the previous methods.

In the second part, the simulation of the floating breakwater performance is complicated by the importance of the mutual interaction between fluid and rigid body. Indeed its displacement is caused by the wave load and the wave propagation is influenced in turn by the floating breakwater kinematics, so that the most interesting

phenomenon, the wave transmission, can only be found if the fully coupled interaction problem is solved. Thus, the fluid flow can be described by a potential which is the sum of an incident, scattered, and radiated fields. The advantage of this decomposition is that the diffraction (scattering) hydrodynamic problem does not involve the floating breakwater dynamics and can be solved first. The radiation hydrodynamic problem, describing the effect of a forced motion, is solved separately. The actual periodic motion of the structure is solved at last by an analytical vibrational model, deriving the hydrodynamic forces from the diffraction problem and the added mass and damping from the radiated potential. This composes a comprehensive study of the sea waves-breakwater interaction, and is capable to implicate the wave height in the fluid domain and especially inside the port region. Second, the optimization problem is introduced by an objective function and its relevant imposed constraints. These latter are enumerated by the floating condition, stability, minimum wave height in the port, and the mechanical resistance. The last constraint demands a finite element formulation to compute the mechanical constraints; while, the wave height constraint is derived from the hydrodynamic problem in the first part. All these constraints are expressed in terms of the geometrical parameters of the design shape, in order to be introduced into the optimization problem. Therefore, we have to solve three main models for each iteration of the optimization procedure:

1-Fluid Mechanics 2-Dynamic Motion 3- Mechanical Resistance

Moreover, the resonance phenomenon plays an important role in such problems, where a structure oscillating in presence of an incoming wave that has its own periodic frequency may enter the resonance bands, and destructive results appear. Then, it must be clear that we are facing two sources of resonance, one being represented by any coincidence between the oscillating frequency of the structure and that of the wave; where the other kind is the wave itself inside the port region. In presence of the sidewall, that really describes a real port problem, it seems to create a bounded domain from the port side or simply an enclosed area. Thus, any wave may be forced to resonance in port side due to specific value of the clearance distance between the sidewall and the breakwater.

For the problem of fluid-structure interaction, it is interesting to consider in the whole thesis the case of a breakwater appearing in ports far from the shore, at a constant depth, and at a fixed point. Then, the problems of waves' propagation over a varying bathymetry and shallow water consequences are eliminated.

Finally, the structure of the report is as follows:

Chapter 2: A short overview of the numerical tools used in modelling and optimisation.

Chapter 3: Analytical and numerical modelling of the sea waves. Dynamical modelling of the floating breakwater. Evaluation and structural parametrical analysis. Analytical and numerical modelling of the mechanical behaviour of the floating breakwater.

Chapter 4: Various methods for shape and topology optimisation of floating breakwaters. Assumptions, calculations parameters and evaluation of the results.

Finally, conclusions will be drawn and recommendations on further research will be given.

Chapter 2

Numerical Tools

This chapter presents the general theory of the numerical tools utilised in the modelling and optimization of floating breakwaters. The first section considers the numerical modelling using the finite element method. It is applied for both wave (fluid) and breakwater (structure) models. The second section illustrates the basics of the optimization algorithms and methods. It covers the deterministic and stochastic methods with some examples to clarify the mathematical formulation of the algorithms.

2.1 General

Engineering consists of a number of well established activities, including analysis, design, fabrication, sales, research, and the development of systems. The process of designing and fabricating systems has been developed over centuries. The existence of many complex and multidisciplinary systems, such as floating breakwaters, ships, bridges, automobiles, airplanes, space vehicles, and others, is an excellent testimonial for this process. However, the evolution of these systems has been slow. The entire process has been both time-consuming and costly, requiring substantial human and material resources. Therefore, the procedure has been to design, fabricate, and use the system regardless of whether it was the best one. Improved systems were designed only after a substantial investment had been recovered. These new systems performed the same or even more tasks, cost less, and were more efficient; where several systems can usually accomplish the same task, and that some are better than others.

The design of complex systems requires data processing and a large number of calculations. In the recent past, a revolution in computer technology and numerical computations has taken place. Today's computers can perform complex calculations and process large amounts of data rapidly. The engineering design and optimization processes benefit greatly from this revolution because they require a large number of calculations. Better systems can now be designed by analyzing and optimizing various

options in a short time. This is highly desirable because better designed systems cost less, have more capability, and are easy to maintain and operate.

The design of systems can be formulated as problems of optimization in which a measure of performance is to be optimized while satisfying all constraints. Many numerical methods of optimization have been developed and used to design better systems. Any problem in which certain parameters need to be determined to satisfy constraints can be formulated as an optimization problem. Therefore, the optimization techniques are quite general, having a wide range of applicability in diverse fields.

In fact, it is a challenge for engineers and scientists to design efficient and cost-effective systems without compromising the integrity of the system. The conventional design process depends on the designer's intuition, experience, and skill. This presence of a human element can sometimes lead to erroneous results in the synthesis of complex systems. Scarcity and the need for efficiency in today's competitive world have forced engineers to evince greater interest in economical and better designs. The computer-aided design optimization process can help in this regard. The main advantage in the conventional design process is that the designer's experience and intuition can be used in making conceptual changes in the system or to make additional specifications in the procedure. For example, the designer can choose the type and the shape of the structure, add or delete certain components of it, and so on. But, when it comes to detailed design, however, the conventional design process has some disadvantages. These include the treatment of complex constraints (such as limits on vibration frequencies) as well as inputs (for example, when the structure is subjected to a variety of loading conditions). In these cases, the designer would find it difficult to decide whether to increase or decrease the size of a particular structural element to satisfy the constraints. Furthermore, the conventional design process can lead to uneconomical designs and can involve a lot of calendar time. The optimum design process forces the designer to identify explicitly a set of design variables, an objective function to be optimized, and the constraint functions for the system. Proper mathematical formulation of the design problem is a key to good solutions. First it starts by a real and comprehensive modelling of the system, and then it moves forward towards imposing an optimization problem

2.2 Numerical Modelling

The numerical analysis of the mechanical and dynamical behaviour of the floating breakwater is based on the finite element method (FEM) using the software Matlab. In fact, Matlab solve the problems of (FEM) under the partial differential equations toolbox (PDE Tool). The elliptic equation, one of the various types of differential equations, satisfies the requirements of the mechanical and dynamical problem. Thus, the attention in this section is concentrated on the specific type of partial differential equations summarized by the elliptic form.

The solutions of simple PDEs on complicated geometries can rarely be expressed in terms of elementary functions. You are confronted with two problems: First we need to describe a complicated geometry and generate a mesh on it. Then we need to discretize the PDE on the mesh and build an equation for the discrete approximation of the solution. Then, the mesh structures and the discretization functions can be accessed and incorporated into specialized applications.
The basic elliptic equation is represented as follows: (expressed in Ω).

$$-\nabla.(c\nabla u)+a.u=f \qquad (2.1)$$

where Ω is a bounded domain in the plane. c, a, f and the unknown solution u are complex functions defined on Ω. The boundary conditions specify a combination of u and its normal derivative on the boundary. We can differentiate three types of boundary conditions:

Dirichlet: $h.u=r$ on the boundary Ω

Newmann: $\vec{n}.(c\nabla u)+q.u=g$ on $\partial\Omega$

Mixed: Only applicable to *systems*. A combination of Dirichlet and generalized Neumann.

where $\partial\Omega$ is the boundary of Ω, $\vec{n}$ is the outward unit normal. $q, g, h, g,$and r are functions defined on $\partial\Omega$.

The approximate solution to the elliptic PDE is found in three steps:
1- Describe the geometry of the domain Ω and the boundary conditions.
2- Build a triangular mesh on the domain Ω. A mesh is described by three matrices of fixed format that contain information about the mesh points, the boundary segments, and the triangles.
3-Discretize the PDE and the boundary conditions to obtain a linear system $Ku = F$. The unknown vector u contains the values of the approximate solution at the mesh points, the matrix K is assembled from the coefficients c, a, h, and q and the right-hand side F contains, essentially, averages of f around each mesh point and contributions from g. Once the matrices K and F are assembled, the required information is at our disposal to solve the linear system and further process the solution.

Starting with the boundary conditions and without restricting the generality, we assume generalized Neumann conditions on the whole boundary. Since Dirichlet conditions can be approximated by generalized Neumann conditions. In the simple case of a unit matrix h, setting $g=q.r$ and then letting $q\to\infty$ yields the Dirichlet condition because division with a very large q cancels the normal derivative terms.

Assume that u is a solution of the differential equation. Multiply the equation with an arbitrary test function v and integrate on Ω:

$$\int_{\Omega}\left(-\nabla.(c\nabla u).v + a.u.v\right).dx = \int_{\Omega} f.v.dx \tag{2.2}$$

Integrate by parts (i.e., use Green's formula) to obtain

$$\int_{\Omega}\left((c\nabla u)\nabla v + a.u.v\right).dx - \int_{\partial\Omega}\vec{n}.(c\nabla u)v.ds = \int_{\Omega} f.v.dx \tag{2.3}$$

The boundary integral can be replaced by the boundary condition:

$$\int_{\Omega}\left((c\nabla u)\nabla v + a.u.v\right).dx - \int_{\partial\Omega}\left(-q.u + g\right)v.ds = \int_{\Omega} f.v.dx \tag{2.4}$$

Replace the original problem with find u such that:

$$\int_{\Omega}\left((c\nabla u)\nabla v + a.u.v - f.v\right)dx - \int_{\partial\Omega}\left(-q.u + g\right)v.ds = 0 \tag{2.5}$$

This equation is called the variational, or weak, form of the differential equation. Obviously, any solution of the differential equation is also a solution of the variational problem. The reverse is true under some restrictions on the domain and on the coefficient functions. The solution of the variational problem is also called the weak solution of the differential equation.

The solution u and the test functions v belong to some function space V. The next step is to choose an N_p dimensional subspace $V_{N_p} \subset V$. Project the weak form of the differential equation onto a finite-dimensional function space simply means requesting u and v to lie in V_{N_p} rather than V. The solution of the finite dimensional problem turns out to be the element of V_{N_p} that lies closest to the weak solution when measured in the energy norm. Convergence is guaranteed if the space V_{N_p} tends to V as $N_p \to \infty$. Since the differential operator is linear, we demand that the variational equation is satisfied for N_p test-functions ϕ_i that form a basis, i.e,

$$\int_{\Omega}\left((c\nabla u)\nabla\phi_i + a.u.\phi_i - f.\phi_i\right)dx - \int_{\partial\Omega}\left(-q.u + g\right)\phi_i ds = 0 \ , \quad i = 1,.....,N_p \tag{2.6}$$

Expand u in the same basis of V_{N_p}

$$u(x) = \sum_{j=1}^{Np} U_j \phi_j(x) \tag{2.7}$$

And obtain the system of equations:

$$\sum_{j=1}^{Np}\left(\int_{\Omega}\left((c\nabla\phi_j)\nabla\phi_i + a.\phi_j.\phi_i\right)dx + \int_{\partial\Omega} q.\phi_j.\phi_i ds\right)U_j = \int_{\Omega} f.\phi_i.dx + \int_{\partial\Omega} g.\phi_j.ds$$

$$i = 1,.....,N_p \tag{2.8}$$

Using the following notations:

$$K_{i,j} = \int_{\Omega}\left(c\nabla\phi_j\right).\nabla\phi_i.dx \tag{2.9}$$

$$M_{i,j} = \int_{\Omega} a\phi_j\phi_i dx \tag{2.10}$$

$$Q_{i,j} = \int_{\partial\Omega} q\phi_j\phi_i ds \tag{2.11}$$

$$F_i = \int_\Omega f\phi_i dx \tag{2.12}$$

$$G_i = \int_{\partial\Omega} g\phi_i ds \tag{2.13}$$

and rewrite the system in the form $(K + M + Q)U = F + G$.
K, M, and Q are N_p-by-N_p matrices, and F and G are N_p-vectors. When it is not necessary to distinguish K, M, and Q or F and G, we collapse the notations to $KU = F$.

When the problem is *self-adjoint* and *elliptic* in the usual mathematical sense, the matrix $K + M + Q$ becomes symmetric and positive definite. Many common problems have these characteristics, most notably those that can also be formulated as minimization problems. For the case of a scalar equation, K, M, and Q are obviously symmetric. If $c(x) \geq \delta > 0$, $a(x) \geq 0$ and $q(x) \geq 0$ with $q(x) > 0$ on some part of $\partial\Omega$, then, if $U \neq 0$.

$$U^T(K + M + Q)U = \int_\Omega \left(c|\nabla u|^2 + au^2\right)dx + \int_{\partial\Omega} qu^2 ds > 0 \qquad \text{if } U \neq 0 \tag{2.14}$$

$U^T(K + M + Q)U$ is the *energy norm*. There are many choices of the test-function spaces. The toolbox uses continuous functions that are linear on each triangle of the mesh. Piecewise linearity guarantees that the integrals defining the stiffness matrix K exist. Projection onto V_{N_p} is nothing more than linear interpolation, and the evaluation of the solution inside a triangle is done just in terms of the nodal values. If the mesh is uniformly refined , V_{N_p} approximates the set of smooth functions on Ω.

A suitable basis V_{N_p} for is the set of "tent" or "hat" functions ϕ_i. These are linear on each triangle and take the value 0 at all nodes x_j except for x_i. Requesting $\phi_i(x_i) = 1$ yields the very pleasant property

$$u(x_i) = \sum_{j=1}^{Np} U_j \phi_j(x_i) = U_i \tag{2.15}$$

That is, by solving the FEM system we obtain the nodal values of the approximate solution. Finally note that the basis function i vanishes on all the triangles that do not contain the node x_i. The immediate consequence is that the integrals appearing in $K_{i,j}$, $M_{i,j}$, $Q_{i,j}$, F_i and G_i only need to be computed on the triangles that contain the node x_i. Secondly, it means that $K_{i,j}$ and $M_{i,j}$ are zero unless x_i and x_j are vertices of the same triangle and thus K and M are very sparse matrices. Their sparse structure depends on the ordering of the indices of the mesh points.

The integrals in the FEM matrices are computed by adding the contributions from each triangle to the corresponding entries (i.e., only if the corresponding mesh point is a vertex of the triangle). The assembling routines scan the triangles of the mesh. For each triangle they compute the so-called local matrices and add their components to the correct positions in the sparse matrices or vectors. (The local 3-by-3 matrices contain the integrals evaluated only on the current triangle. The coefficients are assumed constant on the triangle and they are evaluated only in the triangle barycentre.) The integrals are computed using the mid-point rule. This approximation is optimal since it has the same order of accuracy as the piecewise

linear interpolation. Consider a triangle given by the nodes P_1, P_2, and P_3 as in the following figure.

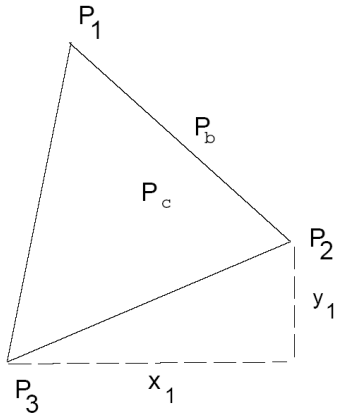

The simplest computations are for the local mass matrix *m*:

$$m_{i,j} = \int_{\nabla P_1P_2P_3} a(P_c)\phi_i(x)\phi_j(x)dx = a(P_c)\frac{area(\Delta P_1P_2P_3)}{12}\left(1+\delta_{i,j}\right) \qquad (2.16)$$

Where P_c is the centre of mass of $\Delta P_1P_2P_3$, i.e,

$$P_c = \frac{P_1+P_2+P_3}{3}$$

The contribution to the right side *F* is just:

$$f_i = f(P_c)\frac{area(\Delta P_1P_2P_3)}{3} \qquad (2.17)$$

For the local stiffness matrix we have to evaluate the gradients of the basis functions that do not vanish on $P_1P_2P_3$. Since the basis functions are linear on the triangle $P_1P_2P_3$, the gradients are constants. Denote the basis functions $\phi_1, \phi_2,$ and ϕ_3 such that $\phi(P_i)=1$. If $P_2 - P_3 = [x_1, y_1]^T$ then we have that

$$\nabla\phi 1 = \frac{1}{2area(\Delta P_1P_2P_3)}\begin{bmatrix} y_1 \\ -x_1 \end{bmatrix} \qquad (2.18)$$

And after integration (taking c as a constant matrix on the triangle)

$$k_{i,j} = \frac{1}{4area(\Delta P_1P_2P_3)}\begin{bmatrix} y_j, -x_j \end{bmatrix} c(P_c)\begin{bmatrix} y_1 \\ -x_1 \end{bmatrix} \qquad (2.19)$$

The toolbox can also handle systems of *N* partial differential equations over the domain Ω, where the elliptic system is expressed by:

$$-\nabla.(\underline{c}\otimes\nabla u) + \underline{a}u = f \qquad (2.20)$$

Where $\underline{c}$ is a 2-by-2 matrix function on Ω

A direct application of the elliptic equation is the mechanical and dynamical equations of the floating breakwater. For example, in structural mechanics the main problem is concentrated in solving the equilibrium equation $\vec{div}\,\sigma + \vec{f}_v = \vec{0}$ in a determined structural domain exposed to different boundary loadings (forces and displacements). To solve this classical equilibrium equation under the elliptic family of equations, the

elliptic coefficients *u, c, a ,f* are defined in terms of their equivalence substitutes in a mechanical problem.

The second basic partial differential equation in this thesis is the Laplace equation describing the wave propagation through the diffraction and radiation theory yielding to study the dynamical behaviour of the floating breakwater. For the wave modelling problem, the state of the fluid can be completely described by the velocity potential. The time independent complex of the latter $\Phi(x,z)$ satisfies the Laplace equation.

$$\nabla^2\Phi(x,z)=0$$

Thus, this simplified form of the elliptic equation is expressed by substituting the elliptic coefficients by their relevant values from the Laplace equation: $c=1$, $a=0$, $f=0$, and the *u* represents the velocity potential of waves.

After defining the elliptic system of both equations, boundary conditions are required to solve the numerical problem.

2.3 Optimization

2.3.1-General:

This section describes the basic concepts of optimization methods and their applications to the design of engineering systems. Optimization theory, numerical methods, and modern computer software can be used as tools to improve the performance of these systems.

The foregoing distinction between the conventional and optimum design indicates that the conventional design process is less formal. An objective function that measures the performance of the system is not identified. Trend information is not calculated to make design decisions for improvement of the system. Most decisions are made based on the designer's experience and intuition. In contrast, the optimization process is more formal, using trend information to make decisions. However, the optimization process can substantially benefit from the designer's experience and intuition in formulating the problem and identifying the critical constraints. Thus, the best approach would be an optimum design process that is aided by the designer's interaction. There are mainly two types of optimization algorithms, i.e., gradient- based method (deterministic methods) and stochastic search method (Genetic Algorithms).

2.3.2 Deterministic Methods

Optimization techniques are used to find a set of design parameters, $x = \{x_1, x_2, ...x_n\}$, that can in some way be defined as optimal. In a simple case this might be the minimization or maximization of some system characteristic that is dependent on x. In a more advanced formulation the objective function, $f(x)$, to be minimized or maximized, might be subject to constraints in the form of equality constraints, $C_i(x) = 0$, $i = 1, ..., m_e$; inequality constraints, $C_i(x) \le 0$, $i = m_e + 1, ..., m$; and/or parameter bounds, x_l, x_u

A General Problem (GP) description is stated as:

$$\underset{x}{Minimize} \quad f(x)$$

Subject to

$$C_i(x) = 0, \ i = 1, ..., m_e$$
$$C_i(x) \le 0, \ i = m_e + 1, ..., m \qquad (2.21)$$

where x is the vector of length n design parameters, $f(x)$ is the objective function, which returns a scalar value, and the vector function $C(x)$ returns a vector of length m containing the values of the equality and inequality constraints evaluated at x.

An efficient and accurate solution to this problem depends not only on the size of the problem in terms of the number of constraints and design variables but also on characteristics of the objective function and constraints. When both the objective function and the constraints are linear functions of the design variable, the problem is

known as a Linear Programming (LP) problem. Quadratic Programming (QP) concerns the minimization or maximization of a quadratic objective function that is linearly constrained. For both the LP and QP problems, reliable solution procedures are readily available. More difficult to solve is the Nonlinear Programming (NP) problem in which the objective function and constraints can be nonlinear functions of the design variables. Numerical methods for nonlinear optimization problems are needed because the analytical methods for solving some of the problems are too cumbersome to use. There are two basic reasons why the methods are inappropriate for many engineering design problems:

1. The numbers of design variables and constraints can be large. In that case, the necessary conditions give a large number of nonlinear equations, which can be difficult to solve. Numerical methods must be used to find solutions of such equations in any case. Therefore it is appropriate to use the numerical methods directly to solve the optimization problems. Even if the problem is not large, these equations can be highly nonlinear and cannot be solved in a closed form.

2. In many engineering applications, cost and/or constraint functions are implicit functions of the design variables; that is, explicit functional forms in terms of the independent variables are not known. These functions cannot be treated easily in the analytical methods for solution of optimality conditions.

For these reasons, we must develop systematic numerical approaches for the optimum design of engineering systems. In such approaches, we estimate an initial design and improve it until optimality conditions are satisfied. Many numerical methods have been developed for NLP (Non Linear Programming) problems. Some are better than others and research in the area continues to develop still better techniques. Detailed derivations and theory of various methods are beyond the scope of the present text. However, it is important to understand a few basic concepts, ideas, and procedures that are used in most algorithms for unconstrained and constrained optimization.

Many numerical solution methods are described by the following iterative prescription:

$x^{(k+1)} = x^{(k)} + \Delta x^{(k)}$

The change in design $\Delta x^{(k)}$ is further decomposed into two parts:

$\Delta x^{(k)} = \alpha_k d^{(k)}$

$d^{(k)}$ the search direction in the design space

α_k step size (positive scalar) in that direction

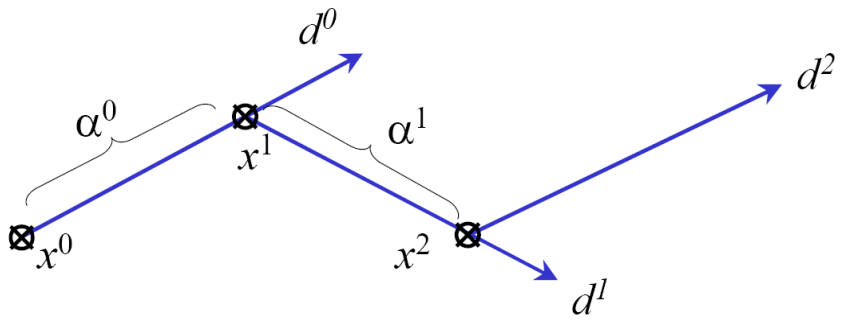

Fig 2.2 Conceptual diagram for iterative steps of an optimization method

In summary, the basic idea of numerical methods for nonlinear optimization problems is to start with a reasonable estimate for the optimum design. Cost and constraint functions and their derivatives are evaluated at that point. Based on them, the design is moved to a new point. The process is continued until either optimality conditions or some other stopping criteria are met. This iterative process represents an organized search through the design space for points that represent local minima. Thus, the procedures are often called the search techniques or direct methods of optimization. The iterative process is summarized as a general algorithm that is applicable to both constrained and unconstrained problems:

Step 1: Estimate a reasonable starting design $x^{(0)}$. Set the iteration counter $k = 0$.

Step 2: Compute a search direction $d^{(k)}$ in the design space. This calculation generally requires a cost function value and its gradient for unconstrained problems and, in addition, constraint functions and their gradients for constrained problems.

Step 3: Check for convergence of the algorithm. If it has converged, stop; otherwise, continue.

Step 4: Calculate a positive step size α_k in the direction $d^{(k)}$.

Step 5: Update the design as follows, set $k = k + 1$ and go to Step 2:
$x^{(k+1)} = x^{(k)} + \alpha_k d^{(k)}$
In the remaining sections of this chapter, we shall present some methods for calculating the step size α_k and the search direction $d^{(k)}$ for unconstrained and constrained optimization problems.

A-Unconstrained optimization

Although a wide spectrum of methods exists for unconstrained optimization, methods can be broadly categorized in terms of the derivative information that is, or is not, used. Search methods that use only function evaluations (e.g., the simplex search of Nelder and Mead 1965) are most suitable for problems that are very nonlinear or have a number of discontinuities. Gradient methods are generally more efficient when the function to be minimized is continuous in its first derivative. Higher order methods, such as Newton's method, are only really suitable when the second order information is readily and easily calculated, because calculation of second order information, using numerical differentiation, is computationally expensive. Gradient methods use information about the slope of the function to dictate a direction of search where the minimum is thought to lie. The simplest of these is the method of steepest descent in which a search is performed in a direction, $-\nabla f(x)$, where $\nabla f(x)$ is the gradient of the objective function $\left(d^k = -\nabla f(x^k)\right)$. This method is very inefficient when the function to be minimized has long narrow valleys as, for example, is the case for Rosenbrock's function

$$f(x) = 100(x_2 - x_1^2)^2 + (1 - x_1)^2 \qquad (2.22)$$

The minimum of this function is at $x = [1,1]$, where $f(x) = 0$. A contour map of this function is shown in Figure 2.1, Steepest Descent Method on Rosenbrock's Function (Eq. 2.22), along with the solution path to the minimum for a steepest descent

implementation starting at the point [-1.9,2]. The optimization was terminated after 1000 iterations, still a considerable distance from the minimum. The black areas are where the method is continually zigzagging from one side of the valley to another. Note that toward the centre of the plot, a number of larger steps are taken when a point lands exactly at the centre of the valley.

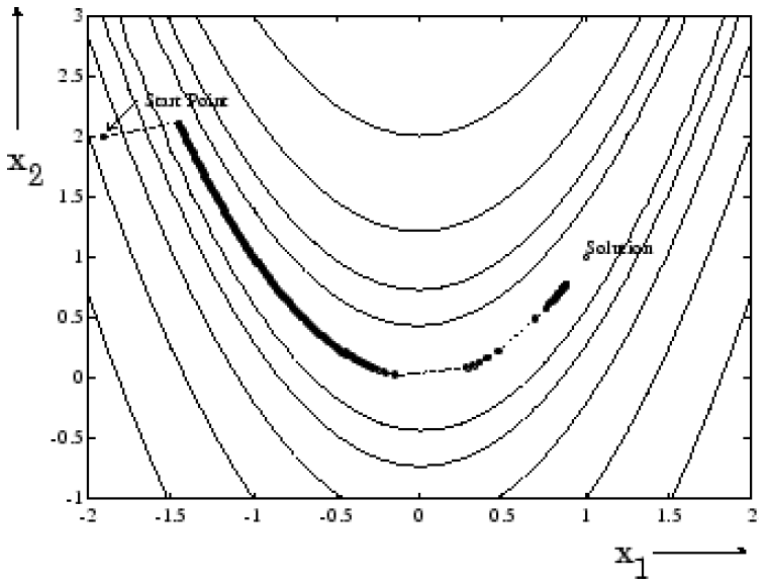

Figure 2.1 Steepest Descent Method on Rosenbrock's Function

This type of function (Equation 2.22), also known as the banana function, is notorious in unconstrained examples because of the way the curvature bends around the origin. Equation (2.22) is used throughout this section to illustrate the use of a variety of optimization techniques. The contours have been plotted in exponential increments because of the steepness of the slope surrounding the U-shaped valley.

In the upper text, the steepest descent method was described. Some of the drawbacks of that method were pointed out. It was noted that the method has a poor rate of convergence because only first-order information is used. This flaw was corrected with Newton's method where second-order derivatives were used. Newton's method has very good convergence properties. However, the method can be inefficient because it requires calculation of $n(n + 1)/2$ second-order derivatives to generate the Hessian matrix (recall that n is the number of design variables). For most engineering design problems, calculation of second-order derivatives may be tedious or even impossible. Also, Newton's method runs into difficulties if the Hessian of the function is singular at any iteration. The methods presented in this section overcome these drawbacks by generating an approximation for the Hessian matrix or its inverse at each iteration. Only the first derivatives of the function are used to generate these approximations. Therefore the methods have desirable features of both the steepest descent and the Newton's methods. They are called quasi-Newton methods.

Quasi-Newton Methods

Of the methods that use gradient information, the most favoured are the quasi-Newton methods. These methods build up curvature information at each iteration to formulate a quadratic model problem of the form

$$\min_x \frac{1}{2} x^T Hx + c^T x + b \qquad (2.23)$$

where the Hessian matrix, $H = \nabla^2 f(x)$, is a positive definite symmetric matrix, *c* is a constant vector, and *b* is a constant. The optimal solution for this problem occurs when the partial derivatives of *x* go to zero, i.e.,

$\nabla f(x^*) = Hx^* + c = 0$

The optimal solution x^* can be written as:

$$x^* = -H^{-1}c \qquad (2.24)$$

Newton-type methods (as opposed to quasi-Newton methods) calculate *H* directly and proceed in a direction of descent to locate the minimum after a number of iterations. Calculating *H* numerically involves a large amount of computation. Quasi-Newton methods avoid this by using the observed behaviour of *f*(*x*) and $\nabla f(x)$ to build up curvature information to make an approximation to *H* using an appropriate updating technique. A large number of Hessian updating methods have been developed. However, the formula of (BFGS) Broyden, Flether, Goldfarb, and Shanno (1970) is thought to be the most effective for use in a General Purpose method.

The formula given by BFGS is

$$H_{k+1} = H_k + \frac{q_k q_k^T}{q_k^T s_k} - \frac{H_k^T s_k^T s_k H_k}{s_k^T H_k s_k} \quad \text{, where} \qquad (2.25)$$

$s_k = x_{k+1} - x_k$

$q_k = \nabla f(x_{k+1}) - \nabla f(x_k)$

As a starting point H_0, can be set to any symmetric positive definite matrix, for example, the identity matrix *I*. To avoid the inversion of the Hessian *H*, you can derive an updating method that avoids the direct inversion of *H* by using a formula that makes an approximation of the inverse Hessian H^{-1} at each update. A well-known procedure is the DFP formula of Davidon (1959), Fletcher, and Powell (1963). This uses the same formula as the BFGS method (Equation 2.25) except that q_k is substituted for s_k.

The gradient information is either supplied through analytically calculated gradients, or derived by partial derivatives using a numerical differentiation method via finite differences. This involves perturbing each of the design variables, *x*, in turn and calculating the rate of change in the objective function.

At each major iteration, *k*, a line search is performed in the direction

$$d = -H_k^{-1} . \nabla f(x_k) \qquad (2.26)$$

The quasi-Newton method is illustrated by the solution path on Rosenbrock's function (Equation 2.22) in Figure 2.2, BFGS Method on Rosenbrock's Function. The method is able to follow the shape of the valley and converges to the minimum after 140 function evaluations using only finite difference gradients.

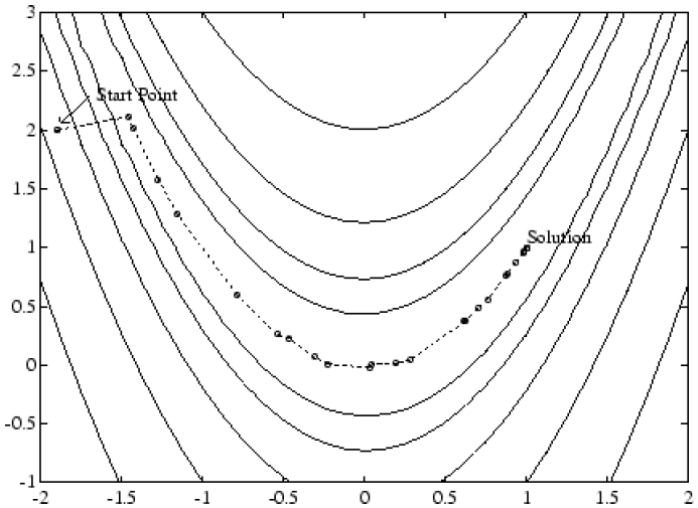

Figure 2.2 BFGS Method on Rosenbrock's Function

Line Search

Line search is a search method that is used as part of a larger optimization algorithm. At each step of the main algorithm, the line-search method searches along the line containing the current point, x_k, parallel to the search direction, which is a vector determined by the main algorithm. That is, the method finds the next iterate x_{k+1} of the form

$$x_{k+1} = x_k + \alpha_k d_k$$

where x_k denotes the current iterate, d_k is the search direction, and alpha α is a scalar step length parameter. The line search method attempts to decrease the objective function along the line $x_k + \alpha_k d_k$ by repeatedly minimizing polynomial interpolation models of the objective function. The line search procedure has two main steps:

- The bracketing phase determines the range of points on the line $x_{k+1} = x_k + \alpha_k d_k$ to be searched. The bracket corresponds to an interval specifying the range of values of α.
- The sectioning step divides the bracket into subintervals, on which the minimum of the objective function is approximated by polynomial interpolation.

The resulting step length α satisfies the Wolfe conditions:

$$(x_k + \alpha d_k) \le f(x_k) + c_1 \alpha \nabla f_k^T d_k \qquad (2.27)$$

$$\nabla f(x_k + \alpha d_k)^T d_k \ge c_2 \alpha \nabla f_k^T d_k \qquad (2.28)$$

Where c_1 and c_2 are constants with $0 < c_1 < c_2 < 1$

The first condition (Equation2.27) requires that α_k sufficiently decreases the objective function. The second condition (Equation 2.28) ensures that the step length is not too small. Points that satisfy both conditions are called acceptable points.

B-Constrained Optimisation

In constrained optimization, the general aim is to transform the problem into an easier subproblem that can then be solved and used as the basis of an iterative process. A characteristic of a large class of early methods is the translation of the constrained problem to a basic unconstrained problem by using a penalty function for constraints that are near or beyond the constraint boundary. In this way the constrained problem is solved using a sequence of parameterized unconstrained optimizations, which in the limit (of the sequence) converge to the constrained problem. These methods are now considered relatively inefficient and have been replaced by methods that have focused on the solution of the Kuhn-Tucker (KT) equations. The KT equations are necessary conditions for optimality for a constrained optimization problem. If the problem is a so-called convex programming problem, that is, $f(x)$ and $C_i(x)$, $i=1,.....,m$, are convex functions, then the KT equations are both necessary and sufficient for a global solution point.
Referring to General Problem (Equation 2.21), the Kuhn-Tucker equations can be stated as

$$\nabla f(x^*) + \sum_{i=1}^{m} \lambda_i . \nabla C_i(x^*) = 0$$
$$\lambda_i . C_i(x^*) = 0 \ , \ i = 1....m$$
$$\lambda_i \geq 0 \ , \ i = m_e + 1,.....,m \qquad (2.29)$$

in addition to the original constraints in Equation (2.21)

The first equation describes a cancelling of the gradients between the objective function and the active constraints at the solution point. For the gradients to be cancelled, Lagrange multipliers $(\lambda_i, i = 1,.....m)$ are necessary to balance the deviations in magnitude of the objective function and constraint gradients. Because only active constraints are included in this cancelling operation, constraints that are not active must not be included in this operation and so are given Lagrange multipliers equal to zeros.

The solution of the KT equations forms the basis to many nonlinear programming algorithms. These algorithms attempt to compute the Lagrange multipliers directly. Constrained quasi-Newton methods guarantee superlinear convergence by accumulating second-order information regarding the KT equations using a quasi-Newton updating procedure. These methods are commonly referred to as Sequential Quadratic Programming (SQP) methods, since a QP subproblem is solved at each major iteration (also known as Iterative Quadratic Programming, Recursive Quadratic Programming, and Constrained Variable Metric methods).

Sequential Quadratic Programming (SQP)

SQP methods represent the state of the art in nonlinear programming methods. Schittkowski (1985), for example, has implemented and tested a version that outperforms every other tested method in terms of efficiency, accuracy, and percentage of successful solutions, over a large number of test problems.

Based on the work of Biggs (1975), Han (1977), and Powell (1978), the method allows you to closely mimic Newton's method for constrained optimization

just as is done for unconstrained optimization. At each major iteration, an approximation is made of the Hessian of the Lagrangian function using a quasi-Newton updating method. This is then used to generate a QP subproblem whose solution is used to form a search direction for a line search procedure. An overview of SQP is found in Fletcher (1987), Gill et. al. (1981), Powell (183), and Hock-Schittkowski (1983). The general method, however, is stated here.

Given the problem description in general problem (Equation 2.21), the principal idea is the formulation of a QP subproblem based on a quadratic approximation of the Lagrangian function.

$$L(x,\lambda) = f(x) + \sum_{i=1}^{m} \lambda_i . c_i(x) \qquad (2.30)$$

Here you simplify Equation (2.21) by assuming that bound constraints have been expressed as inequality constraints. You obtain the QP subproblem by linearizing the nonlinear constraints. Then the Quadratic Programming (QP) Subproblem is expressed as:

$$\begin{aligned} &\underset{d \in R^n}{Minimize}\ \frac{1}{2} d^T H_k d + \nabla f(x_k)^T d \\ &\nabla c_i(x_k)^T d + c_i(x_k) = 0 \qquad i = 1,\ldots\ldots\ldots, m_e \\ &\nabla c_i(x_k)^T d + c_i(x_k) \le 0 \qquad i = m_e + 1,\ldots\ldots\ldots\ldots m \end{aligned} \qquad (2.31)$$

This subproblem can be solved using any QP algorithm. The solution is used to form a new iterate

$$x_{k+1} = x_k + \alpha_k d_k$$

The step length parameter α_k is determined by an appropriate line search procedure so that a sufficient decrease in a merit function is obtained (see "Updating the Hessian Matrix"). The matrix H_k is a positive definite approximation of the Hessian matrix of the Lagrangian function (Equation 2.30). H_k can be updated by any of the quasi-Newton methods, although the BFGS method (see "Updating the Hessian Matrix") appears to be the most popular.

A nonlinearly constrained problem can often be solved in fewer iterations than an unconstrained problem using SQP. One of the reasons for this is that, because of limits on the feasible area, the optimizer can make informed decisions regarding directions of search and step length. Consider Rosenbrock's function (Equation 2.2) with an additional nonlinear inequality constraint, $c(x)$

$$x_1^2 + x_2^2 - 1.5 \le 0$$

This was solved by an SQP implementation in 96 iterations compared to 140 for the unconstrained case. SQP Method on Nonlinear Linearly Constrained Rosenbrock's Function (Eq. 2.22) shows the path to the solution point $x = [0.9072, 0.8228]$, starting at $x = [-1.9, 2]$.

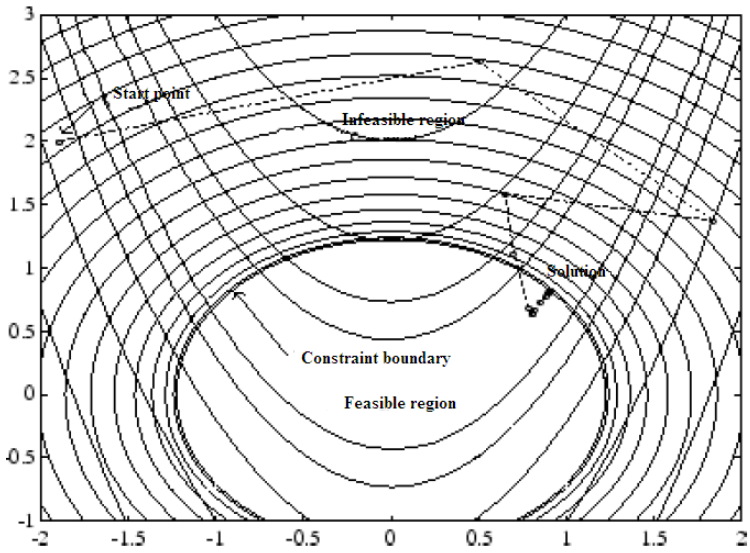

Figure 2.3 SQP Method on Nonlinear Linearly Constrained Rosenbrock's Function

The SQP implementation consists of three main stages, which are discussed briefly in the following subsections:

- "Updating the Hessian Matrix" of the Lagrangian function
- "Quadratic Programming Solution"
- "Line Search and Merit Function"

Updating the Hessian Matrix

At each major iteration a positive definite quasi-Newton approximation of the Hessian of the Lagrangian function, *H*, is calculated using the BFGS method, where $\lambda_i (i = 1,.....m)$ is an estimate of the Lagrange multipliers.

$$H_{k+1} = H_k + \frac{q_k q_k^T}{q_k^T s_k} - \frac{H_k^T H_k}{s_k^T H_k s_k} \quad \text{, where}$$

$$s_k = x_{k+1} - x_k$$

$$q_k = \nabla f(x_{k+1}) + \sum_{i=1}^{n} \lambda_i . \nabla C_i (x_{k+1}) - \left(\nabla f(x_k) + \sum_{i=1}^{n} \lambda_i . \nabla C_i (x_k) \right) \qquad (2.32)$$

Powell [35] recommends keeping the Hessian positive definite even though it might be positive indefinite at the solution point. A positive definite Hessian is maintained providing $q_k^T s_k$ is positive at each update and that *H* is initialized with a positive definite matrix. When $q_k^T s_k$ is not positive, q_k is modified on an element-by-element basis so that $q_k^T s_k > 0$. The general aim of this modification is to distort the elements of q_k, which contribute to a positive definite update, as little as possible. Therefore, in the initial phase of the modification, the most negative element of $q_k s_k$ is repeatedly halved. This procedure is continued until $q_k^T s_k$ is greater than or equal to a small negative tolerance. If, after this procedure, $q_k^T s_k$ is still not positive, modify q_k by adding a vector ν multiplied by a constant scalar ω, that is,

$qk = qk + \omega\nu$, where

$\nu_i = \nabla g_i (x_k + 1).g_i (x_k + 1) - \nabla g_i (x_k).g_i (x_k)$

If $(q_k)_i .\omega < 0$ and $(q_k)_i .(s_k)_i < 0$, $i = 1,.....,m$

$\nu_i = 0$, otherwise increase ω systematically until $q_k^T s_k$ becomes positive

Quadratic Programming Solution

At each major iteration of the SQP method, a QP problem of the following form is solved, where A_i refers to the i[th] row of the *m*-by-*n* matrix A.

$$\underset{d \in R^n}{Minimize}\ q = \frac{1}{2} d^T H_k d + c^T d$$

$$A_i d = b_i \qquad i = 1, \ldots\ldots\ldots, m_e$$

$$A_i d \le b_i \qquad i = m_e + 1, \ldots\ldots\ldots\ldots m \qquad (2.33)$$

The method used in the Optimization Toolbox is an active set strategy (also known as a projection method) similar to that of Gill et. al.(1981). It has been modified for both Linear Programming (LP) and Quadratic Programming (QP) problems. The solution procedure involves two phases. The first phase involves the calculation of a feasible point (if one exists). The second phase involves the generation of an iterative sequence of feasible points that converge to the solution. In this method an active set, $\overline{A}_k$, is maintained that is an estimate of the active constraints (i.e., those that are on the constraint boundaries) at the solution point. Virtually all QP algorithms are active set methods. This point is emphasized because there exist many different methods that are very similar in structure but that are described in widely different terms.

$\overline{A}_k$ is updated at each iteration *k*, and this is used to form a basis for a search direction $\hat{d}_k$. Equality constraints always remain in the active set $\overline{A}_k$. The notation for the variable $\hat{d}_k$ is used here to distinguish it from d_k in the major iterations of the SQP method. The search direction $\hat{d}_k$ is calculated and minimizes the objective function while remaining on any active constraint boundaries. The feasible subspace for $\hat{d}_k$ is formed from a basis Z_k whose columns are orthogonal to the estimate of the active set $\overline{A}_k$ (i.e., $\overline{A}_k Z_k = 0$). Thus a search direction, which is formed from a linear summation of any combination of the columns of Z_k, is guaranteed to remain on the boundaries of the active constraints.

The matrix Z_k is formed from the last *m-l* columns of the QR decomposition of the matrix $\overline{A}_k^T$, where *l* is the number of active constraints and *l* < *m*. That is, Z_k is given by:

$$Z_k = Q[:, l+1:m] \ , \qquad (2.34)$$

where

$$Q^T \overline{A}_k^T = \begin{bmatrix} R \\ 0 \end{bmatrix}$$

Once Z_k is found, a new search direction $\hat{d}_k$ is sought that minimizes $q(d)$ where $\hat{d}_k$ is in the null space of the active constraints. That is, $\hat{d}_k$ is a linear combination of the columns of $Z_k : \hat{d}_k = Z_k p$ for some vector *p*. Then if you view the quadratic as a function of *p*, by substituting for $\hat{d}_k$, you have

$$q(p) = \frac{1}{2} p^T Z_k^T H Z_k p + c^T Z_k p$$

Differentiating with respect to *p*

$$\nabla q(p) = Z_k^T H Z_k p + c^T Z_k$$

$\nabla q(p)$ is referred to as the projected gradient of the quadratic function because it is the gradient projected in the subspace defined by Z_k. The term $Z_k^T H Z_k$ is called the projected Hessian. Assuming the Hessian matrix *H* is positive definite (which is the case in this implementation of SQP), then the minimum of the function *q(p)* in the subspace defined by Z_k occurs when gradient of $\nabla q(p) = 0$, which is the solution of the system of linear equations

$$Z_k^T H Z_k p = -c^T Z_k$$

A step is taken of the form

$$x_{k+1} = x_k + \alpha_k \hat{d}_k \qquad \text{where} \quad \hat{d}_k = Z_k^T p$$

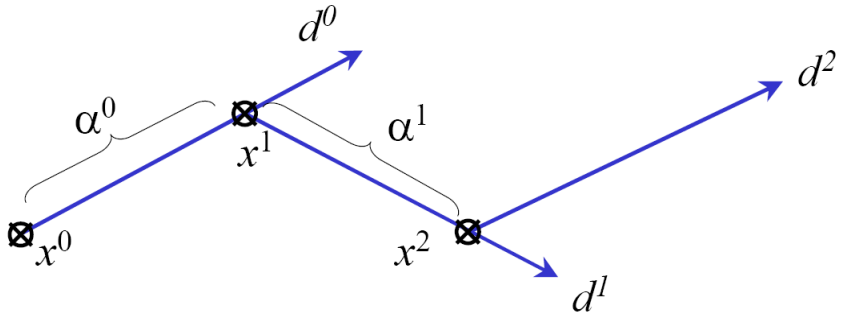

(The step length α_k is chosen in a manner to minimize the function in the direction $\hat{d}_k$)
At each iteration, because of the quadratic nature of the objective function, there are only two choices of step length α . A step of unity along $\hat{d}_k$ is the exact step to the minimum of the function restricted to the null space of $\bar{A}_k$. If such a step can be taken, without violation of the constraints, then this is the solution to QP (Equation 2.34). Otherwise, the step along $\hat{d}_k$ to the nearest constraint is less than unity and a new constraint is included in the active set at the next iteration. The distance to the constraint boundaries in any direction $\hat{d}_k$ is given by

$$\alpha = \min_i \left\{ \frac{-(A_i x_k - b_i)}{A_i \hat{d}_k} \right\} \qquad (i = 1,.....,m) \qquad (2.35)$$

which is defined for constraints not in the active set, and where the direction $\hat{d}_k$ is towards the constraint boundary, i.e., $A_i . \hat{d}_k > 0$, $i = 1,.....,m$.
When *n* independent constraints are included in the active set, without location of the minimum, Lagrange multipliers, λ_k, are calculated that satisfy the non singular set of linear equations

$$\bar{A}_k^T \lambda_k = c$$

If all elements of λ_k are positive, x_k is the optimal solution of QP (Equation 3-30). However, if any component of λ_k is negative, and the component does not correspond to an equality constraint, then the corresponding element is deleted from the active set and a new iterate is sought.

Line Search and Merit Function

The solution to the QP subproblem produces a vector d_k, which is used to form a new iterate

$$x_{k+1} = x_k + \alpha_k d_k$$

The step length parameter α_k is determined in order to produce a sufficient decrease in a merit function. The merit function used by Han (1977) and Powell (1978) of the following form is used in this implementation.

$$\Psi(x) = f(x) + \sum_{i=1}^{m_e} r_i . g_i(x) + \sum_{i=m_e+1}^{m} r_i . \max\{0, g_i(x)\}$$

Powell recommends setting the penalty parameter

$$r_i = (r_k + 1)_i = \max_i \left\{ \lambda_i, \frac{1}{2}\left((r_k)_i + \lambda_i\right) \right\} \qquad i = 1, ..., m$$

This allows positive contribution from constraints that are inactive in the QP solution but were recently active. In this implementation, the penalty parameter r_i is initially set to

$$r_i = \frac{\|\nabla f(x)\|}{\|\nabla g_i(x)\|}$$

where $\| \ \|$ represents the Euclidean norm.

This ensures larger contributions to the penalty parameter from constraints with smaller gradients, which would be the case for active constraints at the solution point.

2.3.2 Stochastic Methods

The GA is a stochastic global search method that mimics the metaphor of natural biological evolution (Holland 1975). Based on the Darwinian survival-of-fittest principle, GAs operate on a population of potential solutions to produce better and better approximations to the optimal solution (Goldberg 1989). The population is a set of configurations called chromosomes and the basic GA operators are selection, crossover and mutation. It produces new individuals that have some parts of both parents genetic material. At each generation, a new set of approximations is created by the process of selecting individuals according to their level of fitness in the problem domain and breeding them together using crossover and mutation operators which are borrowed from natural genetics. This process leads to the evolution of populations of individuals that are better suited to their environment than the individuals that they were created from. You can apply the genetic algorithm to solve a variety of optimization problems that are not well suited for standard optimization algorithms, including problems in which the objective function is discontinuous, non differentiable, stochastic, or highly nonlinear.

The main interest of stochastic methods in engineering sciences is to break the limits of the standard deterministic methods in many optimization problems: when the search space involves both discrete and continuous domains; when the objective function or the constraints lack regularity; or when the objective function admits a huge number of local optima. Moreover, GA employs a random, yet directed, search for locating the globally optimal solution. Therefore, GA is able not only to improve the solution close to a local optimum, but also to explore a larger extension of the design space and to direct the search toward relatively prospective regions in the search space. The following example shows how to find the minimum of Rastrigin's function, to prove the robustness of genetic algorithms. Its many local minima make it difficult for standard, gradient-based methods to find the global minimum. For two independent variables, the Rastrigin's function is defined as:

$$Ras(x) = 20 + x_1^2 + x_2^2 - 10(\cos 2\pi x_1 + \cos 2\pi x_2)$$

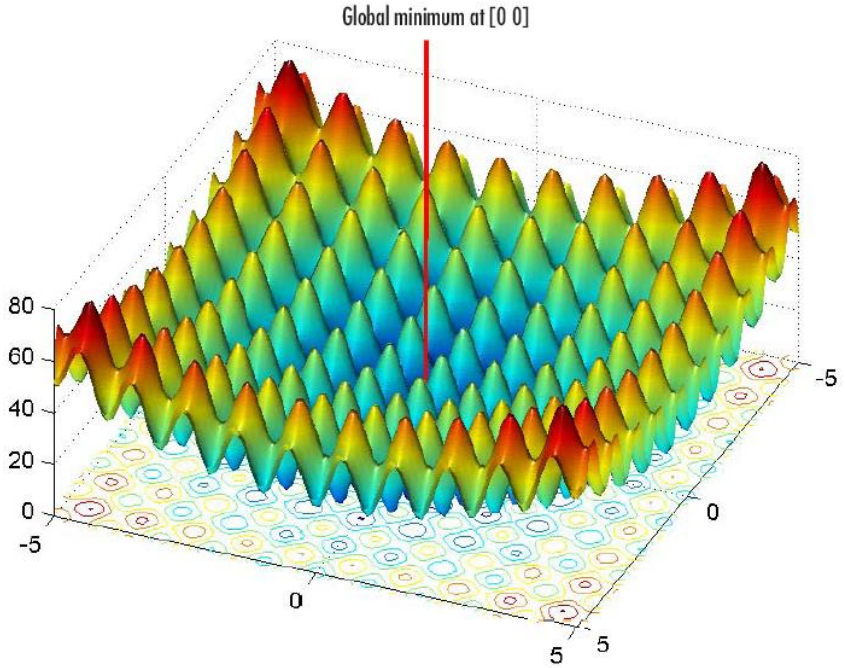

Figure 2.3 Plot of Rastrigin's function

As Fig 2.3 shows, Rastrigin's function has many local minima—the "valleys" in the plot. However, the function has just one global minimum, which occurs at the point [0,0] in the *x*-*y* plane, as indicated by the vertical line in the plot, where the value of the function is 0. At any local minimum other than [0,0], the value of Rastrigin's function is greater than 0. The farther the local minimum is from the origin, the larger the value of the function is at that point. The following contour plot (Figure 2.4) of Rastrigin's function shows the alternating maxima and minima.

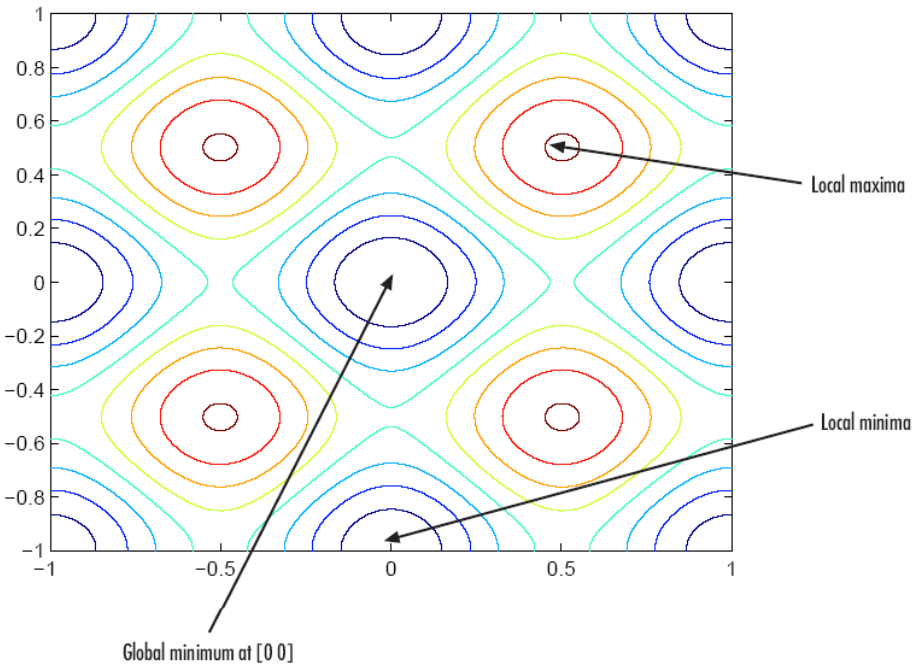

Figure 2.4 Contour Plot of Rastrigin's function

The outline of the genetic algorithm is summarized by the following steps:
1- The algorithm begins by creating a random initial population.
2- The algorithm then creates a sequence of new populations. At each step, the algorithm uses the individuals in the current generation, called parents, who contribute their genes—the entries of their vectors—to their children in order to create the next population. To create the new population, the algorithm performs the following steps:

- Scores each member of the current population by computing its fitness value.
- Scales the raw fitness scores to convert them into a more usable range of values.
- Selects members, called parents, based on their fitness.
- Some of the individuals in the current population that have lower fitness are chosen as elite. These elite individuals are passed to the next population.
- Produces children from the parents. Children are produced either by making random changes to a single parent—mutation—or by combining the vector entries of a pair of parents—crossover.
- Replaces the current population with the children to form the next generation.

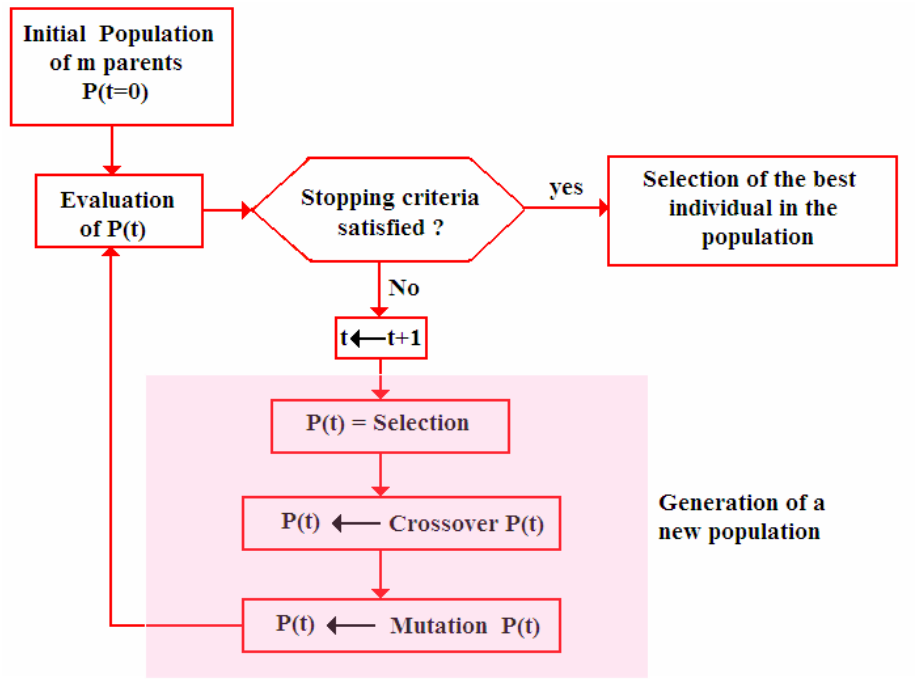

In fact, the reproduction process of the genetic algorithm creates three types of children for the next generation:

- *Elite children* are the individuals in the current generation with the best fitness values. These individuals automatically survive to the next generation.
- *Crossover children* are created by combining the vectors of a pair of parents.
- *Mutation children* are created by introducing random changes, or mutations, to a single parent.

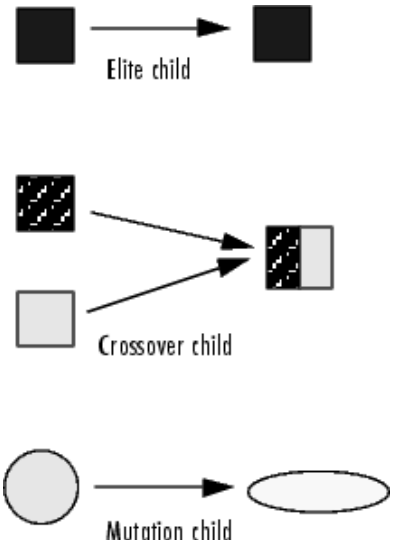

Returning to the example of Rastrigin's function, the following figure shows the children of the initial population, that is, the population at the second generation, and indicates whether they are elite, crossover, or mutation children.

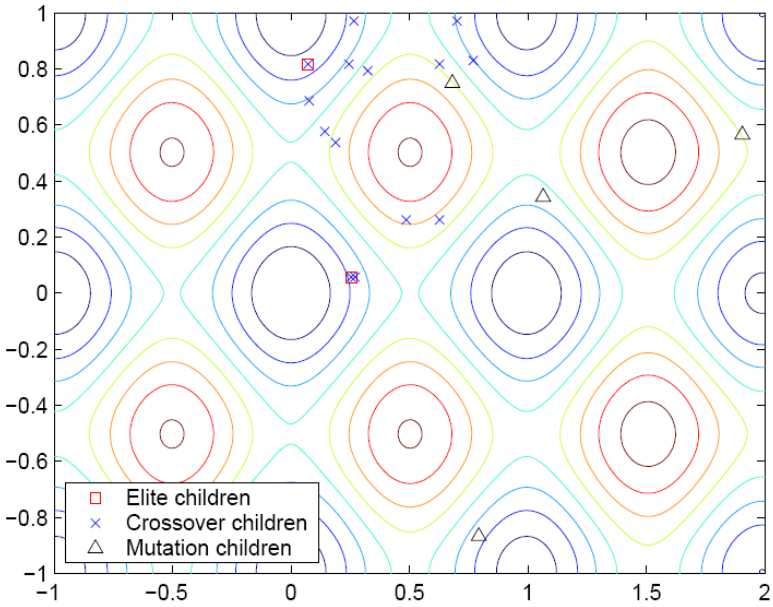

Then, the following figures show the populations at iterations 60, 80, 95, and 100; demonstrating that as the number of generations increases, the individuals in the population get closer together and approach the minimum point [0,0].

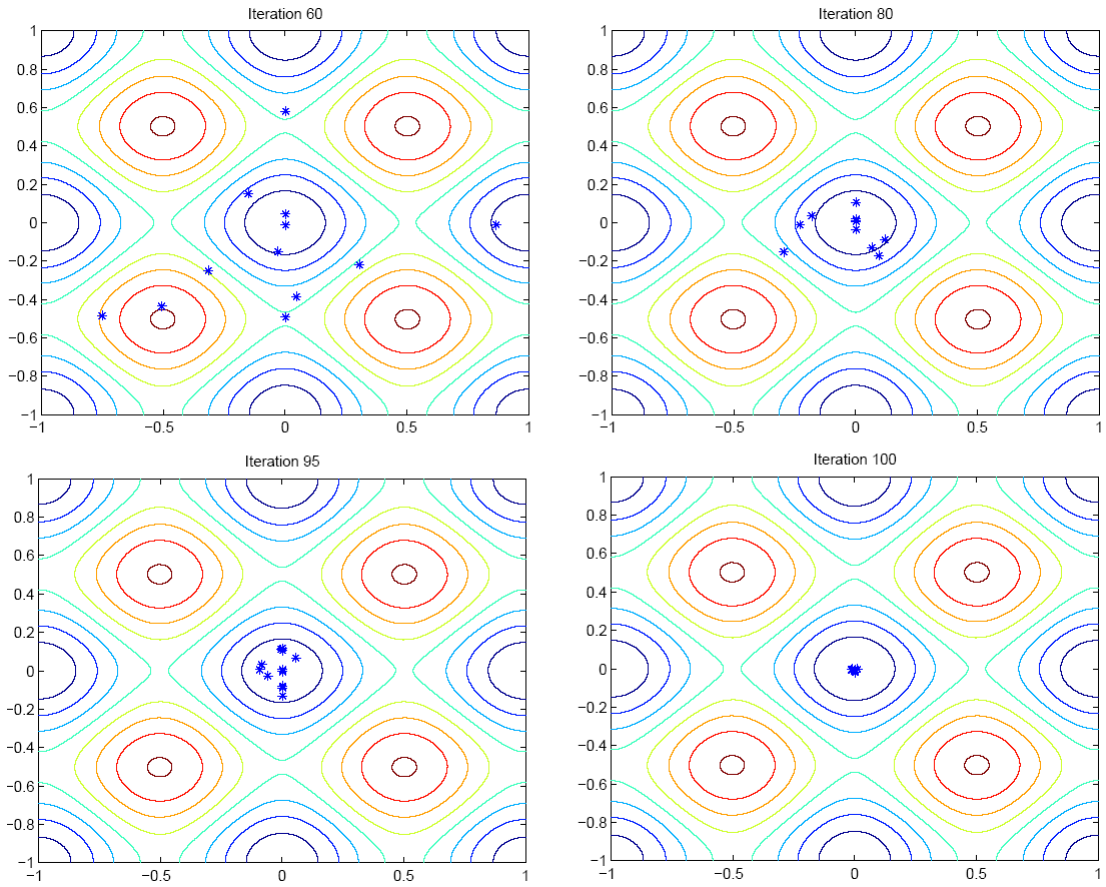

Description of the nonlinear constraint solver

The genetic algorithm uses the Augmented Lagrangian Genetic Algorithm (ALGA) to solve nonlinear constraint problems. The optimization problem solved by the ALGA algorithm is

$$\underset{x}{Minimize} \quad f(x)$$

Subject to

$$C_i(x) = 0\ ,\ i = 1,.....,m$$
$$C_i(x) \le 0\ ,\ i = m+1,.....,m_t$$
$$A.x \le b$$
$$A_{eq}.x = b_{eq}$$
$$LB \le x \le UB$$

where *C(x)* represents the nonlinear inequality and equality constraints, *m* is the number of nonlinear inequality constraints, and m_t is the total number of nonlinear constraints.

The Augmented Lagrangian Genetic Algorithm (ALGA) attempts to solve a nonlinear optimization problem with nonlinear constraints, linear constraints, and bounds. In this approach, bounds and linear constraints are handled separately from nonlinear constraints. A subproblem is formulated by combining the fitness function and nonlinear constraint function using the Lagrangian and the penalty parameters. A sequence of such optimization problems are approximately minimized using the genetic algorithm such that the linear constraints and bounds are satisfied.
A subproblem formulation is defined as

$$\Theta(x,\lambda,s,\rho) = f(x) - \sum_{i=1}^{m} \lambda_i s_i \log(s_i - c_i(x)) + \sum_{i=m+1}^{m_t} \lambda_i c_i(x) + \frac{\rho}{2} \sum_{i=m+1}^{m_t} c_i(x)^2$$

where the components λ_i of the vector λ are nonnegative and are known as Lagrange multiplier estimates. The elements s_i of the vector *s* are nonnegative shifts, and ρ is the positive penalty parameter. The algorithm begins by using an initial value for the penalty parameter (Initial Penalty). The genetic algorithm minimizes a sequence of the subproblem, which is an approximation of the original problem. When the subproblem is minimized to a required accuracy and satisfies feasibility conditions, the Lagrangian estimates are updated. Otherwise, the penalty parameter is increased by a penalty factor (Penalty Factor). This results in a new subproblem formulation and minimization problem. These steps are repeated until the stopping criteria are met.

Reproduction is a process of selecting a set of designs from the current population and carrying them into the next generation. The selection process is biased toward more fit members of the current design set (population). Using the fitness value f_i for each design in the set, its probability of selection is calculated as:

$$P_i = \frac{f_i}{Q} \qquad\qquad Q = \sum_{j=1}^{Np} f_j$$

N_p= number of designs in a population; also called the population size.

It is seen that the members with higher fitness value have larger probability of selection. To explain the process of selection, let us consider a roulette wheel with a handle shown in Fig. 2.4. The wheel has N_p segments to cover the entire population, with the size of the i^{th} segment proportional to the probability P_i. Now a random number *w* is generated between 0 and 1. The wheel is then rotated clockwise, with the

rotation proportional to the random number *w*. After spinning the wheel, the member pointed to by the arrow at the starting location is selected for inclusion in the next generation. In the example shown in Fig. 2.4, member 2 is carried into the next generation. Since the segments on the wheel are sized according to the probabilities P_i, the selection process is biased toward the more fit members of the current population. Note that a member copied to the mating pool remains in the current population for further selection. Thus, the new population may contain identical members and may not contain some of the members found in the current population. This way, the average fitness of the new population is increased.

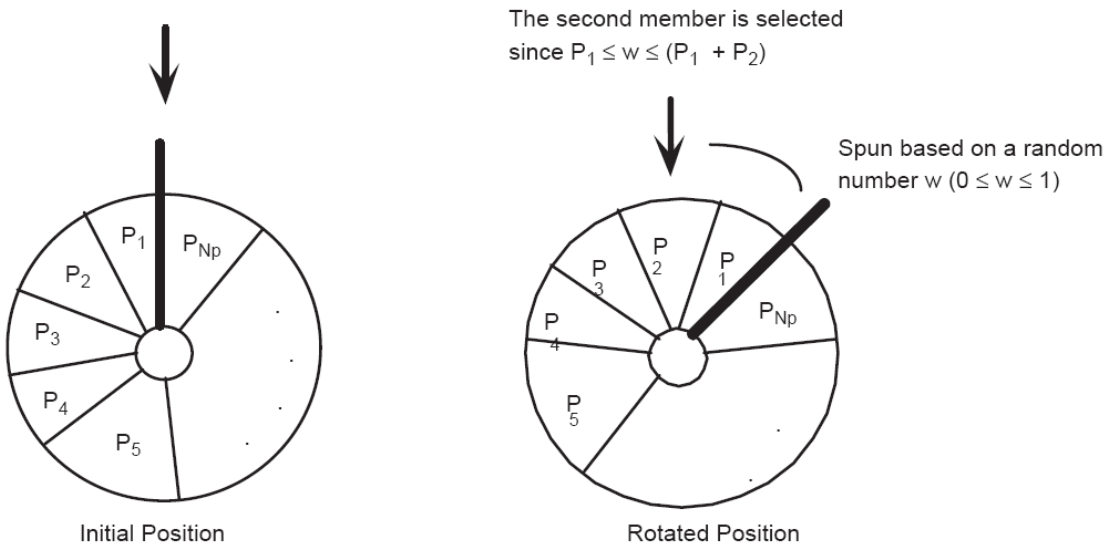

Figure 2.4 Roulette wheel process for selection of designs for new generation (reproduction).

Once a new set of designs is determined, crossover is conducted as a means to introduce variation into a population. Crossover is the process of combining or mixing two different designs (chromosomes) in the population. Although there are many methods for performing crossover, the most common ones are the one-cut-point and two-cut-point methods. A cut point is a position on the genetic string. In the one-cut method a position on the string is randomly selected that marks the point at which two parent designs (chromosomes) split. The resulting four halves then are exchanged to produce new designs (children). The process is illustrated in Fig. 2.5 where the cut point is determined as 4 digits from the right end. The new designs produced $x^{1'}$ and $x^{2'}$ and replace the old designs (parents). Similarly, the two-cut-point method is illustrated in Fig.2.6. Selecting how many or what percentage of chromosomes crossover and at what points the crossover operation occurs are part of the heuristic nature of genetic algorithms. There are many different approaches, and most are based on random selections.

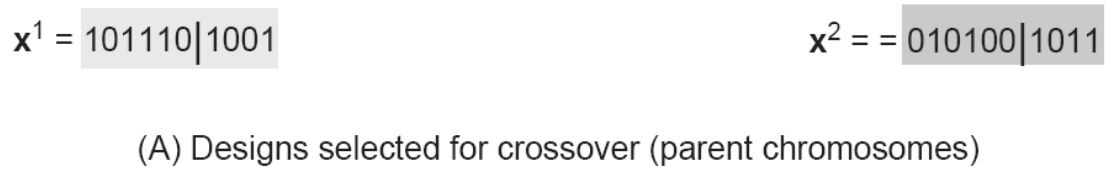

(A) Designs selected for crossover (parent chromosomes)

(B) New designs (children) after crossover

Figure 2.5 Crossover operation with one-cut point

(A) Designs selected for crossover (parent chromosomes)

(B) New designs (children) after crossover

Figure 2.6 Crossover operation with two-cut point

Mutation is the next operation on the members of the new design set (population). The idea of mutation is to safeguard the process from a complete premature loss of valuable genetic material during reproduction and crossover steps. In terms of a genetic string, this step corresponds to selecting a few members of the population, determining a location on each string randomly, and switching 0 to 1 or vice versa. The number of members selected for mutation is based on heuristics, and the selection of location on the string for mutation is based on a random process. Let us select a design as "10 1110 1001" and the location #7 from the right end on its string. The mutation operation involves replacing the current value of 1 at the seventh location with 0 as "10 1010 1001".

Finally, the number of the reproduction operations is always equal to the size of the population, the amount of crossover and mutation can be adjusted to fine-tune the performance of the algorithm.

Chapter 3

Modelling of Waves and Floating Breakwaters

This chapter presents the sea waves modelling and their relative interaction with the floating breakwaters based on both analytical and numerical approaches. Second, the dynamical behaviour of the floating breakwater is introduced by an analytical model applying Lagrange's theorem. Next, the elaborated model is used to identify the influence of the structural parameters on the wave attenuating capacity of the moored floating breakwater through a comprehensive parametrical analysis. Also a comparison with the case of partial reflective sidewalls is introduced. Finally, the mechanical behaviour of the floating breakwater is studied through analytical and numerical models.

3.1-Wave modelling

The mathematical formulation of the water wave problem is derived from fundamental conservation laws. It consists of equations which are valid in the fluid domain and of equations which are valid on the boundaries. Together they define the wave problem in which an analytical solution and a numerical one are presented. For the analytical approach, we consider the oscillating motion of the structure small enough that can be neglected. This constitutes a simple approach that can be easily applied in the optimization chapter, and allows us to elaborate new contributions in the optimization methods with such simplified model. Also, the analytical study is extended towards the non linear theory of waves to improve the results in order to have good agreement with the experimental data. The second one, numerical approach, represents the real model of a floating breakwater that takes into consideration the radiation and the transmission effects together.

3.1.1 Analytical model

Models for propagating free-surface gravity waves are usually based on the potential-flow model. The high values of the density and sound velocity in water render the compressibility effects negligible in sea water. Then, in these models the

fluid is assumed to be incompressible and inviscid and the flow irrotational. Thus, the fluid motion can be described by a velocity potential, Φ, related to the velocity $\vec{U}(u,w)$.

$$\overrightarrow{rot}\left(\vec{U}\right)=\vec{0} \Rightarrow \vec{U}=\overrightarrow{grad}(\Phi) , \qquad (3.1)$$

where $u=\frac{\partial\Phi}{\partial x}$ and $w=\frac{\partial\Phi}{\partial z}$.

A cartesian coordinate system *Oxyz* is employed, where *Oxy* coincide with plane of the free surface at rest, *Oz* directed positive upwards, and *Ox* directed positive in the direction of propagation of the waves. The incident wave propagates in a straight line in the direction defined by the angle γ, formed with the *Ox* axe. In this study, it is supposed that the waves can strike the breakwater in a perpendicular direction to obtain the maximum pressure applied by the waves on the breakwater, in order to study the dangerous case in the construction of a breakwater. Then, the angle is taken as $\gamma=0$ (incident wave normal to the breakwater) and the movement is reduced to two dimensions as in figure 3.1. The fluid motion is defined as follows: Let t denote time, x and z the horizontal and vertical coordinates, respectively, and η the free-surface elevation above the still water level.

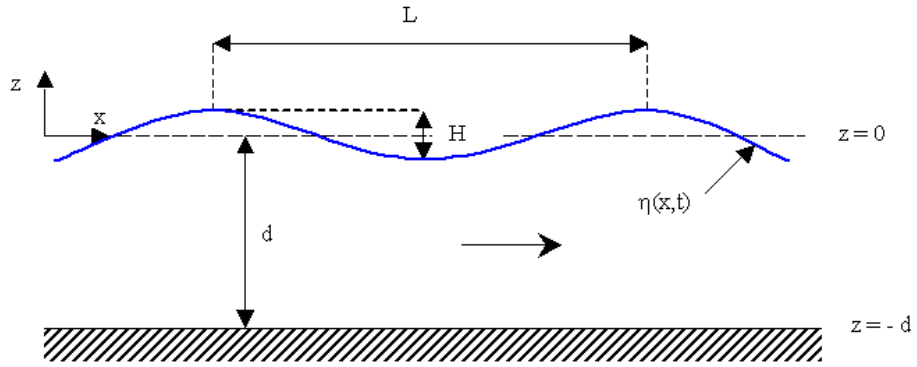

Figure 3.1 Wave notations

Once the parameters characterizing the sea waves are known (Length of wave L, Period T, Height H), a model is needed to study the waves' propagations and transforms their evolution into loads on the breakwater. It is a strict study based on the fundamental physical principles of the conservation of momentum and mass (reduced to Laplace equation). The combination of the equation of momentum conservation and that of mass, yields to the well known equation, Bernoulli-Lagrange, which constitutes the essential equation to determine the field of wave's pressure.

$$\frac{\partial\Phi}{\partial t}+\frac{1}{2}(grad\Phi)^2+\frac{P(x,z,t)}{\rho}+gz=Q(t) \qquad (3.2)$$

In general, the study of marine structures' behaviours due to waves' propagations is mostly made as part of a linear theory (Molin 2004), where the interest in this part is to orient the work towards the non linear approximation (Stokes 2nd order expansion), which yields to a clarified view of the efforts in an enlarged domain of frequencies to have outstanding agreement with the real and experimental data (especially when neglecting the oscillating motion of the breakwater). It is clear that if Φ is known throughout the fluid, the physical quantities pressure and velocity) can be obtained from Bernoulli's equation. Because the free surface is a moving

boundary, we need more than one condition to complete the potential flow model. The first condition is called the kinematic condition where the second one is the dynamic condition. Then, the boundary value problem is then defined as follows:

$\nabla^2\Phi = \Delta\Phi = 0$ Laplace equation in the fluid domain;

$\left(\frac{\partial\Phi}{\partial z}\right)_{z=-d} = 0$ Condition at the sea floor;

$\left(\frac{\partial\Phi}{\partial n}\right)_{x=0} = 0$ Kinematic condition at the solid boundary;

$\left(\frac{\partial\eta}{\partial t} + \frac{\partial\Phi}{\partial x}\frac{\partial\eta}{\partial x} - \frac{\partial\Phi}{\partial z}\right)_{z=\eta} = 0$ Kinematic condition at the free surface;

$\left(\frac{\partial\Phi}{\partial t} + \frac{1}{2}\left(\left(\frac{\partial\Phi}{\partial x}\right)^2 + \left(\frac{\partial\Phi}{\partial z}\right)^2\right) + g\eta\right)_{z=\eta} = Q(t)$ Dynamic equation at the free surface;

The equation of Laplace expresses the mass conservation; the sea bottom condition expresses the impermiability of the sea bed where the normal component of the velocity is zero; the kinematic condition at the solid boundary (breakwater, $x=0$), expresses the static condition of the breakwater (wave reflection) where $\vec{n}$ is the outward normal direction of the solid boundary; the kinematic condition on surface, $z=\eta$, expresses that a fluid particle at the surface should remain there at all times, while the dynamic condition expresses that the pressure on the free surface is zero. The used method for the nonlinear theory (Stockes 2nd order expansion), called perturbation method [5], consists of developing the different variables into power series depending on a parameter $\varepsilon = \frac{H}{L}$, where the linear theory constitutes the first order yielding exact solutions only for waves with infinitesimal amplitudes.

$$\Phi = \varepsilon\Phi_1 + \varepsilon^2\Phi_2 + \varepsilon^3\Phi_3 + \ldots\ldots\ldots + \varepsilon^n\Phi_n \tag{3.3}$$

By considering the amplitudes of the oscillations of the free surface to be small, the terms are then evaluated on the free surface depending on $\eta(x,t)$ due to Taylor series.

$$\Phi(x,\eta) = \Phi(x,0) + \eta\left(\frac{\partial\Phi}{\partial z}\right)_{z=0} + \ldots\ldots\ldots + \frac{\eta^n}{n}\left(\frac{\partial^n\Phi}{\partial z_n}\right)_{z=0} \tag{3.4}$$

The developments are limited to the second order of the camber ε so: $\Phi = \varepsilon\Phi_1 + \varepsilon^2\Phi_2$ and $\eta = \varepsilon\eta_1 + \varepsilon^2\eta_2$. It is convenient to determine $\Phi_2(x,z,t)$ and $\eta_2(x,t)$ knowing Φ_1 and η_1 (linear case), Then the boundary conditions for the free surface for z= $\eta(x,t)$, are transformed into perturbation series. Solving for the 1st order expansion (linear theory)

$$\begin{aligned}\Phi_1 &= \mathrm{Re}\left\{-i\frac{Hg}{2\omega}\frac{ch[k(z+d)]}{ch(kd)}\exp i(kx-\omega t)\right\}\\ \eta_1 &= \mathrm{Re}\left\{\frac{H}{2}\exp i(kx-\omega t)\right\}\end{aligned} \tag{3.5}$$

(Where $k = 2\pi / L$ designates the wave number and ω the frequency). The nonlinear approximation is achieved by substituting for the first order in the perturbation series:

$$\Phi(x,z,t) = \mathrm{Re}\left\{ -i\frac{Hg}{2\omega}\frac{ch[k(z+d)]}{ch(kd)}\exp i(kx-\omega t)\right\} - \frac{\pi g H^2}{4L}\frac{t}{sh(2kd)} + \mathrm{Re}\left\{ -i\frac{3}{8}\left(\frac{H}{2}\right)^2 \frac{gk}{\omega}\frac{ch[2k(z+d)]}{sk^3(kd)ch(kd)}\exp 2i(kx-\omega t)\right\} \quad (3.6)$$

This expression of velocity potential describes the physical properties of the waves in the absence of any structure, where the reflection phenomenon must be taken into consideration during the collision of the waves by the breakwater. Then, a reflected wave identical to the incident one is created but in the opposite sense.

$$\Phi_r(x,z,t) = r \times \Phi_i(-x,z,t)$$

Where r designates the reflection coefficient (coefficient of amplitude reduction), the superposition of the incident and reflected velocity potentials creates a global wave system (Goda 1985) whose velocity potential is defined as: $\Phi_T = \Phi_i + \Phi_r$.

Moreover, the extremity of the breakwater involves the diffraction of the waves and hence concentric circles are formed around its extremity. Considering a semi-infinite breakwater, eliminates this phenomenon and keeps the problem in the domain of wave reflection only; where the global potential velocity describing the problem is maintained as expressed above. The substitution of this value for the velocity potential (Φ_T) in the Bernoulli-Lagrange equation implies the expression of the pressure distribution (pressure at any point in the fluid domain.) in the case of wave-breakwater interaction, where all the waves are reflected by the breakwater (no diffraction or transmission).

$$P(x,z,t) = -\rho g z + \mathrm{Re}\left\{ \begin{array}{l} \frac{1}{2}\rho g H \frac{ch[k(z+d)]}{ch(kd)} \\ \left[\exp i(kx-\omega t) + r\exp i(-kx-\omega t+\beta)\right] \end{array}\right\} + \mathrm{Re}\left\{ \begin{array}{l} \frac{3}{4}\rho g H \frac{\pi H}{L}\frac{1}{sh(2kd)}\left[\frac{ch2k(z+d)}{sh^2 kd} - \frac{1}{3}\right] \\ \left[\exp 2i(kx-\omega t) + (r^2+r)\exp 2i(-kx-\omega t+\beta)\right] \end{array}\right\} + \mathrm{Re}\left\{ r\rho H^2\omega^2 \exp i(-2\omega t+\beta)\right\} - \frac{1}{4}\rho g H \frac{\pi H}{L}\frac{(r+1)}{sh(2kd)}\left[ch2k(z+d)-1\right] \quad (3.7)$$

Hydrodynamic pressure

The exerted pressure by waves on the vertical breakwater is deduced from the computed fluid problem in the first section. This hydrodynamic pressure has a complicated expression different from the hydrostatic one that is linear, its repartition over the breakwater has a curved shape (obtained using Matlab); where its maximum is around the still water level and it decreases to zero at the top of the breakwater (with the wave height) and also decreases with water depth (figure 2). Fixing $x = 0$ (exterior breakwater surface), and the phase angle $\beta = 0$ (vertical impermeable wall, Tadjbkhsh and Keller 1960), the pressure distribution over the vertical breakwater is obtained.

The hydrodynamic pressure exerted by the waves on the breakwater is acting on the exterior surface of the breakwater due to the assumption that all the waves propagating from the ocean side are totally reflected outside the port and the radiated

waves are neglected. Hence, it can be simply deduced that there are no dynamic pressure acting on the interior surface of the breakwater due to the absence of waves' propagations inside the port. It can be written as follows:

$$P = a\cosh k(z+d) + b\cosh 2k(z+d) + f \tag{3.8}$$

$$a = \frac{\rho g H}{2}\frac{(r+1)}{chkd}\cos(\omega t),\ b = \frac{\rho g \pi H^2}{4Lsh2kd}\left[\frac{(3r^2+3r+3)\cos(2\omega t)}{sh^2 kd} - r - 1\right]$$

$$f = \frac{\rho g \pi H^2}{4Lsh2kd}\left[(-r^2 - r - 1)\cos(2\omega t) + r + 1\right] + \rho H^2 \omega^2 r\cos(2\omega t)$$

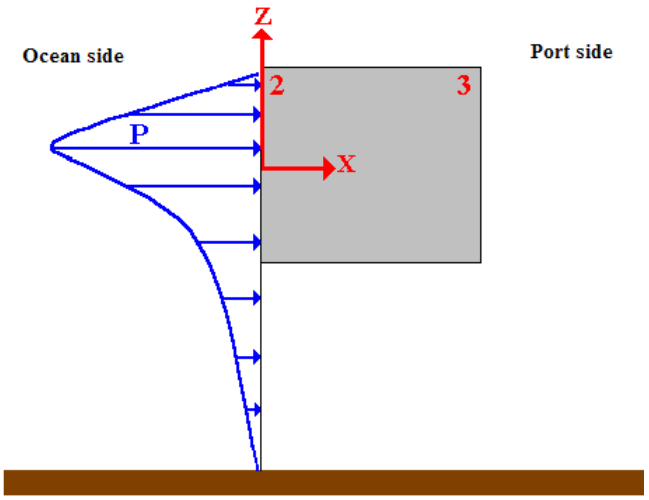

Figure 3.2 Hydrodynamic pressure distribution over the breakwater

It is reduced to an equation with hyperbolic functions of z (height), where the other variables independent of the altitude are collected together in the terms $a, b,$ and f .

3.1.2 Numerical model

A floating harbour has a complex dynamic behaviour. In contrast to a normal harbour, where only ship motions occur, a floating harbour will be completely influenced by the wave conditions. Lots of structural and hydraulic factors influence the hydrodynamic behaviour of the floating breakwater. Determining the relations and the influence of these factors on the wave attenuating capacity of the floating breakwater is the main objective of this study.

With this knowledge a model can be developed that can be used as a design tool to determine the magnitude of the floating breakwater elements in an early stage of the design process. It is therefore important to structuralize the problem to be a base for later, more detailed assessment and model testing. The dynamic behaviour of a floating breakwater is influenced by many factors. The influence factors that can be distinguished are shown in Figure 3.3 and can roughly be divided into two parts:

- The interference of the floating breakwater with the environment
- The interference of the floating breakwater with the mooring system

The symbols, used in figure 3.3 are:
k_m : Spring stiffness of the mooring system (N/m)
L_w : Length of the floating breakwater element (m)
b : Draft of the floating section of the breakwater. (m)
a : Width of the floating section of the floating breakwater (m)
ζ_a : Incoming wave amplitude (m)
ζ_R : Radiated / reflected wave amplitude to the sea side of the floating breakwater (m)
ζ_T : Radiated / transmitted wave amplitude to the harbour side of the floating breakwater (m)

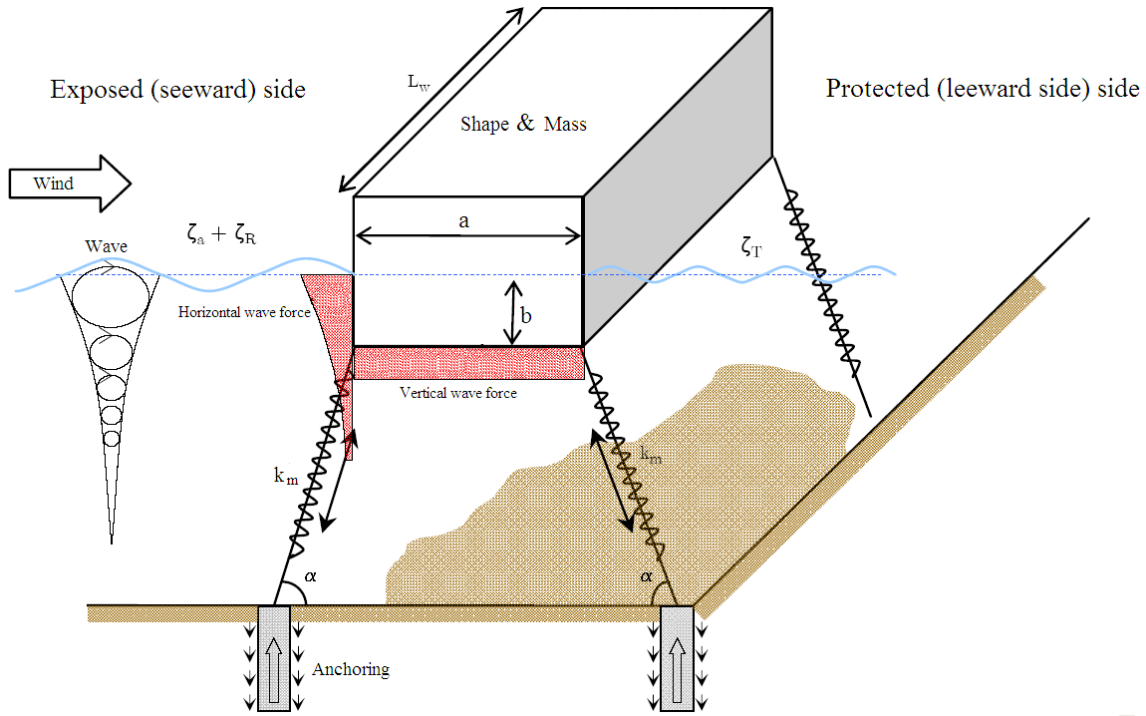

Figure 3.3 Structural and hydrodynamic factors

The interference of the floating breakwater with the environment is mainly related to the movement of the sea waves. These local waves produce the forces that will put the floating breakwater into motion. Since the largest part of the floating breakwater will be submerged, the influence of the wave forces will be large. The dynamic behaviour of a mass-spring system, like a floating body, is affected by the mass of the structure and the hydrodynamic parameters. The magnitude of the hydrodynamic parameters, as they will be discussed later, depends on the frequency of motion and the structural dimensions. The shape and the dimensions do affect the structural behaviour and are the factors that determine the performance of the floating breakwater.

Regarding the second type of interference, the anchoring of the floating breakwater is necessary to keep the structure at the position where it is supposed to be. Besides the station keeping property, the mooring system is an important parameter that determines the dynamic behaviour of the mass-spring system. There are two types of restraint are generally adopted to keep a floating breakwater at a designated location: either piles or mooring lines. Piles have the advantage of restricting sway and roll motions almost completely, resulting in lower transmission coefficients. However, they have the disadvantage of wear problems at the points of contact with the breakwater. And their use may be limited by large water depths and poor soil conditions at the seabed. On the other hand, mooring lines may be more suitable in deeper water, but may give rise to problems related to connection points to the breakwaters lifting or dragging anchors and they may not limit sufficiently the breakwater motions leading to increased transmission coefficients. Thus, the choice of the mooring lines is selected in all the optimization problems to hold the structure at its position.

The concept of wave interaction with floating breakwaters constitutes a multidisciplinary problem, where a combination of fluid mechanics, dynamic behaviour of mechanical systems, and the vibration theory are introduced to perform a complete analysis capable to clarify the interference between the design parameters. In fact, the simulation of the floating breakwater performance is complicated by the importance of the mutual interaction between fluid and rigid body. Indeed its displacement is caused by the wave load and the wave propagation is influenced in turn by the floating breakwater kinematics, so that the most interesting phenomenon, the wave transmission, can only be found if the fully coupled interaction problem is solved. Thus, the fluid flow can be described by a potential which is the sum of an incident, scattered, and radiated fields. The advantage of this decomposition is that the diffraction (scattering) hydrodynamic problem does not involve the FB dynamics and can be solved first. The radiation hydrodynamic problem, describing the effect of a forced motion, is solved separately. The actual periodic motion is solved at last by a vibration model, deriving the hydrodynamic forces by the diffraction problem and the added mass and damping by the radiated potential.

Formulation of boundary value problem

Fluid is assumed to be ideal, flow is considered as irrotational, so we can apply a linear wave theory. The body is assumed to be rigid. It is assumed that no flow of energy takes place through the bottom surface or the free surface. Energy is gained or lost by the system only through waves arriving or departing at infinity or due to the

external forces acting on the body. The motions are assumed to be small, so that the body boundary conditions are satisfied very close to the equilibrium position of the body. The fluid domain of calculation is defined in Fig 3.4, it is bounded by an artificial radiation boundary at the ocean side and by the reflective sidewall, representing the port terminals, from the right side. A Cartesian coordinate system is used, with the origin at the mean free surface, *Oz* directed positive upwards and *Ox* directed positive in the direction of propagation of waves. The state of the fluid can be completely described by the velocity potential, $\phi(x,z,t) = \mathrm{Re}[\Phi(x,z)e^{-i\omega t}]$, where *Re* denotes the real part of the complex expression $i = \sqrt{-1}$ and t is the time. For the two-dimensional problem considered here, the time independent complex velocity potential $\Phi(x,z)$ satisfies the Laplace equation.

$$\nabla^2\Phi(x,z) = 0 \tag{3.9}$$

The general configuration of an infinitely long floating structure interacting with a monochromatic linear wave of height, *H*, and wave angular frequency, $\omega = 2\pi/T$ is shown in Fig.3.4, where both the diffraction (waves incident on fixed structure) and radiation (structure oscillating in otherwise calm fluid) problems have been treated. It is generally convenient to separate the total velocity potential into incident potential, Φ_I, scattered potential, Φ_S, radiation potentials, Φ_j, j = 1, 2, 3 in three modes, heave, sway and roll. This is mathematically represented as

$$\Phi(x,z) = \Phi_I + \Phi_S + \sum_{j=1}^{3}\Phi_j \tag{3.10}$$

Where $\Phi_j = X_j'\varphi_j$ in which, φ_j is the radiation potential per unit body velocity, X_j'.

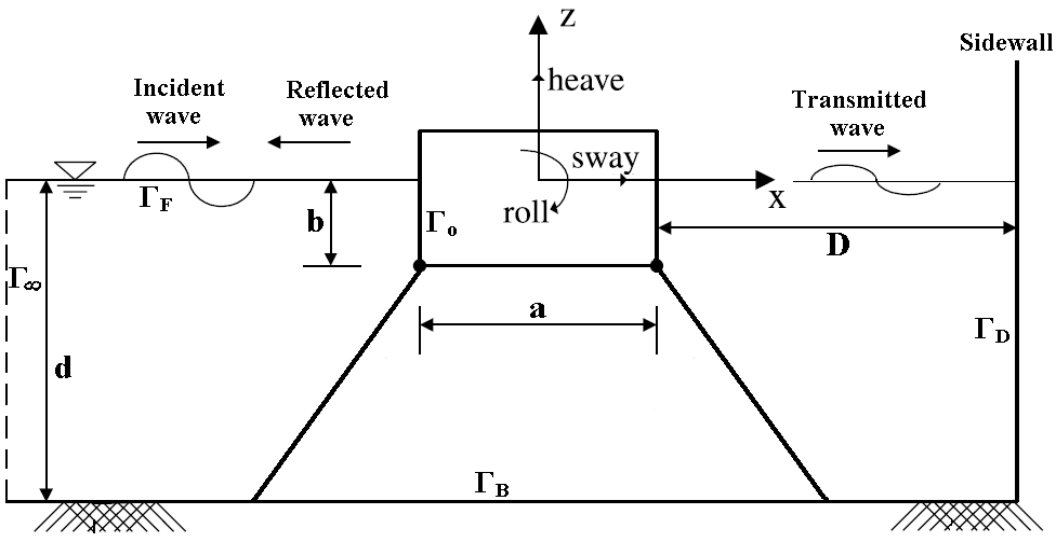

Fig.3.4 Definition sketch for theoretical analysis with a sidewall

It is well known that the incident velocity potential of linear waves propagating from $x = -\infty$ to the positive direction is represented by:

$$\Phi_I = -\frac{igA}{\omega}\frac{\cosh[k(z+d)]}{\cosh(kd)}e^{ikx} \tag{3.11}$$

where *g* is the gravitational acceleration, *d* is the water depth, *A* is the amplitude of wave and *k* is the wave number satisfying the dispersion relation,

$$\omega^2 = gk\tanh(kd) \tag{3.12}$$

Since numerical models based on the linear potential theory have proven to be efficient tools to predict the sea keeping behaviour of floating breakwaters; it is useful to apply it for the diffraction-radiation model and then to use it in evaluating the hydrodynamic coefficients and wave exciting forces.

Diffraction problem

The boundary value problem for the diffracted potential (Φ_D) can be defined by the governing Laplace equation and the boundary conditions as defined below:

$$\Phi_D = \Phi_I + \Phi_S \tag{3.13}$$

$$\nabla^2\Phi_D = 0 \quad \text{in the fluid domain } \Omega \tag{3.14}$$

$$\frac{\partial\Phi_D}{\partial z} - \frac{\omega^2}{g}\Phi_D = 0 \quad \text{at the free surface, } \Gamma_F,\ z = 0 \tag{3.15}$$

$$\frac{\partial\Phi_D}{\partial z} = 0 \quad \text{at the sea bed, } \Gamma_B,\ z = -d \tag{3.16}$$

$$\frac{\partial\Phi_D}{\partial z} + ik\Phi_D = 0 \quad \text{at the radiation boundary, } \Gamma_\infty,\ x \to -\infty \tag{3.17}$$

The infinite boundary Γ_∞ is fixed at a finite distance, $x = x_R$. The position of the radiation boundary relative to the characteristic dimension of the structure and water depth is described in detail by Bai (1977). In the diffraction problem the rigid body is restrained from all its degrees of freedom, the kinematic boundary condition on the body can be expressed as follows:

$$\frac{\partial\Phi_D}{\partial z} = 0 \quad \text{on the body surface, } \Gamma_0,\ z = -b,\ -a/2 \le x \le a/2 \tag{3.18}$$

$$\frac{\partial\Phi_D}{\partial x} = 0 \quad \text{on the body surface, } \Gamma_0,\ x = \pm a/2,\ -b \le z \le 0 \tag{3.19}$$

$$\frac{\partial\Phi_D}{\partial z} = ik\frac{k_r - 1}{k_r + 1}\Phi_D \quad \text{on the sidewall surface, } \Gamma_D,\ x = a/2 + D,\ -d \le z \le 0 \tag{3.20}$$

where $k_r = 1$: corresponds to total reflective sidewall

$k_r = 0.3$: corresponds to partial reflective sidewall

Radiation problem

The wave radiation problem can also be described by a radiated potential represented as

$$\Phi_j(x,z) = -i\omega X_j\varphi_j(x,z) \tag{3.21}$$

The linear radiation boundary value problem is defined by the Laplace equation as a governing equation, and the boundary conditions are as given below:

$$\nabla^2\varphi_j = 0 \quad \text{in the fluid domain } \Omega \tag{3.22}$$

$$\frac{\partial\varphi_j}{\partial z} - \frac{\omega^2}{g}\varphi_j = 0 \quad \text{at the free surface, } \Gamma_F,\ z = 0 \tag{3.23}$$

$$\frac{\partial\varphi_j}{\partial z} = 0 \quad \text{at the sea bed, } \Gamma_B,\ z = -d \tag{3.24}$$

$$\frac{\partial \varphi_j}{\partial z} + ik\varphi_j = 0 \qquad \text{at the radiation boundary, } \Gamma_\infty,\ x \to -\infty \qquad (3.25)$$

For the radiation potentials, φ_j, $j = 1,2,3$, the kinematic body boundary condition or the body-fluid interface may be written as:

$$\frac{\partial \varphi_j}{\partial x} = ik\frac{k_r - 1}{k_r + 1}\varphi_j \qquad \text{on the sidewall surface, } \Gamma_D,\ x = D + a/2 \qquad (3.26)$$

$$\frac{\partial \varphi_j}{\partial n} = n_j \qquad \text{on the body surface, } \Gamma_0 \qquad (3.27)$$

Where n_1 and n_2 are the x and z components of the unit inward normal to the body and $n_3 = (x - x_c)n_2 - (z - z_c)n_1$, in which (x_c, z_c) are the coordinates of the centre of rotation.

The numerical model for water waves can be divided into two parts. On the one hand we have boundary conditions describing the evolution of the boundaries and the potential on the boundaries in time. On the other hand we have an elliptic problem (Laplace's equation) in a domain whose boundaries change in time. These two parts are handled alternately by the numerical model. The boundary conditions are the demanded information to solve the basic equation of wave propagation presented by Laplace equation. This latter is solved using the finite element method described in chapter 2. In more detail, it can be described as follows. At *t* = 0 we have an initial configuration described by a domain Ω_0 and initial conditions for ϕ or $\frac{\partial \phi}{\partial n}$ on the boundary $\partial\Omega_0$ of the domain. For the free surface we specify ϕ and for the bottom we specify $\frac{\partial \phi}{\partial n}$ (=0). Then Laplace's equation is solved in this domain in which all parts of the boundary can be specified as either a Dirichlet boundary (if ϕ is specified) or a Neumann boundary (if $\frac{\partial \phi}{\partial n}$ is specified).

Returning again to chapter 2, we can assimilate the relative values of the elliptic coefficients in Eq. 2.1. $-\nabla.(c\nabla u) + a.u = f$

where the Laplace equation describing the wave propagation is $\nabla^2\Phi(x,z) = 0$,

and *u* stands for the velocity potential of waves Φ. Substituting the relative values of the elliptic coefficients, we obtain the complete form of our specific type of elliptic equation : $c = 1$, $a = 0$, and $f = 0$. Moreover, the entire boundary conditions Eqs. 3.15, 3.16, 3.17, 3.18, 3.19, 3.20, 3.23, 3.24, 3.25, 3.26, and 3.27 are expressed in terms of Dirichlet ($h.u = r$) or Newmann condition ($\vec{n}.(c\nabla u) + q.u = g$) to solve the finite element problem.

A practical application can be considered to explain the phenomenon of floating breakwaters and to show how the radiated waves are an important factor that plays an essential role in the breakwater performance beside the diffraction theory. The wave forces will put the floating breakwater in a harmonic oscillation. The oscillating floating breakwater will produce waves, the so called radiation waves in the three directions (heave- sway-roll). The heights of these radiated waves are directly related to the shape and mass of the structure. These latter are computed with respect to structure velocity as described in Eq. 3.27. As deduced from Fig. 3.5, it is clear that such waves can have high amplitudes that must be minimized by sufficient

mooring system. Thus, reducing the wave heights can be managed by reducing the velocity or simply the breakwater motion along the three directions. (The white area corresponds to the floating breakwater).

In the first figure (diffraction), we notice the wave height reduction between the ocean side (right side of the breakwater) and the port side (left side of the breakwater) due to the presence of the floating breakwater. Where, the underflow (The part of the wave energy that is not influenced by the presence of the floating breakwater) presenting the wave energy underneath the floating breakwater propagates to the leeward protected side. In the rest figures (heave-sway-roll), we can clearly notice the effect of the breakwater oscillations. Radiated waves are generated on the two sides of the breakwater, where the performance of the breakwater is achieved by optimal shape, mass, and mooring system that is capable to reduce the heights of these waves to a minimum. In addition, it can be stated that a structure that performs less sway and roll motions will radiate less wave energy. Because of these arguments, the shape of the floating breakwater is taken rectangular for the rest of this thesis.

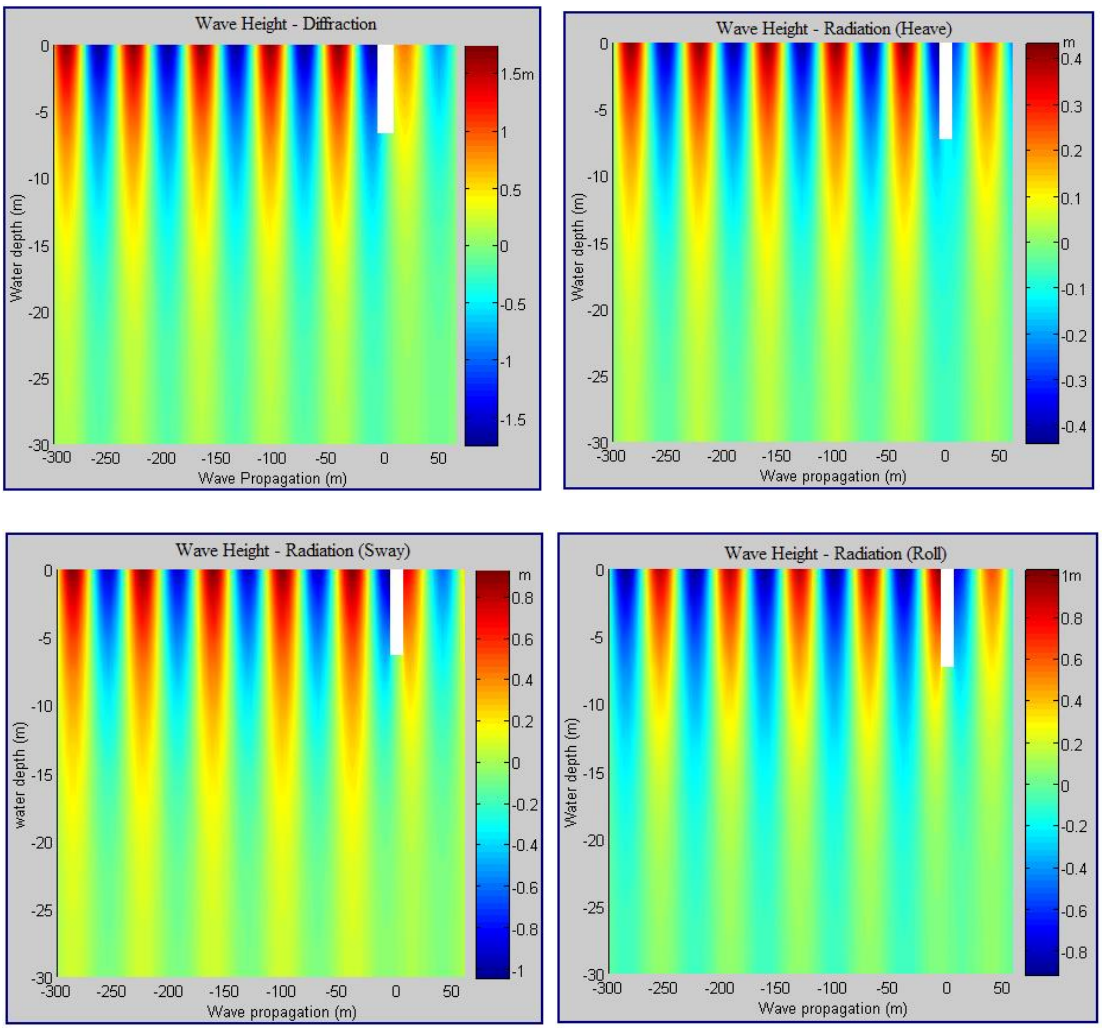

Figure 3.5 Diffracted and radiated waves generated from a floating breakwater
From left to right: Diffraction – Heave – Sway - Roll

3.2-Dynamical behaviour of the floating breakwater

After applying the diffraction-radiation model, the hydrodynamic forces are derived by the hydrodynamic forces and the added mass and damping by the radiated potential. In order to proceed forward and determine the transmission coefficient, an analytical modelling for the vibrating structure is developed. The equations of motions are solved to evaluate structure responses in the three modes of motion, and hence vibrational effects are determined and discussed.

Hydrodynamic forces

The hydrodynamic pressure at any point in the fluid can be expressed as,

$$P(x,z,t) = -\rho \frac{\partial \phi}{\partial t} = i\omega\rho\phi \tag{3.28}$$

Where ρ is mass density of fluid. The hydrodynamic forces can be determined by integrating the pressure over the wetted body surface Γ_0.

$$F_j(x,z,t) = i\omega\rho \int_{\Gamma_0} \phi n_j d\Gamma \tag{3.29}$$

The hydrodynamic forces thus calculated can be separated into wave exciting forces governed by the diffraction problem and the hydrodynamic restoring forces governed by the radiation problem. The wave exciting forces, F_j^e due to the diffracted potential can be expressed as

$$F_j^e(x,z,t) = i\omega\rho \int_{\Gamma_0} (\phi_I + \phi_S) n_j d\Gamma \tag{3.30}$$

Where $j = 1,2,3$ correspond to heave, sway, and roll modes respectively.

Concerning the hydrodynamic restoring forces, a chain of progressive outgoing waves is generated on the free surface from an oscillating floating body. The energy of these waves is that taken away from the energy supplied to the body to sustain its motion. The energy loss to the surrounding fluid is characterized as hydrodynamic damping of the body. This wave damping force constitutes a harmonic conjugate to the added mass force for the oscillating floating body. Then from the radiation potential, the hydrodynamic restoring forces, F_j^h can be evaluated as:

$$F_j^h = \int i\omega\rho X_k^{'} \varphi_k n_j d\Gamma = -\mu_{jk} X_k^{''} - \lambda_{jk} X_k^{'} \tag{3.31}$$

Where μ_{jk} is the added mass coefficient proportional to the body acceleration and λ_{jk} is the damping coefficient proportional to the body velocity. Then, μ_{jk} and λ_{jk} are evaluated from the real and imaginary parts of the complex radiation potential, respectively:

$$\mu_{jk} = \rho \,\mathrm{Re}[\int_{\Gamma_0} \varphi_k n_j d\Gamma] \tag{3.32}$$

$$\lambda_{jk} = \rho\omega \,\mathrm{Im}[\int_{\Gamma_0} \varphi_k n_j d\Gamma] \tag{3.33}$$

Numerical models based on the linear potential theory have proven to be efficient tools to predict the sea keeping behaviour of floating breakwaters; hence, it is useful to apply it to solve the diffraction-radiation problem. The numerical model is based on the finite element method, and then all the integrals defining the hydrodynamic coefficients are also computed numerically.

Structural Dynamic Response

Considering that the floating breakwater will not produce any waves by itself due to structural movements when floating in still water, the only hydro mechanical reaction will occur after the structure is loaded with exciting forces deduced from the incoming waves. These exciting forces and motions will put the floating breakwater in a harmonic oscillation. Once the floating breakwater has been put into oscillation by the incoming waves, it generates radiated waves on its two sides and moreover its motion is affected by the stiffness of the mooring lines and its natural frequency.

Although a floating body seems to have the same dynamic characteristics as a mechanic mass-spring system, there is an important difference that affects the dynamic behaviour. The water, surrounding the oscillating floating breakwater will determine the total mass and the damping of the system (Fig. 3.6). Since the magnitude of the so-called added mass and hydrodynamic damping parameters depend on the motion amplitude and frequency, these parameters are never constant. Therefore, the linear analysis procedure used to analyze the breakwater's motion is similar to the free vibration theory in air (Fig. 3.6). However, three new elements are introduced here. The motions are forced due to the waves passing over the structure, damping due to the fluid structure interaction is included, and the added mass term is included to account for the decreased response of the structure due to the presence of the external water. Then, the equation of motion, in matrix form, that describes the motion of the floating breakwater is given as:

$$[M+\mu]X^{''}+\lambda X^{'}+KX=F_j^e(t) \qquad (3.34)$$

Where the matrices of additional mass, μ, the damping matrix, λ, and the exciting forces, F_j^e, are determined from the previous parts. The resting terms or matrices M and K (body mass matrix and rigidity matrix) are derived from the Lagrange equations for the oscillating system considered in air and having three degrees of freedom. In the frequency domain, and due to the harmonic type of exciting forces ($F_j^e = f_j^e e^{-i\omega t}$), the response of the structure in waves can be found by:

$$[-\omega^2(M+\mu)-i\omega\lambda+K]\delta_j = f_j^e \qquad (3.35)$$

δ_j is the complex amplitude of the motion response, $X_j = \delta_j e^{-i\omega t}$.

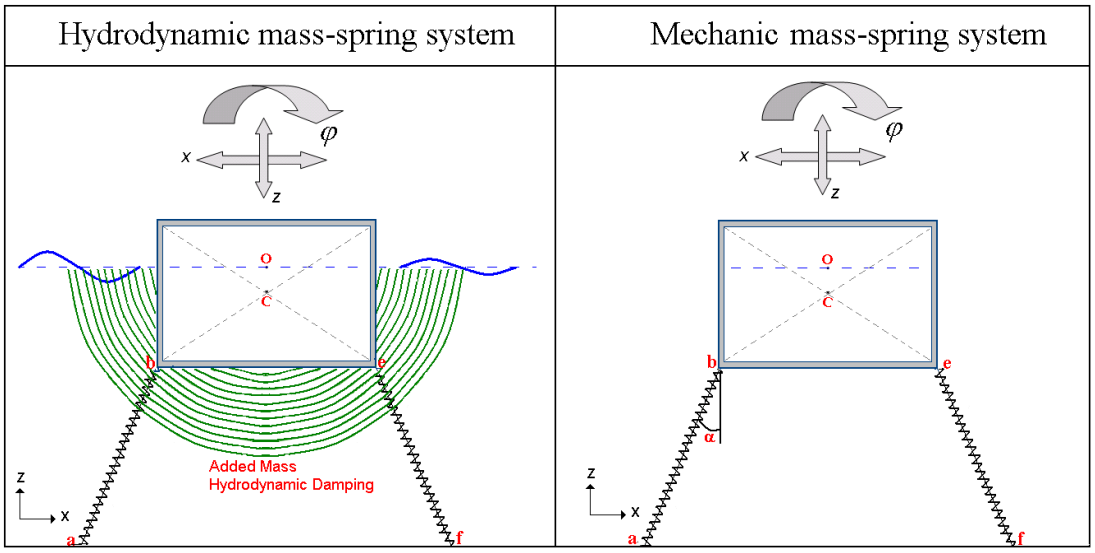

Fig.3.6 Representation of a hydrodynamic and a mechanic mass-spring system

The structural response will be analyzed by assuming that the breakwater behaves as a two dimensional rigid body undergoing small amplitude heave, surge, and pitch motions. The Lagrange expression is:

$$L = \frac{1}{2}Mx_c^{'2} + \frac{1}{2}Mz_c^{'2} + \frac{1}{2}I\theta^{'2} + \frac{1}{2}k\left(\sqrt{(x_e - x_f)^2 + (z_e - z_f)^2} - l^2\right) + \frac{1}{2}k\left(\sqrt{(x_a - x_b)^2 + (z_z - z_b)^2} - l^2\right) \tag{3.36}$$

To trace the rotational motion of the body and likewise any point on the body other than the centre of gravity, the Euler angles will be used. And then the points of connection (e and b) of body to the mooring lines of length (l) can be expressed in terms of translation of the centre of gravity and the body angle of rotation as follows:

$x_e = x_c + e_1\cos\theta + e_2\sin\theta$

$z_e = z_c + e_1\cos\theta - e_2\sin\theta$

Hence, the three equation of motion based on Lagrange equation can be expressed in terms of the three degrees of freedom (x_c, y_c, θ):

$$\frac{d}{dt}\left(\frac{\partial L}{\partial q'}\right) - \frac{\partial L}{\partial q} = 0 \tag{3.37}$$

This formulation yields to nonlinear equations, which can be linearized by assuming small perturbations around the equilibrium positions.

$x_c = x_{ceq} + x_{cnew}$, $z_c = z_{ceq} + z_{cnew}$, $\theta = \theta_{eq} + \theta_{new}$

Finally, the equations of motions of the breakwater acted upon by the waves may be written as:

$$\begin{aligned} &Mx''_{cnew} + kx_{cnew}[2 + lG^{-3/2}r^2 - lG^{-1/2} + lH^{-3/2}u^2 - lH^{-1/2}] + kz_{cnew}[lG^{-3/2}rs + lH^{-3/2}uv] + \\ &k\theta_{new}[e_2 + lG^{-3/2}(e_2r^2 - e_1sr) - lG^{-1/2}e_2 + b_2 - lb_2H^{-1/2} + lH^{-3/2}(b_2u^2 - b_1uv)] = 0 \end{aligned} \tag{3.38}$$

$$\begin{aligned} &Mz''_{cnew} + kx_{cnew}[lG^{-3/2}rs + lH^{-3/2}uv] + kz_{cnew}[2 + lG^{-3/2}s^2 + lG^{-1/2} + lH^{-3/2}v^2 + lH^{-1/2}] + \\ &k\theta_{new}[-e_1 + lG^{-3/2}(e_2rs - e_1s^2) + lG^{-1/2}e_1 - b_1 + lb_1H^{-1/2} + lH^{-3/2}(b_2uv - b_1v^2)] = 0 \end{aligned} \tag{3.39}$$

$$\begin{aligned} &I\theta''_{new} + kx_{cnew}[e_2 + lG^{-3/2}\left(e_2r^2 - e_1rs\right) + lH^{-3/2}\left(b_2u^2 - b_1uv\right) + b_2 - le_2G^{-1/2} - lb_2H^{-1/2}] + \\ &kz_{cnew}[-e_1 + lG^{-3/2}\left(e_2rs - e_1s^2\right) + lH^{-3/2}\left(b_2uv - b_1v^2\right) - b_1 + le_1G^{-1/2} + lb_1H^{-1/2}] + \\ &k\theta_{new}[e_1^2 - e_2s + lG^{-3/2}(e_er - e_1s)^2 - lG^{-1/2}(e_2^2 - e_1r + e_1^2 - e_2s) + b_1^2 - b_2v + e_2^2 - e_1r + b_2^2 - b_1u + \\ &\quad lH^{-3/2}(b_2u - b_1v)^2 - lH^{-1/2}(b_2^2 - b_1u + b_1^2 - b_2v)] = 0 \end{aligned} \tag{3.40}$$

Where:

$r = x_{ceq} + e_1 - f_1$ $\quad s = y_{ceq} + e_2 - f_2$ $\quad G = r^2 + s^2$

$u = x_{ceq} + b_1 - a_1$ $\quad v = y_{ceq} + b_2 - a_2$ $\quad H = u^2 + v^2$

And,

$e(e_1, e_2)$, $f(f_1, f_2)$, $a(a_1, a_2)$, $b(b_1, b_2)$

$x_{ceq} = 0$, $\theta_{eq} = 0$

These three equations of motion are assembled in matrix form in order to directly substitute the elements of the K and M matrices in the principal equation (Eq. 3.34).

$$\begin{bmatrix} M & 0 & 0 \\ 0 & M & 0 \\ 0 & 0 & I \end{bmatrix} \begin{bmatrix} x'' \\ z'' \\ \theta'' \end{bmatrix} + \begin{bmatrix} K_{11} & K_{12} & K_{13} \\ K_{22} & K_{22} & K_{23} \\ K_{31} & K_{32} & K_{33} \end{bmatrix} \begin{bmatrix} x \\ z \\ \theta \end{bmatrix} = 0$$

Now, the response amplitude can be directly derived from Eq. 3.35, and the total velocity potential (Eq. 3.10) can be simply calculated. Thus, the surface elevation for any point in the fluid domain can be derived by:

$$\eta(x,t) = \frac{i\omega}{g}\phi(x,z,t) \tag{3.41}$$

And the transmission coefficient is given by

$$C_T = \frac{H_T}{H_I}, \tag{3.42}$$

where H_T, H_I are the transmitted and the incident wave heights respectively.

3.3 Parametrical Analysis

A lot of research has been done on the hydrodynamic behaviour of floating breakwaters. The main focus of all these studies has always been to obtain transmission coefficients that are as small as possible. The transmission coefficient is the ratio between the wave height at the leeward (harbour) side of the floating breakwater relative to the wave height of the incident wave. In order to obtain satisfactory results, many designs were model-tested. Although the tested models do vary in design, the common research topics can be split into the influence of the structural design and the structural dynamics on the wave attenuating capacity of the structure. The novelty in this study is the inclusion of the reflective sidewall of the port in the domain of computation. When a ship is parked in the port, the waves are reflected due to a vertical sidewall. So it is different to the problems of structures oscillation on water surface with unbounded domain. Moreover, in presence of this sidewall, that really describes a real port problem, it seems to create a bounded domain from the port side or simply an enclosed area (Fig 3.4). Thus, any wave may be forced to resonance in port side due to specific value of the clearance distance between the sidewall and the breakwater. Finally, it must be clear that we are facing two sources of resonance, one being represented by any coincidence between the oscillating frequency of the structure and that of the wave; where the other kind is the wave itself inside the port region. Thus, the resonance phenomenon plays an important role in such problems, especially when a structure oscillating in presence of an incoming wave that has its own periodic frequency may enter the resonance bands, and destructive results appear. The major aspects of the structural design that have been tested and that really influence the (hydro)dynamic behaviour of the floating breakwater:

- Shape
- Width of the floating section of the structure
- Draft of the structure
- Mass of the structure
- Mooring system

The model that was discussed in the previous section is used to verify the influence of the structural variables on the wave attenuating capacity of the floating breakwater. The transmitted wave height depends on width, draft, stiffness, mooring angle, wave period or frequency, incident wave height, and finally the clearance distance**;** hence it can be expressed as: $H_T = f(a,b,k,\alpha,T,H_I,D)$**.** The table below (Table 3.1) summarises the different types of structures and their relevant properties considered during the analysis study. The grey spaces correspond to the varying parameters in the various type of analysis listed in column1. The influence of the motion and the structural parameters on the total wave transmission is determined in presence of the reflective sidewall, where resonance peaks and high transmission coefficients are obtained due to its presence. In order to reduce this phenomenon, we have tried to change the characteristics of this wall by proposing it as partial reflective $(k_r = 0.3)$. This surely contributes to scatter the waves in all the directions instead of reflecting it in the same path and also to reduce the quantity of reflected one, and hence wave energy is diffused. Finally, its influence on the wave transmission is studied and compared to the totally reflective wall.

Parameters Analysis	Width (m)	Draft (m)	Clearance Distance (m)	Wave Period (s)	Mooring stiffness (N/m)	Mooring angle (º)	Floating Mass (kg)
1-Clearance (D)	16	12	[40-300]	[4-14]	$5x10^6$	30	$1.9x10^5$
2-Draft (b)	16	[2-20]	180	[4-18]	$5x10^6$	30	
3-Width (a)	[2-26]	12	180	[4-18]	$5x10^6$	30	
4-Angle (α)	16	12	180	9	$[2-7]x10^6$	[0-90]	$1.9x10^5$
5-Stiffness (k)	[2-30]	12	180	9	$[3-8]x10^6$	30	

Table 3.1 Different configuration structures and their relevant parameters

Sidewall Clearance Distance

The important effect of the clearance on the transmitted wave height is examined in detail. It is found that the transmitted wave height has great change over certain values of the parameter D. This is called the resonance, and is mainly caused by energy accumulation in enclosed domain or the interference between the reflected waves from the sidewall and the incident waves (radiation waves) in the port side regardless from the oscillation frequency of the structure itself.

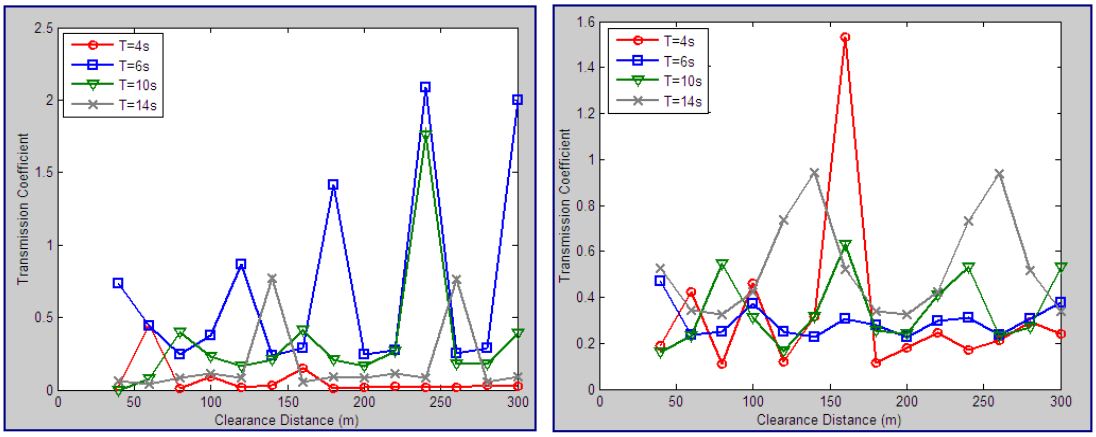

Fig.3.7 Effect of clearance distance on the transmitted wave height (k_r=1,left ; k_r=0.3, right)

In Figure 3.7, the effect of the clearance distance on the transmission coefficient is studied for different wave periods, and we can conclude the following:

1 Repetition of resonance peaks over a distance of $D = L/2$ as Hsu and Wu (1996) have concluded (L denotes the wavelength).
2 The problem of resonance cannot be avoided but can be dominated by varying the distance D.
3 There is an influence of the partial reflection coefficient (k_r) on the transmitted wave height. Sharp resonance peaks for the waves ($T = 6\text{sec}, T = 10\text{sec}$) have disappeared, where we can notice exceptionally an increase in the value for $T = 4\text{sec}$.

Finally, we can deduce that the effect of the clearance distance can be controlled by a partial sidewall for a two dimensional model to reduce the energy accumulation in the bounded region of the port. Also, this approaches it from the real case of a three dimensional port, where the clearance distance varies from point to other (Fig. 3.8). Hence, this will automatically diffuse the energy waves inside the port even though total reflective walls are considered.

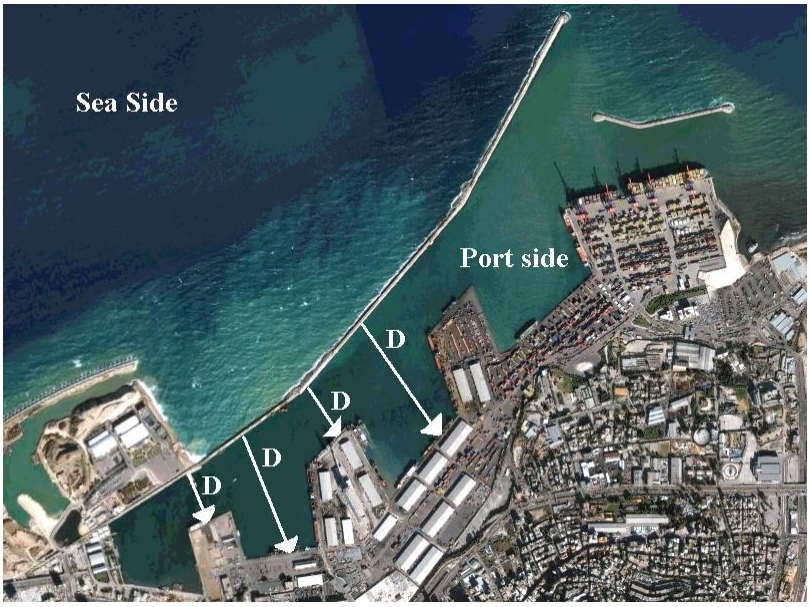

Figure 3.8 Variation of clearance distance in a real port

Draft

The influence of the draft on the transmission coefficient of the floating breakwater is presented in Figure 3.9; a variable draft with different wave periods is considered. The mass automatically changes when the draft is changed and the width is kept constant, this causes a change in the natural frequency of the body and influences also the hydrodynamic coefficients.

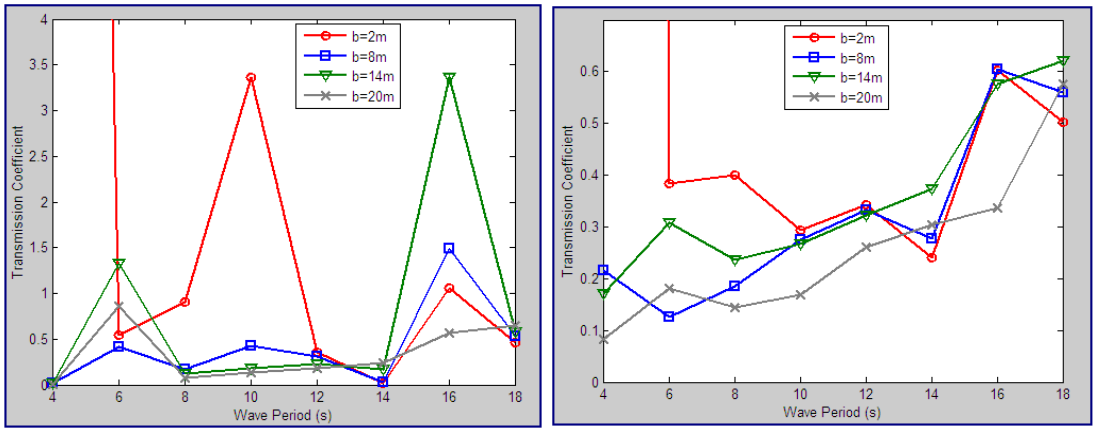

Figure 3.9 Effect of breakwater draft on the transmission coefficient (k_r=1,left ; k_r=0.3, right)

From Fig.3.9, we can deduce the following:

1 Resonance peaks mainly occurring at 6 and 16 sec, this return to the considered value of clearance distance D (Fig.3.7).
2 Increasing the draft yields to decrease the transmission coefficient and especially in the resonance bands, since a heavier structure is hard to put it into oscillation. Therefore optimal solution exists.
3 A draft of 2m is the worse over all the range of wave periods.

4 Decreasing the value of k_r will decrease the values of the transmission coefficients over all the range. Transmission values decreased from [0-3.5] to [0-0.6].
5 Moreover, the importance of increasing the draft appears clearly with decreasing the reflection coefficient. (Fig.3.9 right)
6 At longer periods, all the curves intersect around a value of 60%. This is due to the small variation of the incident potential inside the fluid domain over the vertical direction, and hence the major part of the underflow is being transmitted to the port side. This verifies that the floating breakwaters are less efficient for long wave periods.

Width

The influence of the width on the wave transmission depends on the draft and the weight of the structure. When the structural width is increased while the draft is kept constant, the mass will increase too. Although the horizontal wave force on the structure will not change, the increase of the mass is the reason why the motion amplitude decreases. The decrease of the resonance peak for structures with a large width is due to the large hydrodynamic damping. Similar to draft analysis, important reductions in the transmission values and resonance limitations are obtained by reducing the reflection coefficient (Fig.3.10).

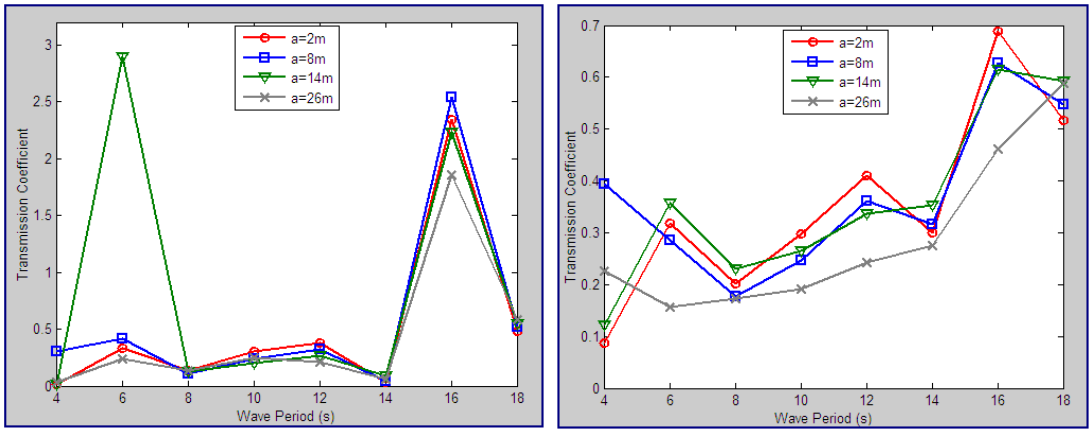

Fig.3.10 Effect of breakwater width on the transmission coefficient (k_r=1,left ; k_r=0.3, right)

Angle of inclination of mooring lines

The angle of inclination of mooring line α (Fig. 3.6) constitutes an important effect in determining the natural frequency of the breakwater. Its value is introduced in the elements of the stiffness matrix K, through the coordinates of the points a and f (Fig.3.6). In Fig.3.11, the study is elaborated for the effect of the line angle and the stiffness on the structural motions of the breakwater for a given wave characteristics.

1 It is observed at an inclination angle range (10°-20°), sharp resonance peaks occur, and then the transmission coefficient stabilise whatever the value of the mooring stiffness.
2 The mooring lines with high stiffness values have the lowest resonance peaks.
3 Therefore, we can conclude that a useful domain of inclination angle can be taken from (30°-80°), but surely the 30° angle will be the optimal value for an inclination angle from the economic point also, since higher angles yields to longer cables.

4 Normally, the reflection coefficient has no visible effect on the mooring angles for a given breakwater, since it will affect neither the stiffness nor the mass.

5

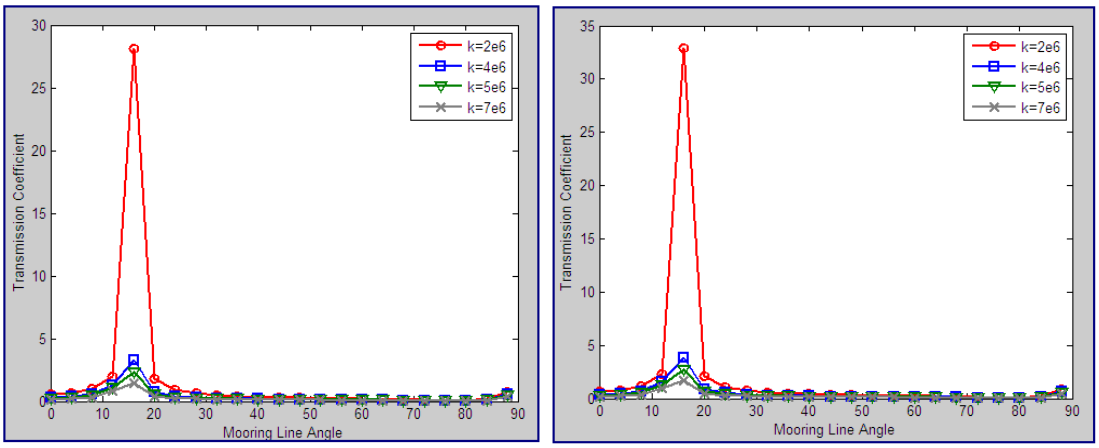

Fig.3.11 Effect of the mooring line inclination angle on the transmission coefficient (k_r=1,left ; k_r=0.3, right)

Mooring stiffness

The mooring stiffness plays an important role in structure stability and its vibrational effects. All the wave generating factors change when the mooring stiffness is changed.

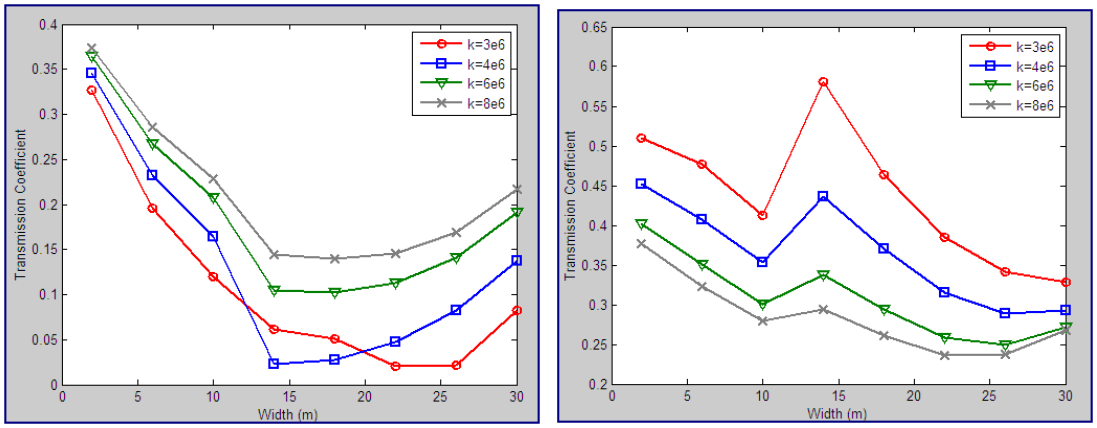

Fig.3.12 Effect of the mooring line stiffness on the transmission coefficient (k_r=1,left ; k_r=0.3, right)

From Fig.3.12 we can conclude:

1 For a total reflective sidewall, the curves are almost the same, thus the stiffness does not constitute an important factor in wave attenuation. This is due to the reflected waves that put the structure in a motion opposite to that derived from the incoming waves which is dominating over the stiffness values.

2 For a partial reflective sidewall, the stiffness holds its natural role in stabilizing the structure. Thus, higher stiffness yields to reduce the structure oscillations and hence lower transmission coefficients.

3 Also, it is noticed that the width plays an important role in structure stability or simply in reducing the movement of the oscillating structure. Therefore, the larger the width, the lower the transmission coefficient regardless of the stiffness values.

4 A shift of the resonance peak is achieved when the mass or the spring stiffness of the system is changed. This is due to the fact that a change of mass or spring stiffness results in a different natural frequency.

Finally, this parametrical analysis demonstrates the complexity of a floating breakwater design due to repetitive resonance bands and the interference between the structural parameters. Thus, it is very important to orient the problem towards an optimization approach that can consider all the dangerous regions. Also, we have considered here the variation of the structural parameters without taking into consideration the mechanical resistance of this proposed structure. Then, an additional constraint would be introduced in the optimization problem, holding the mechanical constraints of the structure into account. This may yields to mass variation due to the variation of the internal rectangular section causing changes in the natural frequency.

3.4 Mechanical Modelling

This part is also based on analytical and numerical models. For the first part, the breakwater is divided into four beams and the traditional method of calculating the moments and stresses are applied for each beam. The second part covers the numerical analysis by applying the finite element method. This constitutes a pure structural analysis of the floating breakwater that must be included in the optimization constraints. It yields to compute the mechanical stresses that must be restricted to a certain limit in the optimal design.

Analytical model

The floating breakwater is modelled as a frame structure fixed on two simple supports at its bottom, where it can be simply divided into four beams with assimilating the upper rectangular wall as a concentrated force on the upper beam.

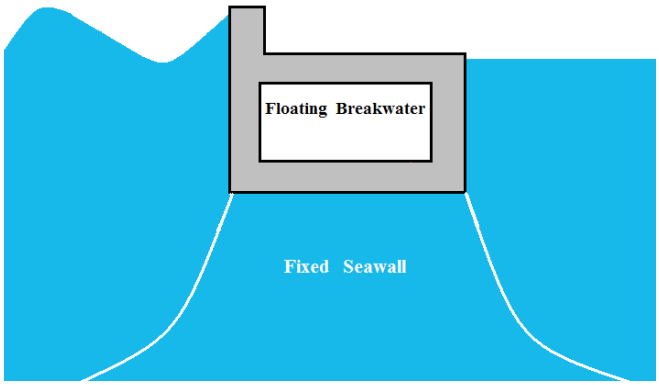

Figure 3.13 Floating breakwater with an additional wall

Each beam is equilibrated by the internal reactions and moments generated from frame division, and hence the equilibrium conditions can be applied for each beam alone to determine the internal efforts and moments yielding to the deflection and stress calculations, (Fig.7) $\Sigma F_x = 0$, $\Sigma F_y = 0$, $\Sigma M = 0$. All the forces are distinguished from each other by different colours and are well explained in the figure below.

This constitutes a problem of 12 variables (Ni, Vi, and Mi where $i = 1,2,3,4$) with 12 equations, but in fact there is only 9 effective equations (equilibrium conditions for beam 1-4, 1-2, 2-3) and the last 3 equations (beam 3-4) are linearly dependant and will not help to solve the system of 12 variables.

This problem is of the hyper-elastic type, where the number of equations is not sufficient to determine the corresponding variables [11], and it is necessary to include three other relations deduced from applying Castigliano's theorem on the fixed nodes (beam 1-4 and 1-2).

$\lambda_i = \frac{\partial W}{\partial F_i} = \int M \frac{\partial M}{F_i} \frac{dx}{EI}$, λ_i being the displacement of the node where the force F_i is applied, and M the distribution of moment along the beam.

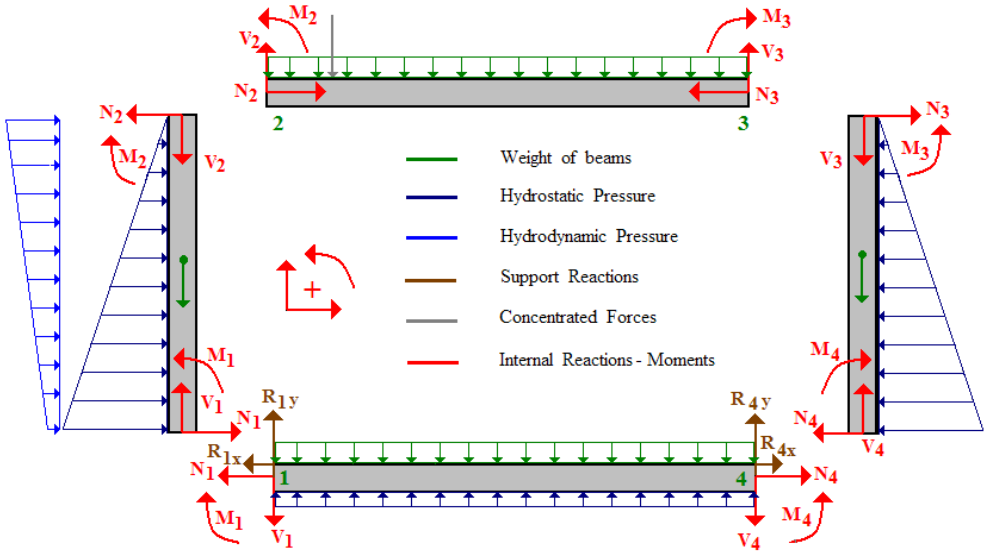

Fig. 3.13 Forces and moments distributions

The bending moments along each beam is determined by the traditional way of beam theory, $\Sigma M_I = 0$:

Applying the global equilibrium conditions for the whole frame: $\Sigma F_x = 0$, $\Sigma F_y = 0$, $\Sigma M = 0$, the support reactions are expressed in terms of the variable vector x by:

$$R_{1y} = (\rho_m x_4 - \rho L) g \frac{x_1}{2} - (a\cosh(kd) + b\cosh(2kd) + f)\frac{L^2}{3x_1} + \rho_m g x_3 \frac{x_1}{2} + \rho_m g x_5 L + \rho_m g H c\left(1 - \frac{c}{2x_1}\right) \tag{3.43}$$

$$R_{4y} = (\rho_m x_4 - \rho L) g \frac{x_1}{2} + (a\cosh(kd) + b\cosh(2kd) + f)\frac{L^2}{3x_1} + \rho_m g x_3 \frac{x_1}{2} + \rho_m g (x_1 - x_2 - x_5) L + \rho_m g H \frac{c^2}{2x_1} \tag{3.44}$$

$$R_{1x} - R_{4x} = (a\cosh(kd) + b\cosh(2kd) + f)\frac{L}{2} \tag{3.45}$$

Applying the local equilibrium conditions for each beam:

Beam 2-3:

$$\begin{cases} V_2 + V_3 = \rho_m g x_1 x_3 + \rho_m g c H \\ N_2 - N_3 = 0 \\ M_2 - M_3 + V_3 x_1 = \frac{1}{2}\rho_m g x_3 x_1^{\,2} + \frac{1}{2}\rho_m g c^2 H \end{cases}$$

Beam 1-2:

$$\begin{cases} V_1 - V_2 = \rho_b g x_5 L \\ N_2 - N_1 = \frac{\rho g L^2}{2} + (a\cosh(kd) + b\cosh(2kd) + f)\frac{L}{2} \\ M_1 - M_2 + N_2 L = (a\cosh(kd) + b\cosh(2kd) + f)\frac{L^2}{3} + \frac{\rho g L^3}{6} \end{cases}$$

Beam 1-4:

$$\begin{cases} V_1 + V_4 = R_{1y} + R_{4y} - (\rho_b x_4 - \rho L) g x_1 \\ N_4 - N_1 = R_{1x} - R_{4x} \\ M_4 - M_1 - V_4 x_1 = (\rho_b x_4 - \rho L) \dfrac{g x_1^2}{2} - R_{4y} x_1 \end{cases}$$

Castigliano's theorem is applied in beam 1-4 on the node1 and on the node 4, and beam 1-2 on the node 1; which give 3 new equations to complete the system. (The vertical displacement of the nodes 1 and 4 are equal to zero since it simply supported)

$$\begin{cases} \dfrac{M_1 L^2}{2} + \dfrac{N_1 L^3}{3} + \dfrac{11 \rho g L^5}{120} + (a\cosh(kd) + b\cosh(2kd) + f)\dfrac{L^4}{30} = 0 \\ -\dfrac{M_1}{2} + \dfrac{V_1 x_1}{3} + (\rho_b x_4 - \rho L) g \dfrac{x_1^2}{8} - R_{1y} \dfrac{x_1}{3} = 0 \\ -\dfrac{M_4}{2} + \dfrac{V_4 x_1}{3} + (\rho_b x_4 - \rho L) g \dfrac{x_1^2}{8} - R_{4y} \dfrac{x_1}{3} = 0 \end{cases}$$

Finally, it ends up with a system of 12 variables with 12 equations, where these 12 variables ($Ni, Vi,$ and Mi) are determined in terms of the breakwater geometrical dimensions x_1, x_2, x_3, x_4, x_5.

The next step in this structural part, after determining the internal efforts and moments, is to develop the expressions of the bending stresses, and the deflections, in order to present them as new constraints needed to be respected in design. Having the bending moments calculated before in terms of $Ni, Vi,$ and Mi; the vertical displacements and the bending stresses can be easily deduced based on the following: $EIy'' = M(x)$, where y'' is the second derivative of the beam deflection, E is the Young Modulus of the inside material, I is the moment of Inertia of the corresponding beam.

$\sigma = \dfrac{Me}{2I}$, where e is the beam thickness

The deflections' constraints are expressed as follows:

$$f_3(x_2, x_3, x_4, x_5) = \frac{1}{EI_{23}}[-\frac{\rho_m g x_3}{24} x^4 + \frac{V_2}{6} x^3 - \frac{M_2}{2} x^2 - \frac{\rho_m g c^2 H}{4} x^2 - \frac{M_2 x_1}{2} x - \frac{v_2 x_1^2}{6} x + \frac{\rho_m g x_3 x_1^3}{24} x + \frac{\rho_m g c^2 H x_1}{4} x] \quad (3.46)$$

$$f_4(x_2, x_3, x_4, x_5) = \frac{1}{EI_{14}}[-\frac{(\rho_m x_4 - \rho L) g}{24} x^4 - \frac{V_1}{6} x^3 + \frac{R_{1y}}{6} x^3 + \frac{M_1}{2} x^2 - \frac{M_1 x_1}{2} x + \frac{V_1 x_1^2}{6} x + \frac{(\rho_m x_4 - \rho L) g x_1^3}{24} x - \frac{R_{1y} x_1^2}{6} x] \quad (3.47)$$

$$f_5(x_2, x_3, x_4, x_5) = \frac{1}{EI_{12}}\left[\frac{\rho g}{120}(1 - \frac{H}{L}) y^5 - \frac{\rho g L}{24} y^4 - \frac{N_1}{6} y^3 - \frac{M_1}{2} y^2\right] \quad (3.48)$$

The bending stresses' constraints are expressed as follows:

$$f_6(x_2, x_3, x_4, x_5) = \left[M_1 - V_1 x - (\rho_m x_4 - \rho L) g \frac{x^2}{2} + R_{1y} x\right] \frac{x_4}{2I_{14}} \quad (3.49)$$

$$f_7(x_2, x_3, x_4, x_5) = \left[-M_2 + V_2 x - \rho_m g x_3 \frac{x^2}{2} - \rho_m g H \frac{c^2}{2}\right] \frac{x_3}{2I_{23}} \quad (3.50)$$

$$f_8(x_2, x_3, x_4, x_5) = \begin{bmatrix} -M_1 - N_1 y - \dfrac{(a\cosh(kd) + b\cosh(2kd) + f)y^3}{6L} \\ -\dfrac{\rho g y^3}{3} - \dfrac{\rho g (L-y) y^2}{2} \end{bmatrix} \frac{x_5}{2I_{12}} \qquad (3.51)$$

Numerical model

The numerical analysis of the mechanical behaviour of this floating breakwater is based on the finite element method (FEM) using the software Matlab. In fact, Matlab solve the problems of (FEM) under the partial differential equations toolbox (PDE Tool), where the mechanical problem is assimilated to an elliptic equation under the form: $-div(c \times grad(u)) + a \times u = f$ in Ω, where Ω is a bounded domain in the plane, *u* is the solution vector, *c, a ,f* are complex functions defined on Ω. In structural mechanics the main problem is concentrated in solving the equilibrium equation $\vec{div}\,\sigma + \vec{f}_v = \vec{0}$ in a determined structural domain exposed to different boundary loadings (forces and displacements).

To solve this classical equilibrium equation under the elliptic family of equations, the elliptic coefficients *u, c, a ,f* are defined in terms of their equivalence substitutes in a mechanical problem. The *u* represents the nodal displacement vector in the two directions, *a* equals to zero, *f* represents the volume forces or simply the weight $(-\rho_m \times g)$, and *c* stands for the matrix deduced from the stress-strain relation, assuming isotropic and isothermal conditions.

$$\begin{pmatrix} \sigma_x \\ \sigma_y \\ \tau_{xy} \end{pmatrix} = \frac{E}{1-\upsilon^2} \begin{pmatrix} 1 & \nu & 0 \\ \nu & 1 & 0 \\ 0 & 0 & (1-\upsilon)/2 \end{pmatrix} \begin{pmatrix} \varepsilon_x \\ \varepsilon_y \\ \gamma_{xy} \end{pmatrix} \qquad (3.52)$$

where σ_x and σ_y are the stresses in the *x* and *y* directions, and τ_{xy} is the *shear stress*. The material properties are expressed as a combination of *E*, the elastic modulus or Young's modulus, and υ Poisson's ratio. The basic finite element procedure starts by describing the geometry of the domain Ω and the boundary conditions. The boundary conditions specify a combination between *u* and its normal derivative on the boundary, and are defined either under the Dirichlet form (defining displacement) or under the Neumann form (defining forces). Second, a triangular mesh is built up on the domain Ω; and finally the structure is discretized into many subregions and for each subregion the displacement field is written in terms of nodal values. The total potential energy is then minimized with respect to the nodal values to give the equilibrium relation:

$\{F\} = [k] \times \{u\}$, where *{u}* is the vector of nodal displacements, *{F}* is the vector of element nodal forces, and [*k*] is the element stiffness matrix. Once the displacement vector *u* is computed, it is easy to move deeper and calculate the mechanical stresses and finally the principal stresses, where these latter stresses are the one substituted in the structural constraint expression.

3.5 Conclusion

Although a lot of theoretical and practical research has been done, no practical solution has been found for the general problem of creating an optimal floating breakwater, able to attenuate strong waves. The floating breakwaters that have been built in real situations were designed to serve at specific locations with mild wave conditions. This resulted in huge and expensive constructions, like the Monaco floating breakwater (Fig 1.9), or cheap and temporary structures like the RIBS floating breakwater (Fig 1.5). From the model tests, it can be concluded that there seems to be an optimal floating breakwater design for every wave frequency. The structural appearance of the floating breakwater might change whenever the frequency of the incoming wave train changes in order to attenuate the wave optimal.

Chapter 4

Optimization of Floating Breakwaters

Several optimization problems of floating breakwaters are studied in this chapter. It is divided into two parts: The first one considers a simplified model of the interaction waves-breakwater, where the motion of the latter is neglected; therefore no radiating waves are generated. It constitutes from shape optimization with a predefined shape, then a topology optimization, and the last method concerns the shape optimization with a variable number of points forming a geometrical shape. The second part, takes into consideration the dynamical behaviour of the floating breakwater. Thus, it compromise a complete model of the floating breakwater and its shape optimization is an important problem where the dimensions, shape, mass, and mooring system plays an effective role in the design. Moreover, the optimal shape is also affected by the resonance phenomenon that also must be included.

4.1 General

Structural optimization is a subject which has attracted the interest of the researches for many years. It refers to the optimal design of the shape or topology of structural components and is of great importance in structural and mechanical engineering. The problem consists in finding the best design of a structural component under certain loading, in order to have minimum weight, or uniformly distributed equivalent stresses. It consists of an iterative process in which repeated improvements are carried out over successive designs until the optimal design is acceptable. In this chapter, we consider the problem of determining the optimal shape and topology of a floating breakwater, which constitutes an ascending type of coastal structures.

Current designs of floating breakwaters are reasonably effective at attenuating moderate to high frequency waves. Although most of the energy in a deep-water wave is concentrated near the surface, some of it is contained in the water at depth. Breakwaters of practical dimensions can therefore intercept only a part of the total wave energy. Typically, floating breakwaters have been used at locations where the wave period ranges up to about 5 sec and wave heights up to about 1 m. Moreover,

the present practice relating to floating breakwater designs is often based on experience with past designs. The large number of variables involved and the variety of existing breakwaters have made it difficult for empirical relationships to be derived. For most large scale applications, it has therefore been necessary to reason to site-specific physical model tests before a particular breakwater design is adopted. Therefore, an optimal design is an essential demand in order to achieve a satisfactory floating breakwater with a minimum weight, or simply to represent a new resistive form, in accordance to the physical and mechanical constraints.

A moored floating breakwater should be properly designed in order to ensure: (a) effective reduction of the transmitted energy, hence adequate protection of the area behind the floating system, (b) non-failure of the floating breakwater itself and (c) non-failure of the mooring lines. The satisfaction of these 3 requirements represents the overall desired performance of the floating breakwater. The reduction of the transmitted energy is achieved by satisfactory dimensions and mass of the floating structure itself, which are important parameters that can be used to optimize its performance. On the other side, the anchoring of the floating breakwater is necessary to keep the structure at the appropriate position. Besides the station keeping property, the mooring system is an important parameter that determines the dynamic behaviour of the mass-spring system. The non-failure analysis of these mooring lines is mainly included in the hydrodynamic behaviour study. Moreover, for a breakwater to float it is obviously designed with a hollow form to reduce the total weight of the structure; where such form complicates the problem and implicates more constraints to be considered during the design.

This study will concentrate on several aspects in order to design a floating breakwater that is capable of attenuating strong waves to satisfy the harbour demands. Both analytical and numerical model will be used as a design tool to optimize the shape and topology of these floating breakwaters that must meet or satisfy the requirements needed in ports. This demonstrate the contribution of the most basic design elements such as draft, width, weight and mooring line stiffness to the performance of the floating breakwater.

4.2 Optimization without dynamical behaviour

In this section, the dynamical behaviour of the floating breakwater is excluded from our study. Thus, we can consider that there are no radiated waves in the port side.

4.2.1 Optimization problem

The reduction of the transmitted energy is achieved by the floating breakwater itself due to a considerable depth and by the fixed seawall concept under the breakwater for the rest underwater region. Moreover, for a breakwater to float, it is obviously designed with a hollow form to reduce the total weight of the structure; where such form complicates the problem and implicates more constraints to be considered during the design.

Fig.4.1 Characteristics of floating breakwater

Thus, improving the performance of floating breakwaters could open up multiple of possible cases and this because the floating breakwater has many parameters characterizing its geometry (Fig.4.1). Some of these parameters are related to the same physical constraint where the rest are determined from other independent constraints, and therefore determining its topology or inward shape cannot be performed as an ordinary calculation problem but it needs an optimisation process in order to compute these parameters taking into consideration their effects on each other. Therefore, the optimisation problem is assumed to be finite dimensional constrained minimization problem, which is symbolically expressed as:

Find a design variable vector x;
to minimize the weight function $f_{ob}(x)$
subjected to the n constraints $C_i(x) < 0, \quad i = 1,....,n$
$G_i(x) = 0, \quad i = 1,....,m$

Objective function

The optimal solution is to design a breakwater respecting all the constraints with a minimum volume, hence the objective is to minimize the weight of the breakwater.
$f_{ob} = \min(Weight)$

Dynamic pressure constraint

The concept of the fixed seawall permits to determine the height of the breakwater in accordance with low hydrodynamic pressure acting on this seawall. The dynamic

wave pressure is mainly concentrated near the free surface and its induced perturbation is low under a certain height (Fig.4.2); then the height of the breakwater can be limited to where the pressure is approximately unvarying corresponding to an approximate value of $P-0.1P\max=0$, where $P\max=P(z=0)$. Finally, the height can be considered to be $L=4m$, where this height is indeed satisfactory for a strong wave $(H=2m)$.

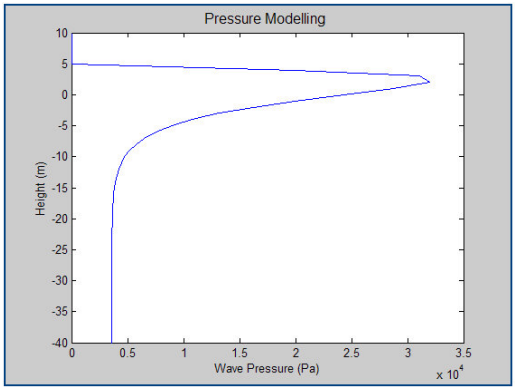

Fig.4.2 Wave Pressure Modelling

This constraint is independent of the other constraints, and then the height of the breakwater is determined only from it and no need to still consider the height as a variable for the rest of the optimization process.

Floating constraint

It is obvious to mention that the floating breakwater must be designed with a hollow form to equilibrate the total weight of the breakwater with the submerged volume, where this yields to an important constraint relating the external dimensions to that of the hollow form**.** It is a direct application of Archimedes principle where the equilibrium equation for floating can be written as: $-\rho_m V_m g+\rho_e V_T g=0$, where ρ_m and ρ designates the densities of the material (concrete) and the sea water respectively, V_m designates the volume of the inside material of the whole breakwater, where V_T designates the volume of the submerged part of the breakwater. In fact, for a moored structure the floating law can be expressed in an inequality in order to minimize the weight, where the difference between the buoyancy force and the weight can be compensated by the tension in the mooring lines.

$$C_1(x)=-\rho_m V_m g+\rho_e V_T g\le 0 \qquad (3)$$

Stability constraint

Stability is defined as the ability of the breakwater to right itself after being heeled over. This ability is achieved by developing moments that tend to restore the breakwater to its initial position. There are a number of calculated values that together determine the stability of a floating breakwater: 1- Initial horizontal equilibrium, 2- Heeled angle, 3- Tension in mooring lines.

First of all, this floating breakwater has a rectangular shape with an arbitrary core, so initially (before any disturbance) it is necessary to maintain a horizontal

equilibrium position. The calculation is based on the basic formula of determining the centre of gravity (G) for a structure composed from different well known determined geometrical shapes and then aligning it with the centre of buoyancy (B) of the floating breakwater (Fig.4) which lies at the geometric centre of volume of the displaced water ($D/2$).

$x_g = \frac{\sum A_i \times x_i}{\sum A_i}$ where A_i and x_i are respectively the area and the centre of gravity of the composing geometries. Therefore, the horizontal equilibrium constraint is expressed as follows:

$$G_1(x) = x_g - \frac{D}{2} = 0$$

Second, when the breakwater is disturbed by a wave, the centre of buoyancy moves from B to B_1 (Fig.4.3) because the shape of the submerged volume is changed; then the weight and the buoyancy force form a couple capable to restore the breakwater to its original position. Moreover, the distance GM known as the metacentric height illustrates the fundamental law of stability, where it must be always positive to create a restoring couple and maintain stability $G\overline{M} \geq 0$.

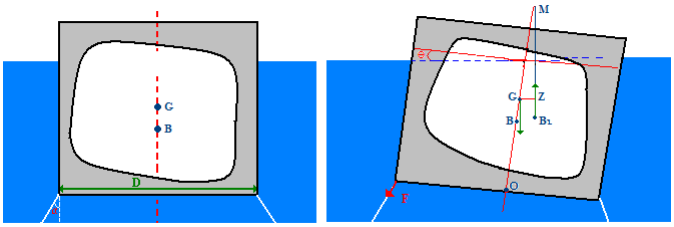

Fig.4.3 Stability of floating breakwater

Finally, stability is achieved by the restoring couple (weight-buoyancy) and by the tension in the mooring lines. This stability is determined around the centre of gravity, hence the moments developed by the restoring couple and the tension in cables must equilibrate the moment derived from the incoming waves.

$|Mp| - M_F - M_B = 0$, where Mp is the moment of the disturbing force (wave), M_F is the moment of the tension in the mooring lines, and M_B is the moment of the buoyant fore (restoring couple). The absolute value of the disturbing moment guarantees the flexibility of the stability relation in the two senses of rotation. Hence, the stability constraint can be expressed by an inequality:

$$C_2(x) = -W\left(\frac{D^2}{12L} - y_g + \frac{L}{2}\right)\sin\theta - F\cos(\alpha-\theta)x_g + F\sin(\alpha-\theta)y_g$$

$$+\left|\int_{-L+y_g}^{0}(a\cosh k(z+d-y_g)+b\cosh 2k(z+d-y_g)+f)zdz\right.$$

$$\left.+\int_{0}^{h-yg}(a\cosh k(z+d-y_g)+b\cosh 2k(z+d+y_g)+f)zdz\right| \leq 0$$

h is the height of the breakwater portion above the still water, α being the angle formed by the mooring lines and the vertical (α=20°), and θ is the angle of disturbance (heeled angle); in fact it is fixed by the designer, and since the breakwater must be very rigid and stable in order to protect the ports from waves, it is taken 1.2°.(slope of 2%)

Structural constraints

The main purpose of this constraint is to compute the mechanical stresses in order to be restricted to a certain limit. It constitutes a pure structural analysis of the floating breakwater. For the case of analytical modelling, the equations of section 3.4 are applied; while, for the case of numerical analysis a finite element method is requested in order to determine the mechanical stresses. In general, it can be summarized by maximizing the stiffness of the structure having a given shape. The floating breakwater is subjected to the hydrostatic forces on its sides and also the hydrodynamic forces exerted by the incoming waves. The forces in the anchoring system are also introduced, which equilibrates the difference between the weight and the pressure exerted on the bottom of the breakwater (Fig.5).

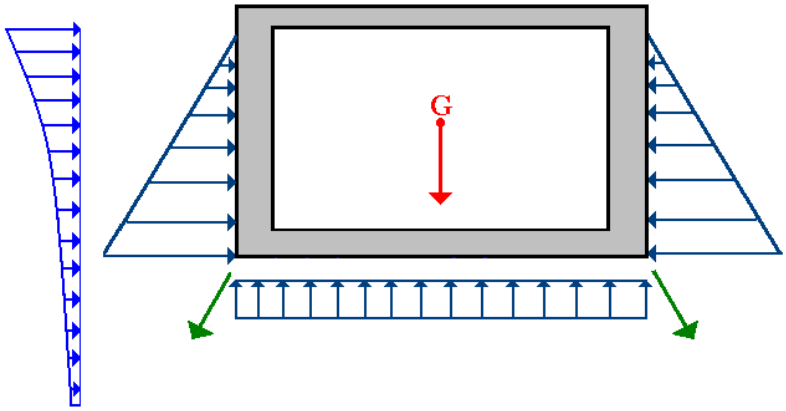

Fig.5 Floating breakwaters subjected to hydrostatic and hydrodynamic forces

It is well known that the concrete have different compression and traction limits due to its nature, and so the well known formula of Von Mises for elastic materials cannot be used. A special criterion, named the Parabolic Criteria, (Garrigues.J, 2001) mainly used for concrete is introduced in terms of the principal stresses of the breakwater and the limit stresses for the material, and is written directly in the form of optimization constraint:

$$C_4(x_1,x_2,x_3,x_4,x_5,x_6)=(\sigma_1-\sigma_2)^2-(\sigma_t+\sigma_c)(\sigma_1+\sigma_2)-\sigma_t\sigma_c\le 0 \qquad (38)$$

where σ_1,σ_2 represent the principal stresses of the structure and σ_t,σ_c represent the limiting stresses for the material constituting the studied structure (hardened concrete: $\sigma_t=6MPa$, $\sigma_c=-60MPa$). This constraint as the others must be computed in each iteration, which yields to solve the FEM problem in each iteration and for each new defined geometry in order to define the principal stresses.

Finally, the optimization problem defined atop, by the objective function and the related constraints, constitutes the theory of the floating breakwater optimization problem. An application of various methods concerning shape and topology optimization are applied and thoroughly discussed. In fact, all the preceding optimization constraints are theoretically reserved through out the different methods, but what is altering is the representation manner of these latter who are directly related to the type of representation of the optimization method itself.

4.2.1- Shape optimization with a predefined geometry

Analytical

All the constraints are expressed in long and complicated equations in terms of the four geometrical parameters x_2, x_3, x_4, x_5, characterising the floating breakwater. Finally, the optimization problem is summarized as follows:

The objective function f_{ob}, establishing the minimum weight of the floating breakwater, has been minimized to design relative breakwater dimensions according to the following non linear constraints:

Objective function:

$$Min \quad f_{ob}(x_2, x_3, x_4, x_5) = Lx_1 - x_2(L - x_3 - x_4) + Hc$$

Constraints:

$$\begin{cases} f_1(x_2, x_3, x_4, x_5, F) = 0 \\ f_2(x_2, x_3, x_4, x_5) = 0 \\ Max(f_3(x_2, x_3, x_4, x_5)) < 0.01m \\ Max(f_4(x_2, x_3, x_4, x_5)) < 0.01m \\ Max(f_5(x_2, x_3, x_4, x_5)) < 0.01m \\ Max(f_6(x_2, x_3, x_4, x_5)) < 3MPa \\ Max(f_7(x_2, x_3, x_4, x_5)) < 3MPa \\ Max(f_8(x_2, x_3, x_4, x_5)) < 3MPa \end{cases}$$

Aside from the constraints of stability, structural, and floating, it was also necessary to establish some additional geometrical constraints:

$$\begin{cases} x_2 - x_1 < 0 \\ x_3 - x_4 < 0 \\ -x_1 < 0, \quad -x_2 < 0, \quad -x_3 < 0, \quad -x_4 < 0, \quad -x_5 < 0, \end{cases}$$

Using the Matlab optimization toolbox and mainly the function ***fmincon***; which is based on the SQP method (sequential quadratic programming), the problem can be solved to determine the variables x_2, x_3, x_4, x_5, F. (same sea wave and material parameters applied for the fixed bottom breakwater)

$$\begin{cases} x_1 = 8.35m, \qquad x_2 = 6.2m, \\ x_3 = 0.8m, \qquad x_4 = 0.8m \\ x_5 = 0.79m, \qquad F = 2.3 \times 10^5 N/1m \end{cases}$$

In order to validate this analytical calculation, a comparison is realized with a numerical approach using the ABAQUS software, one of the leading softwares in the domain of finite element calculation.

The comparison comprises the deflections and the bending stresses of the most affected and most feeble beams (1-4 and 2-3), where in fact the lower beam is holding the weight and the vertical displacement of all the structure, and the upper beam (2-3) is mainly exposed to the horizontal effort (displacement) and its induced moments caused by the sea waves. Using the Matlab, all the preceding equations (moments, deflections, stresses) can be programmed to yield to explanatory curves defining the real state of the floating breakwater when exposed to sea waves.

The upper and lower beam deflections are described by the below curves, showing good agreement with the ABAQUS results. First, the upper beam (2-3) has a decreasing-increasing deflection, where it is obviously explained by the subjected moment of the hydrodynamic pressure on the left side of the breakwater causing the decreasing part ($-8x10^{-5}m$) and moreover due to the weight of the vertical wall fixed on the left side of the floating breakwater; where the compression stresses derived form the hydrodynamic pressure on both sides causes a positive deflection attaining a maximum of $4.8x10^{-4}m$. The same trace has been drawn by ABAQUS with a close maximum deflection of $5.7x10^{-4}m$.

The lower beam is supporting all the weight and also the hydrostatic pressure applied at its bottom which is strong enough to cause an upper deflection ($9.28x10^{-4}m$) towards the hollow section and very close to the results given ABAQUS ($1.1x10^{-3}m$), except for the position of the upward maximum deflection where it is approximately located in the middle of the beam in our analytical calculation and shifted smoothly towards the right in ABAQUS.

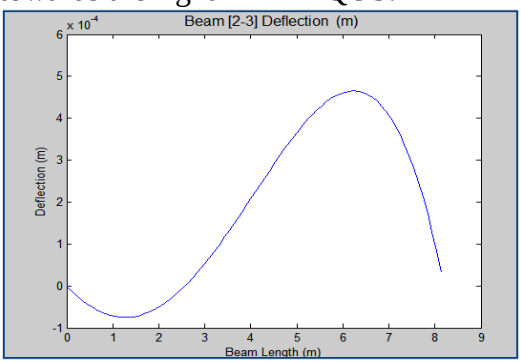

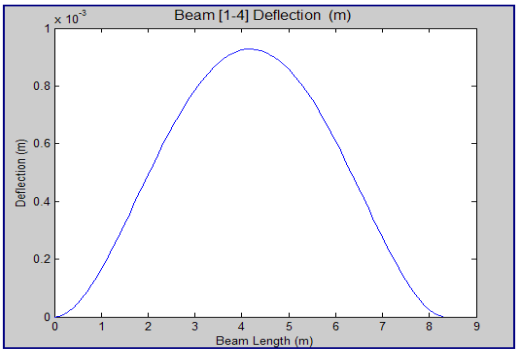

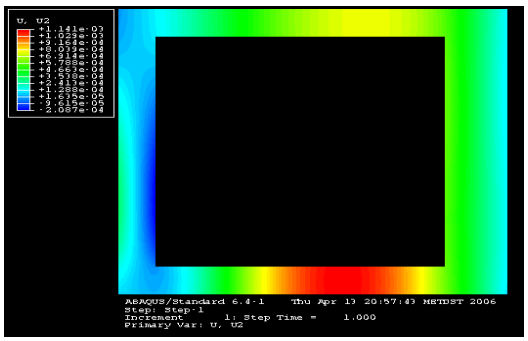

Concerning the bending stresses, a similar comparison to the deflection is realized. The bending stress in the upper beam (2-3) is increasing from *0.9 MPa* on the left side to a value of *2.7MPa* on the right side where it is reaching *2.51 MPa* in ABAQUS. For the lower beam it is decreasing from *3.4 MPa* to a minimum of *-1.7 MPa* and then increasing again. In fact the only value not being respected in the constraints is the bending stress at the node1 and 4, and this is due to the calculation manner of $\max(f_6(x_2, x_3, x_4, x_5))$, where the maximum is located due to the derivative of the function. Despite this, it is normal to have always the large bending stresses located at the fixed supports. In ABAQUS, we can notice that the bending stress is decreasing from *4.34 MPa* to *-1.14 MPa* and then increasing again.

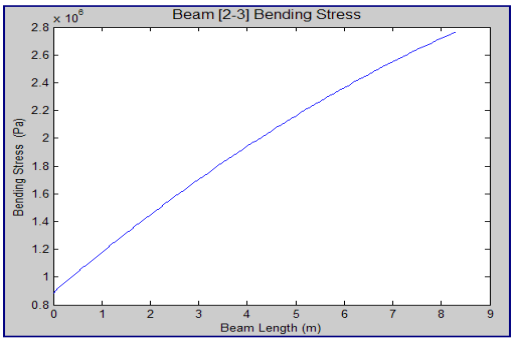

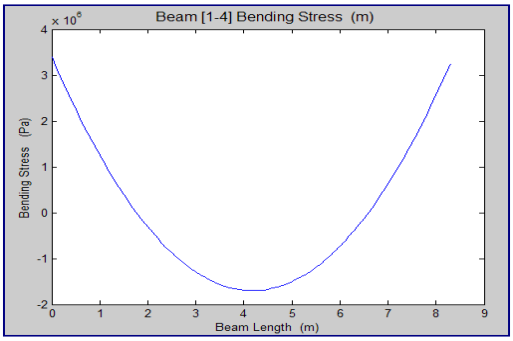

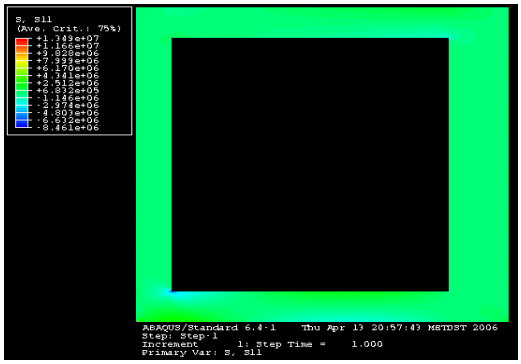

Numerical

A moored floating breakwater should be properly designed in order to ensure: (a) effective reduction of the transmitted energy, hence adequate protection of the area behind the floating system, (b) non-failure of the floating breakwater itself and (c) non-failure of the mooring lines. The satisfaction of these 3 requirements represents the overall desired performance of the floating breakwater. The non-failure of the mooring lines has been widely studied and discussed, so the efforts in this paper are directed towards the first two issues.

The reduction of the transmitted energy is achieved by the floating breakwater itself due to a considerable depth and by the fixed seawall concept under the breakwater for the rest underwater region. Moreover, for a breakwater to float it is obviously designed with a hollow form to reduce the total weight of the structure; where such form complicates the problem and implicates more constraints to be considered during the design. Also, an additional rectangular wall (Fig.4.4) can be used to protect the sheltered regions from high waves; where it is sufficient to place it only from the ocean side since it has non sense to construct a rectangular breakwater with its height over the free surface level equals to a strong wave height. Then, it can be simply deduced that a floating breakwater can be assimilated to two parts: the main rectangular body possessing sufficient dimensions considering the fixed seawall concept, and a second part formed by a small rectangular wall fixed on the ocean side of the breakwater to attenuate the high waves. The dimensions of the second part are easily determined, where its height is equal to the wave height H, and its width c is taken to be 0.8 m (Bonnefille 1976).

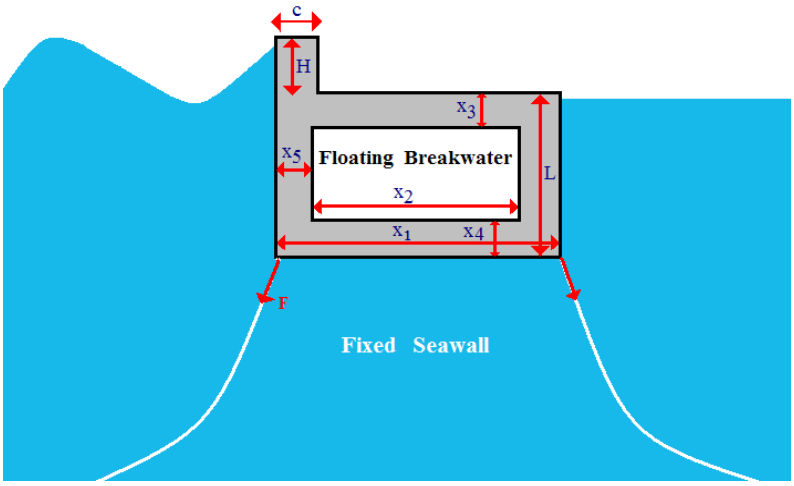

Fig.4.4 Characteristics of floating breakwater

In fact, the problem of shape optimization has been widely explored in the structural optimization area along with the rapid development of fast digital computers and numerical methods such as the finite element method. The usual shape optimization procedures start from the given initial design, where the boundary of the structure is described and parameterized using a set of simple segments such as straight lines, and then the shape is varied iteratively using the information from the shape design sensitivity to achieve finally the optimal shape design. Therefore, improving the performance of floating breakwaters could open up multiple of possible uses and this because the floating breakwater, in contrary to the fixed one (the only parameter to calculate is the width being deduced from the stability condition), has many parameters characterizing its geometry and defining its shape $L, x_1, x_2, x_3, x_4, x_5$ (Fig.3). Some of these parameters are related to the same physical constraint where the rest are determined from other independent constraints, and therefore determining its geometrical dimensions cannot be performed as an ordinary calculation problem but it needs an optimisation process in order to compute these parameters taking into consideration their effects on each other. Hence, the optimisation problem is assumed to be finite dimensional constrained minimization problem, which is symbolically expressed as:

Find a design variable vector x;
to minimize the weight function $f(x)$
subject to the *n* constraints $C_i(x) < 0$

The design variable vector represents a one row vector whose elements $L, x_1, x_2, x_3, x_4, x_5$, (constitute the geometrical dimensions of the breakwater) are to be determined by the optimization procedure. This section commences by a brief definition of the optimization methodology of the SQP, and then moves forward towards introducing the optimization problem.

Optimization Problem

The optimization problem is summarized by the objective function and the related imposed constraints including both physical and mechanical constraints.

1-Objective Function: The optimal solution is to design a breakwater respecting all the constraints with a minimum volume, hence the objective is to minimize the weight of the breakwater,

$$f_{ob}(x_1, x_2, x_3, x_4, x_5) = Lx_1 - x_2(L - x_3 - x_4) + Hc \qquad (3)$$

2-Floating Constraint: The floating of the breakwater is a direct application of Archimedes principle where the equilibrium equation for floating can be written as: $-\rho_m(V_m + V_r)g + \rho_e V_T g = 0$, where ρ_m and ρ_e designates the densities of the material (concrete) and the sea water respectively, V_m designates the volume of the inside material of the whole breakwater without the upper rectangular wall, V_o designates the volume of the hollow part (atmospheric pressure inside), V_r designates the volume of the upper rectangular part, where V_T designates the volume of the submerged part of the breakwater , and then $V_m + V_o = V_T$

A relation between the hollow volume and the submerged volume can be simply deduced: $V_o = \frac{\rho_m - \rho_e}{\rho_m} V_T + V_r$

The floating constraint can be expressed as follows:

$$C_1(x_1, x_2, x_3, x_4, x_5) = x_2(L - x_3 - x_4) - \frac{\rho_m - \rho_e}{\rho_m} Lx_1 - V_r \qquad (4)$$

But, really the floating constraint yields to a simple relation between the variables that can be used to reduce the number of variables in the optimization.

3-Stability Constraint: Stability is defined as the ability of the breakwater to right itself after being heeled over. This ability is achieved by developing moments that tend to restore the breakwater to its original condition. There are a number of calculated values that together determine the stability of a floating breakwater: 1- Initial horizontal equilibrium, 2- Heeled angle, 3- Tension in mooring lines.

First of all, this floating breakwater has a non-symmetrical shape, so initially (before any disturbance) it is necessary to maintain a horizontal equilibrium position. In this case, it can be benefited from the numerical analysis of the structure to calculate in an interesting method the new centre of gravity and then aligning it with the centre of buoyancy for the floating breakwater (Fig.6) which lies at the geometric centre of volume of the displaced water ($x_1/2$). It is based on calculating the centre of gravity of each triangle in the whole mesh triangulation process and its corresponding area instead of dividing the structure into five rectangles and writes the analytical equations of their centres (Fig.5). In fact, it is based on the basic formula of determining the centre of gravity for a structure composed from different well known determined geometrical shapes and applied for each triangle in the meshed domain. $x_g = \frac{\sum A_i \times x_i}{\sum A_i}$ where A_i and x_i are respectively the area and the centre of gravity of the composing geometries. Then, the relevant constraint is $x_g = x_1/2$ (horizontal equilibrium condition) $C_2(x_1, x_2, x_3, x_4, x_5) = \frac{\sum_{i=1}^{n} A_i \times x_i}{\sum_{i=1}^{n} A_i} - \frac{x_1}{2} = 0$ (5)

where *n* is the number of triangles in the meshed domain.(Fig.5)

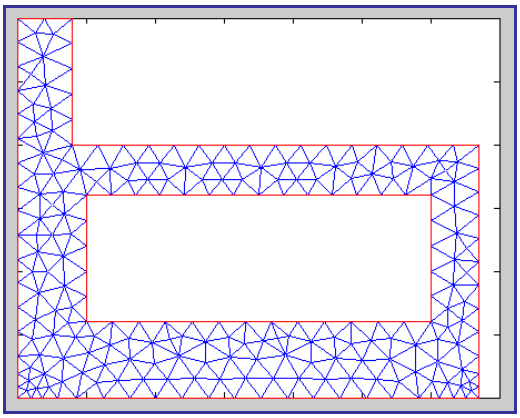

Fig. 5 Determination of centre of gravity

Moreover, the distance GM known as the metacentric height illustrates the fundamental law of stability, where it must be always positive to create a restoring couple and maintain stability $G\overline{M} \geq 0$.

The equation of motion can be written as: $\sum M = I\ddot{\theta} \Rightarrow$ at equilibrium $|Mp| - M_F - M_B = 0$, where *Mp* is the moment of the disturbing force (wave), M_F is the moment of the tension in the mooring lines, and M_B is the moment of the buoyant fore (restoring couple). The absolute value of the disturbing moment guarantees the flexibility of the stability relation in the two senses of rotation; that is the couple produced by the weight must also be in opposite sense of the disturbing moment to be capable to right the structure to its initial position. Hence, the stability constraint can be expressed as: (where x_i represents the variables, i=1,2,3,4,5)

$$C_3(x_i) = -W\left(\frac{x_1^2}{12L} - y_g + \frac{L}{2}\right)\sin\theta - F\cos(\alpha-\theta)x_g + F\sin(\alpha-\theta)y_g$$

$$+\left|\int_{-L+y_g}^{0}(a\cosh k(z+d-y_g)+b\cosh 2k(z+d-y_g)+f)zdz\right.$$

$$\left.+\int_{0}^{h-yg}(a\cosh k(z+d-y_g)+b\cosh 2k(z+d+y_g)+f)zdz\right| \leq 0 \qquad (6)$$

h is the height of the breakwater portion above the still water, α being the angle formed by the mooring lines and the vertical (α=20°), and θ is the angle of disturbance (heeled angle); in fact it is fixed by the designer, and since the breakwater must be very rigid and stable in order to protect the ports from waves, it is taken 1.2°.(slope of 2%)

5-Structural constraint: The real applied forces (pressures) on the floating breakwater are modelled as five separate forces divided as follows: 2 hydrostatic forces on the left and right sides, one hydrostatic force on the bottom, one hydrodynamic force exerted by the wave motion on the left side (Eq.2), and finally the atmospheric pressure exerted on the upper part. (Fig.7)

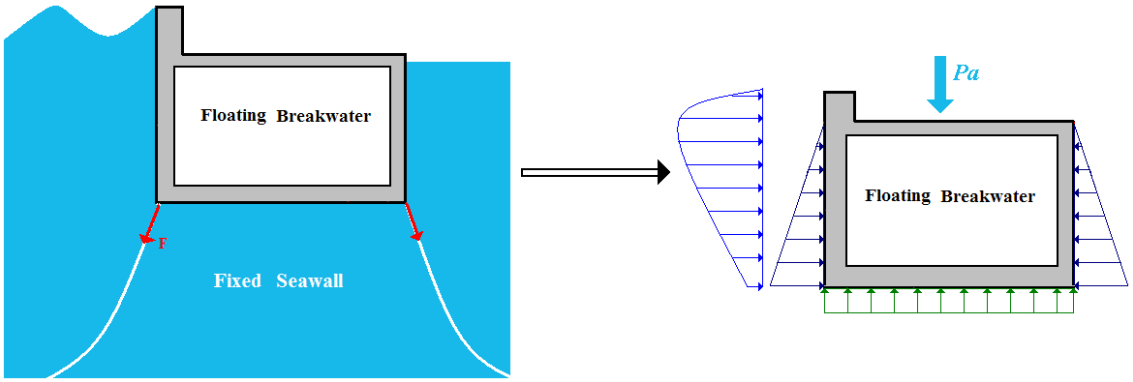

Fig.7 Modelling of various pressures on the floating breakwater

Application and Results

Without any further doubt, the applied method will produce a floating breakwater with a new shape providing an idea of an efficient breakwater. In this section a numerical application is developed and results are obtained based on the following numerical setup for the waves and the breakwater:

$$\text{wave}\begin{cases} L=120m & T=9\sec \\ H=2m & t=0 \\ d=40m & r=0.8 \end{cases} \qquad \text{Breakwater}\begin{cases} \rho_m=2300Kg/m^3 \\ F=10^4\,N \\ D=6m \end{cases}$$

The optimization problem, outlining the whole environmental conditions in floating breakwater design, is solved by the SQP method in Matlab, leading to the following results (Fig.8):

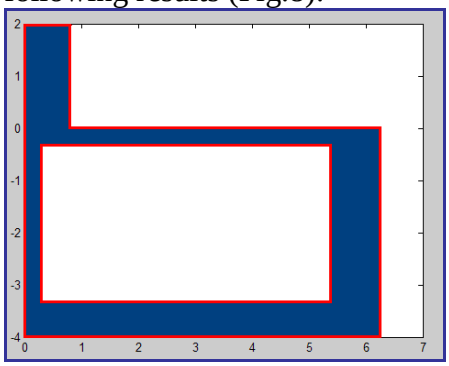

Fig.8 Floating breakwater using shape optimization

$$\begin{cases} x_1=6.25m, & x_2=5.09m, \\ x_3=0.3m, & x_4=0.66m \\ & x_5=0.3m, \end{cases}$$

As mentioned before, these constraints (physical and mechanical) are obviously written in form of mathematical equations in order to be introduced in the optimization problem. But in fact, it is not a classical optimization problem where all the constraints are only defined in terms of mathematical equations without affecting the physical or geometrical significance of the latter whatever is the response in each iteration. So, in such problems that handle

in addition to the physical constraints, a mechanical problem where the mechanical stresses has to be calculated for a new defined geometry in each iteration, any non logical iteration response will yield to arrest the optimization procedure directly without any solution. We can simply summarize our problem as optimizing a void surface translating or moving inside another geometrical shape that also needs to be optimized. Hence, errors can occur when an iteration produces the void geometry partially outside the other geometry or intersecting with it, leading to a non meaningful geometry lacking off course the capability of meshing a non sensible geometry.

In Matlab, it is possible to overcome such difficulties by introducing a conditional algorithm in the programming to sustain the execution of the rest of the optimization iterations although one of them or more falls in such error. This is done by providing a large stress tensor value $(\sigma = 9MPa)$ for this failure case; forcing the optimization procedure to skip directly to the next iteration without executing the rest of the finite element procedure in the previous one.

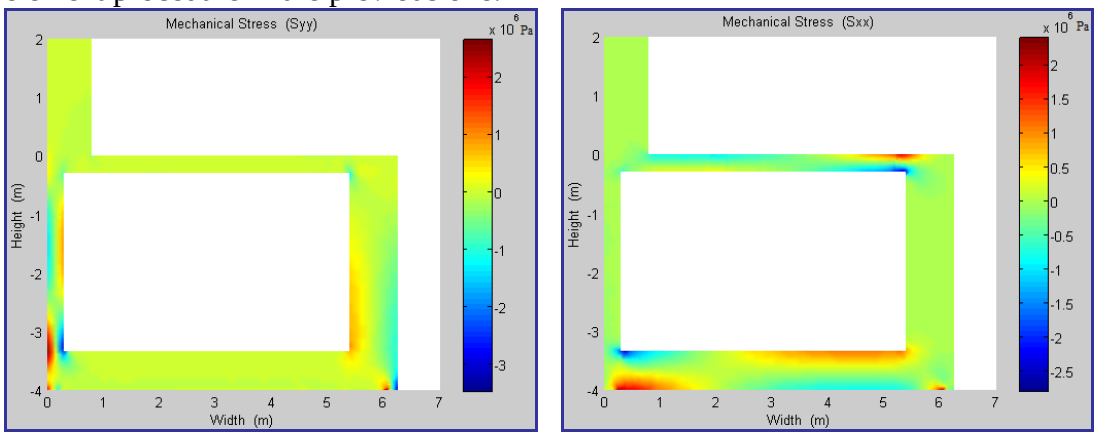

Figure 9 Mechanical stresses σ_x (left) and σ_y (right)

In consequence to our applied method, it is apparent that we ended up with a very logical and accepted solution to our problem considering an overall breakwater problem. In fact, it is not only a problem of volume consuming, but also a structural advantage where the floating breakwater is working approximately in the same stress domain (Fig.9); while in the case of a fixed bottom breakwater (filled material breakwater) the stress domain is largely varying between the points inside the breakwater. This is an additional advantage for the floating breakwater, since the more the inside points are working on closer stresses values the more the extended life of the structure is expected and vice versa. Moreover, we can notice (Fig. 9) the respected limits of the mechanical stresses due to the imposed structural constraints, where the concrete has its traction and compression limits as follows: $\sigma_t = 4MPa$, $\sigma_c = -40MPa$.

4.2.2 Topology Optimization

Topology optimization is one of the most important subset approaches of structural optimization which aims to find the best possible structure that meets different multidisciplinary requirements such as functionality and manufacturing. Generally, structural topology optimization is a powerful tool which can help the designer select suitable initial structural topologies and more importantly, it is identified as economically the most rewarding task in structural design. Structural topology optimization as a generalized shape optimization problem has received considerable attention recently. Various families of structural topology optimization methods have been extensively developed. One of the most established families of methods is the one based on the homogenization approach proposed by Bendsøe and Kikuchi (1988), in which the structural form is represented by a sponge-like material with infinite micro-scale cells with voids and the material throughout the structure is redistributed by using an optimality criteria procedure. As an important alternative approach within this family, the power-law approach, which is also called the SIMP (Solid Isotropic Micro-structure with Penalization) method (Sigmund-2001) and originally introduced by Bendsøe (1989), has got a fairly general acceptance in recent years. It adopts the element relative density as the design variable and assumes that the material properties within each element are uniform, which are modelled as the relative material density raised to some power times the material properties of solid material. A more recent development is the one based on implicit functions such as the regularization method (Belytschko et al, 2003) and level-set methods (Allaire et al. 2002, 2003) It is shown that the regularization method is a dual of the homogenization method and the level-set methods can be as efficient as the homogenization method with a good initialization.

Another well-developed family of structural optimization methods is the one based on the evolutionary structural optimization (ESO) approach proposed by Xie and Steven (1993), in which the material in a design domain which is not structurally active is considered as inefficiently used and can thus be removed by using some element rejection criteria. Both the homogenization method and the ESO method have been further developed by a large number of researchers, leading to the extensive exposition and exploration of these two families of methods. Although computationally effective, both cannot perform a global search and thus do not necessarily converge to the global optimal solution for the given objective function and constraints (Rozvany, 2001 - Zhou and Rozvany, 2001). Another emerging family of structural topology optimization methods is the one using Genetic Algorithms (GA), which are based on the Darwinian survival-of-the-fittest principle to mimic natural biological evolution. GAs have been gradually recognized as a kind of powerful and robust stochastic global search method (Jenkins, 2001- Kane and Schoenauer, 1996) since the seminal work of Holland (1975) and the comprehensive study of Goldberg (1989). More recently, GAs have been increasingly employed in the structural topology optimization field in order to perform a global search in the design domain (Jensen 1992, Schoenauer 1995, Schoenauer 1996, Tai et al. 2002, Fanjoy and Crossley 2002 ,Wang and Tai, 2004).

It is well known that for the GAs, the choice of a representation method (the definition of the search space) is of vital importance. Currently, the bit-array or binary-string representation method has been widely adopted. The bit-array

representation method (Schoenauer 1995, Kane and Schoenauer-1996, Hamda et al.2002), which is similar to the binary-string representation method adopted by Chapman et al (1994), Chapman and Jakiela (1996), Jakiela et al. (2000), as well as Fanjoy and Crossley (2002), is an intuitive and straightforward method to represent the two-dimensional topology for the optimum design problems using the GAs. A bit array or binary string is mapped into the two-dimensional design domain discretized by a fixed regular mesh, where each of the small, square elements contains either material or void, where not intermediate densities are allowed, and is thus treated as a binary design variable. It was also pointed out that since the design domain is discretized by a regular finite element mesh, the complexity of the resulting topology is dependent on that of the given mesh and thus high computational cost may be required for a fine mesh. In spite of its success in solving topology optimization design problems, bitarray representation suffers from a strong limitation due to the dependency of its complexity on that of the underlying mesh. Indeed the size of the individual (the number of codes used to encode a structure) is the size of the mesh. Unfortunately according to both the theoretical results and empirical considerations, the critical population size required for convergence should be increased at least linearly with the size of the individuals. Moreover, larger populations generally require a greater number of generations to converge. Hence it is clear that the bitarray approach will not scale up when using very fine meshes. This greatly limits the practical application of this approach to coarse 2D meshes and obviously fine 3D meshes. These considerations appeal for some more compact representations whose complexity does not depend on a fixed discretization.

An attempt to overcome such problems is the Voronoi-based representation (Schoenauer 1995, Schoenauer 1996, Kane and Schoenauer 1996,) first introduced by Schoenauer, where a finite number of Voronoi sites being labeled 0 or 1 are used to define the Voronoi diagram and to represent a partition of the design domain into two subsets and thus the Voronoi representation of shapes and topologies does not depend on the mesh that will be used to compute the behavior of the shapes. These representations do not involve exactly components, but do require some elementary alleles to be defined by the programmer; such alleles can be viewed as some sort of variable components: due to the high degree of epistasis of those representations, the phenotypic expression of each allele strongly depends on the other alleles. Consequently, the basic blocks that build the structure had to be designed by the programmer, and wrong choices can bias the search in a wrong direction. Moreover, just as in the case of bit-array or binary-string representation, the problem of design connectivity and some boundary control problems still exists. In fact, the Vornoi–based representation allows one to push further the limits of Evolutionary Topological Optimization but doesn't solve the imposed problems. Another relatively new representation method is the morphological representation proposed by Tai and Chee (2000). Simple parametric curves (Bezier curves) with varying thickness to connect the input/output (I/O) regions are used to represent the topology and shape in the two dimensional design domain, but really the morphological representation is essentially an intuitive method without a strong mathematical or theoretical background. Then, the morphological representation method is further developed into a graph-theoretic representation method based on graph theory and cubic Bezier curves with varying thickness (S.Y. Wang, K.Tai) and mainly developed to overcome the problem of design connectivity. The main disadvantage in such methods is that the complexity of

the resulting topology would greatly rely on the complexity of the connection curves, and it is difficult to be applied in complicated mechanical problems.

The objective of this section is to further address the representation form using an ordinary triangular mesh. In fact, this work combines the concept of the traditional bitarray representation from the point of view of the relation between the structure itself and its regular partition, and that of the Vornoi representation in differentiating between the geometrical detection and the FEM computation. In this manner, the structural domain is decomposed into small partitions due to a triangular mesh that is totally different from the mesh used in the FEM computation (Fig 1). Therefore, this triangular mesh is utilized just to determine the geometrical shape or more clearly to define the void and present material inside this studied domain, and then any meshing type might be used for the rest of the problem. This, it is just a technical operation for dividing the geometrical shape into small finite shapes to be easily defined in the optimization process. The mesh used for representing the structure is shown in the left figure, while a refined mesh is applied after the new representation (structure with void domain) in the finite element method to compute the mechanical stresses. (right figure).

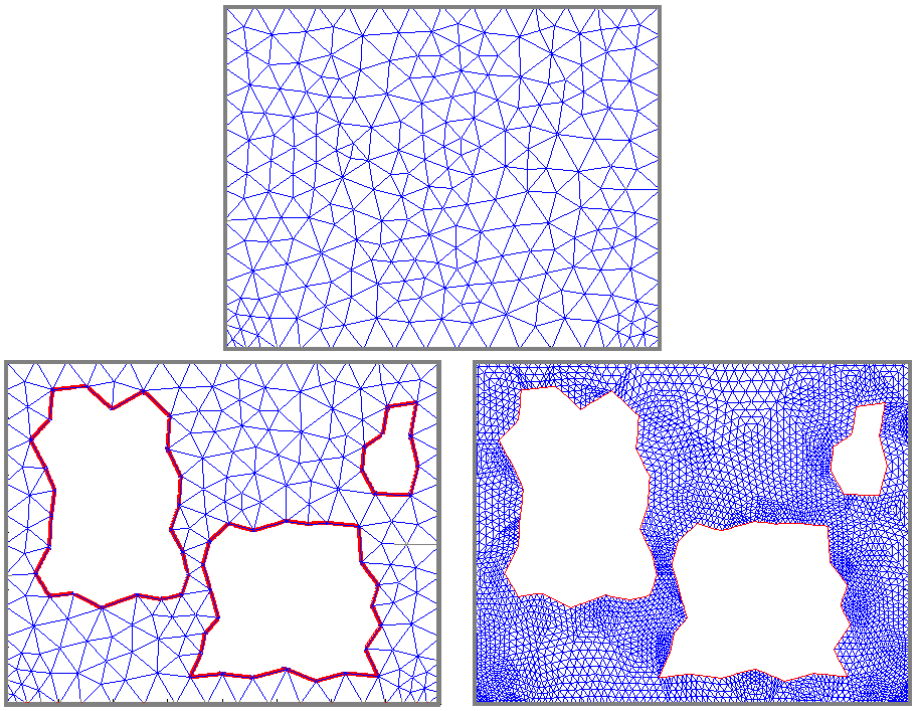

Figure 1 Differentiating between meshes for triangular representation and those for mechanical computations

This new type of representation holds up many advantages when compared to the others. First of all, the triangular mesh is much better than the particular rectangular mesh, used in traditional bitarray representation, in discretizing complicated and non rectangular geometries. The meshing generation process is also better when compared to Voronoi partition due to the latter irregularity and its high dependence on the predefined Voronoi sites (points), where this can be clearly observed from the obtained geometrical results after decoding. Second, each element in the triangular mesh is defined by its geometrical location, so it is easy now to escape from the problems of fine tuning of the domain boundary by reserving all the

elements adjacent to the boundaries. Third, a density vector is introduced having a length equals to the total number of meshing triangles and holding only the values 0 or 1 corresponding to filled or void triangles, describing the density distribution inside the geometrical domain. This density vector establish a relation between the geometrical identification of each triangle, its location inside the domain, and its value in the density vector, yielding to a full control on the boundaries in each iteration ignoring the mutation and crossover operations in specific and undesirable regions through the Genetic Algorithm procedure. Thus, the optimal shape can be reached in reasonable time since the algorithm is able to precisely control the boundaries of the individuals in the population. Moreover, the initial population is given in a very comprehensive form, where it is not combination of arbitrary void and filled triangles like the preceding methods, but it describes void and filled geometrical forms which will also increase the velocity of convergence towards the optimal shape. Finally, a practical example, discussing the optimization of floating breakwaters, is considered with nonlinear physical and mechanical constraints. In contrary to the preceding studies and methods that were applied only on a simple mechanical problem (the cantilever beam) to optimize its weight under displacement constraints, the objective function and all the constraints here are formulated in terms of this density vector. The implementation of this new contribution in the bitarray representation is introduced through several steps:

a-Triangular representation

The method relies on dividing the design domain into a finite number of unequal random triangles. This discretization operation is executed by an arbitrary triangular mesh generation for the design domain based on the Delaunay Triangulation method. The number of triangles indicates the total number of variables for the optimization problem; where the latter is initially indicated and controlled by us upon choosing the appropriate triangular mesh form (Fig. 4). It is important to note that this triangular mesh is not the same one used for computing the mechanical stresses, but it is just a technical operation for dividing the geometrical shape into small finite shapes to be easily defined in the optimization process. This importance appears in differentiating between the size of the individuals (the density vector used to encode a structure) and the size of the mesh for the mechanical computation, and by this way we can use very fine meshes without affecting the scale of the general problem. In fact, the triangular meshing is the best way to discretize any geometrical domain, since the regular rectangular mesh which constitutes the subject of previous bitarray representations is used only for particular rectangular domains. This is mainly due to the simplicity in determining the weight of the optimized structure, since all the finite rectangles are equally sized. By this representation, one can deal with any mechanical problem holding an arbitrary geometrical domain; and the weight can be formulated by a numerical calculation of the area of each triangle alone since the latter is expressed in terms of its nodes' coordinates.

Another benefit from such triangular representation, is the regular description of the final shape when compared to that deduced from Vornoi representation. In fact, it can be clearly observed in (Fig.1) the great difference in domain partition when describing the same geometry (square divided into 100 repartition); moreover another huge difference also in describing the geometry after a topology optimization process (Fig.2). For example, if it is decided to extract all the elements of a square except

those that are adjacent to the square boundaries (the control of this procedure is explained after); the triangular representation will produce a very smooth shape and nearly a rectangular one, where the voronoi representation is clearly irregular and not accepted at all in practical applications. It is important to note that when using a refined mesh for the same problem it will lead up to more comfortable results, but in the figures below, we demonstrate the capability of triangular mesh in describing and expressing the same problem and with the same number of divisions.

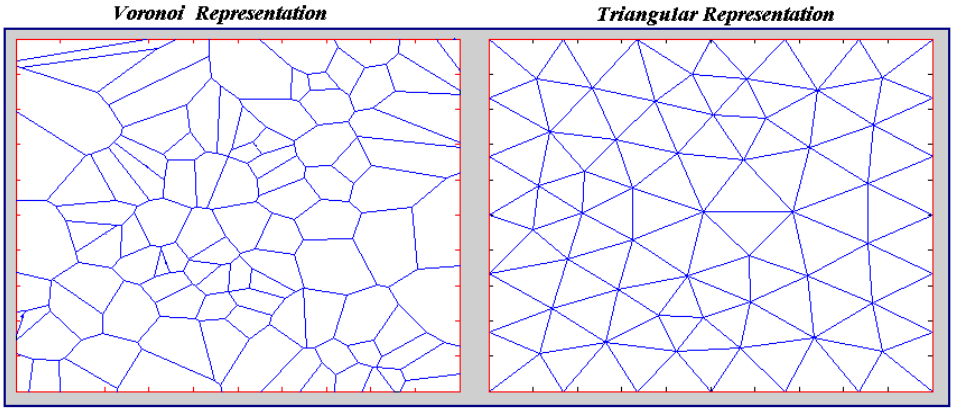

Figure 1 Comparison between triangular and voronoi representation

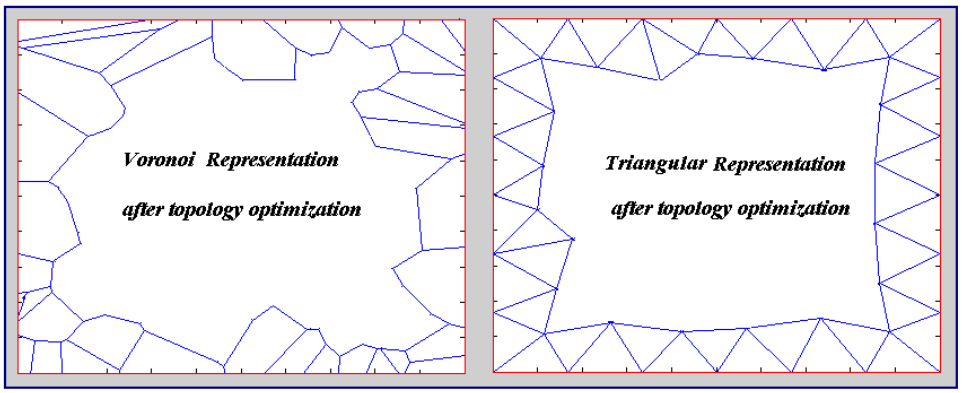

Figure 2 Comparison after topology optimization

Thus, it will be very difficult to obtain symmetrical shapes when using the voronoi representation, especially for problems in ocean fields where the floating condition of the structure and its stability around the centre of gravity are essential constraints in an optimization problem.

b-Density vector

After defining the triangular representation for a geometrical domain, a density vector is created having the same length as the number of meshing triangles in the design domain and holding only the values 0 or 1 corresponding to filled or void triangles; where this latter describes the density distribution inside the studied domain.

$$\rho = (\rho_1, \rho_2, ..., \rho_n)$$

The index associated to each element in the density vector, ρ, represents the density of the triangle having the same index, where it creates the relation between the geometrical identification of this triangle, its location inside this domain, and its value in the density vector. This labelling or numbering is an arbitrary process where

adjacent bits in the bit string representation do not necessarily correspond to neighbour elements of the domain. The number of triangles indicates the total number of variables for the optimization problem; where this number is initially indicated and controlled by us upon choosing the appropriate triangular mesh form (Fig. 4). The interest in this problem lies in the geometry description where it can be written or expressed in terms of triangles, which in their term are expressed in terms of their corresponding densities giving them the ability of presence or absence. In fact, this significance is not only limited to the expression of complicated and arbitrary geometries in mathematical formulas, but also in the control of keeping or removing boundary segments in the problem. For example, this density vector signifies the capability of this representation by controlling the presence or absence of all the triangular elements by the corresponding values in it (Fig.3). The control over this vector is deduced only from the geometrical coordinates of the triangle nodes and not from their numbers, since this labelling or numbering is an arbitrary process where adjacent bits in the bit string representation do not necessarily correspond to neighbour elements of the domain (Fig.3)

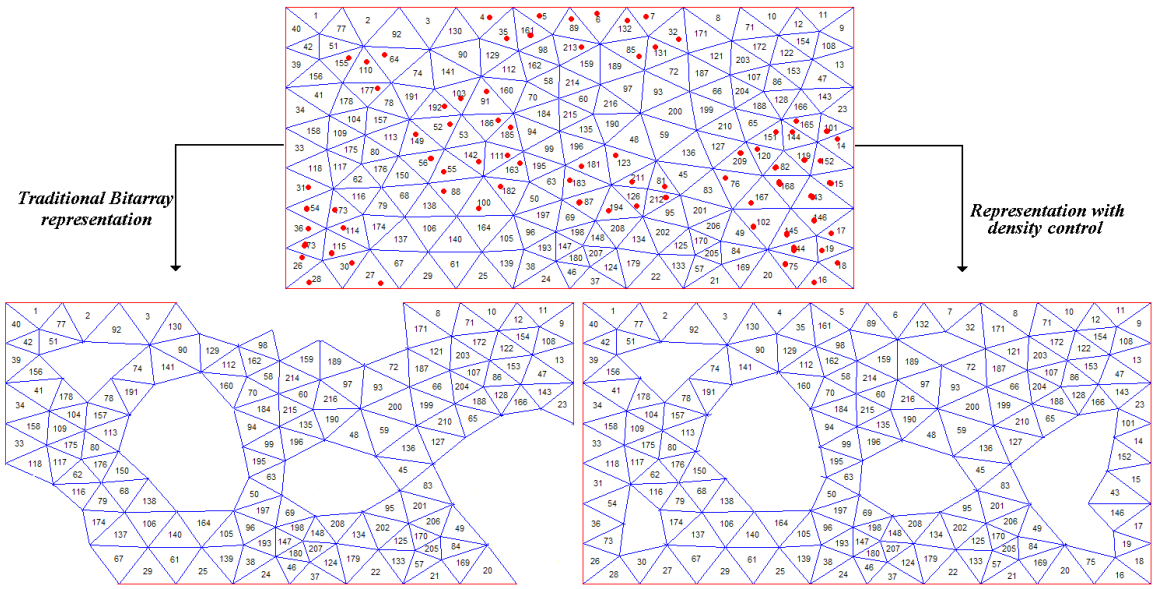

Figure 3 Representation with and without density control

As afore-mentioned, the bit-array representation is adopted as the chromosome representation method to define the distribution of material and void of the design domain. To translate such a bit-array genotype into a phenotypic topology, the chromosome is directly mapped into the design domain, where elements with allele values of 1 become material while those with allele values of 0 become void, as shown in Fig. 3. However, this representation method does not prevent the formation of unanalyzable structures, checkerboard patterns, and boundary problems. Additional strategies must be taken to prevent the biases resulting in the formation of invalid structures during the GA iterations to finally improve the GA performance. The example illustrated in (Fig.3) clarifies the main difference between the traditional representation and the triangular one with density control. The rectangular domain is subjected to various forces from the four sides and it also has fixed supports at its bottom edges. However, numerous design problems have no connected individuals and boundary problems existing in the population in the early generations [31]. For example, if the one of the generations during the GA procedure produces a bitarray

giving the red pointed elements in Fig.3 the values of zeros, it is obvious that the such unviable structures may lead to the failure of the convergence of the GA, since part of the boundaries are eliminated, and the node where the fixed support is applied is also extracted. Including the control of the density vector in the GA procedure, will definitely solves the problem of unanalyzable structures by reserving all the triangular elements adjacent to the boundary giving them the values 1 whatever was their original values in the preceding iteration. Whatever was the bitarray produced after mutation and crossover operations, the control on the density vector will always fix the boundary problem before evaluating the objective function, finite element computation for each new structure in each iteration, and the rest of the constraints imposed in the optimization problem. Mathematically, it is expressed as follows:

$$\text{If } \begin{cases} x_{i,k} = a \\ or(and) \\ y_{i,k} = b \end{cases} \quad \Rightarrow \quad \rho_i = 1$$

$$\text{for } i = 1,.....,n \text{ , and } k = 1,2,3$$

where n is the total number of triangles or simply it is the total number of variables in the GA, k represents the number of node in each triangle; $x_{i,k}$ represents the x coordinates of the node k in the triangle number i; $y_{i,k}$ stands for the y coordinates, finally a and b stands for the boundary coordinates that needs to be conserved in all the optimization problem (they can take positive or negative values or even linear equations). Furthermore, it is possible now to favour the occurrence of valid designs from those invalid designs and the problem of representation degeneracy are not ignored like the previous bitarray representations.

c- Population Initialization

Usually, population initialization is achieved by generating the required number of individuals using a random number generator that uniformly distributes numbers in the desired range [19]. However, by using this initialization method on the bit-array representation, it is often found that there is no viable structure in the initial and early generations and the GA may sometimes fail to converge if the mesh is not too coarse or if the problem involves long narrow design domains [30]. To guarantee the existence of analyzable structures in the population for such problems, an identical population initialization method is proposed. The initial individuals will obviously hold the values 0 and 1, but in a comprehensive manner. That is, each individual in the initial population will represent a void domain in the structure and not arbitrary filled and void material elements. Thus, an algorithm is developed to create void domains in the basic design domain as follows:

$$\text{If } \begin{cases} h_1 < x_{i,k} < h_2 \\ and \\ h_3 < y_{i,k} < h_4 \end{cases} \quad \Rightarrow \quad \rho_i = 0$$

$$\text{for } i = 1,.....,n \text{ , and } k = 1,2,3$$

where h_1,h_2,h_3,h_4 represents correspondingly the x and y limits of this void domain. For better performance of the GA, each individual in the initial population stands for a different domain. Hence, the design domain validity can be guaranteed. It is important to note here that also these initial individuals will be passé under the density control to confirm the boundary reservation before any computation. Furthermore, with the

appropriately selected GA operators, the convergence of this GA can also be obtained, since the diversity of the population in the early generations can be achieved mainly through mutation operations.

d-Crossover and Mutation

Crossover (recombination) is the main GA operator to produce new individuals that have some parts of both parents genetic material. Handling the bit-array representation as a bit string, Specific two-dimensional crossover operators have been proposed to overcome this drawback [22,31]. Nevertheless, the scattered crossover method is adopted in the present work to maintain complete combination between the parents which are initially reproduced in the initial population. Physically, it will combine different void domains and not void elements, and so reduces any form of bias associated with the bit-array representation. Mutation is usually used as a background GA operator to enforce a random walk in the design domain so that the probability of searching any given point in this domain will never be zero and the diversity in the population will thus be increased. In the present study, mutation operation is chosen as adaptive feasible to respect the limit bounds of the density vector.

Finally, after defining the new representation procedure, a Matlab program is developed to define in each iteration a new density vector defining a new corresponding geometrical structure. This new structure is the one passed for the mechanical behaviour study, based on the finite element method, and the rest of the optimization constraints. This program is developed in conjunction of the GA (Genetic Algorithm) toolbox and the PDE (Partial Differential Equation) toolbox in Matlab.

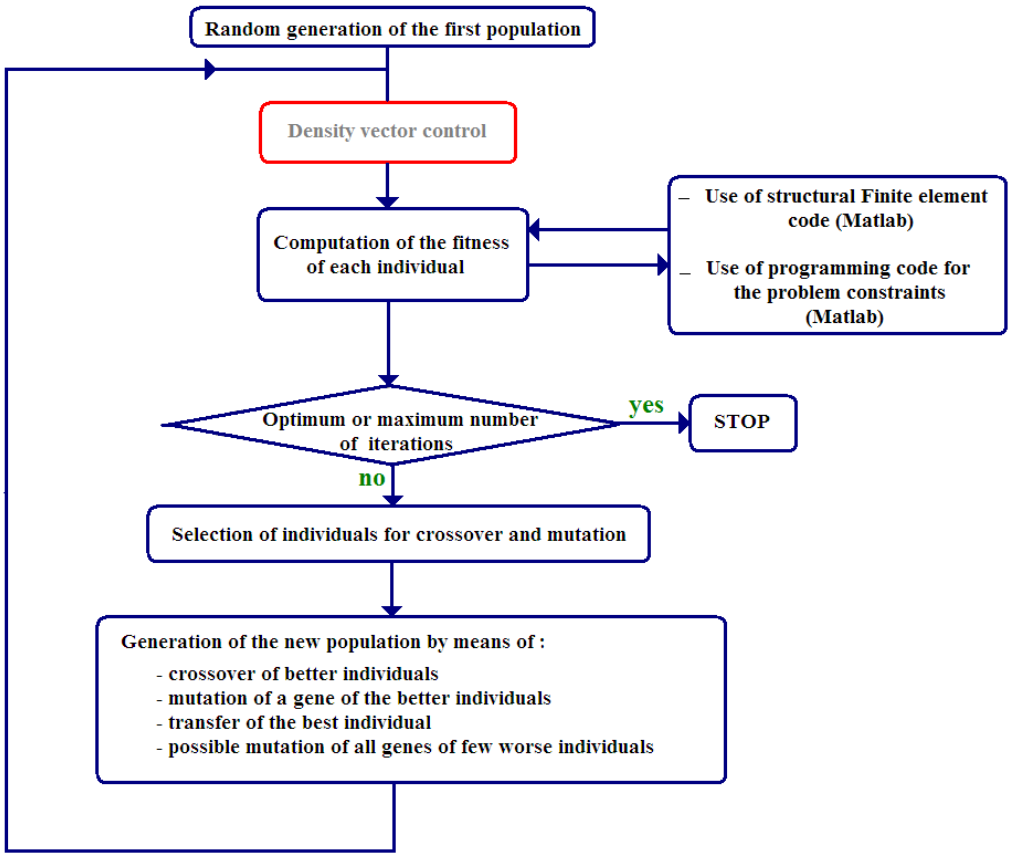

The optimization problem for the case of topology study is defined as follows:

Objective function

Since the geometry of the structure is expressed in terms of the density distribution or mesh triangulation, the weight will be expressed in terms of the latter.

$$f_{ob}(\rho) = \rho_m \sum_{i=1}^{n} \rho_i \times A_i \qquad (3)$$

where n is the number of triangles, ρ_i and A_i are the densities and areas of the corresponding triangles. In this way the complicated geometrical form or its arbitrary distribution is simply expressed by this simple formula, since the presence or absence of each triangle in the weight calculation is guaranteed by its corresponding density value in the density vector.

Floating constraint

A relation between the hollow volume (area) and the submerged volume can be directly expressed, in terms of the densities of the meshing triangles, as the floating constraint. (S_T designates the submerged area of breakwater)

$$C_1(\rho) = \sum_{i=1}^{n} \rho_i \times A_i - S_T \frac{\rho_e}{\rho_m} \le 0 \qquad (4)$$

Stability constraint

In such problems where the geometry is taking different shapes and varying its topology in each iteration, it will be impossible to calculate the centre of gravity in the traditional or analytical methods. Benefiting from various numerical tools, the centre of gravity and area of each triangle are calculated in the whole mesh triangulation domain including both filled and void triangles. Then, we multiply their product by the density vector excluding in this manner all the void triangles from the real calculation of the centre of gravity. $x_g = \dfrac{\sum_{i=1}^{n} \rho_i \times A_i \times x_i}{\sum_{i=1}^{n} \rho_i \times A_i}$ and $y_g = \dfrac{\sum_{i=1}^{n} \rho_i \times A_i \times y_i}{\sum_{i=1}^{n} \rho_i \times A_i}$

where x_i and y_i are the coordinates of the centre of gravity of each triangle. Then, the relevant horizontal stability constraint $(x_g = D/2)$ is written as follows:

$$G_1(\rho) = \frac{\sum_{i=1}^{n} \rho_i \times A_i \times x_i}{\sum_{i=1}^{n} \rho_i \times A_i} - \frac{D}{2} = 0$$

Application and results

The problem is reduced to the optimal design of the inward domain of the floating breakwater, since the height is indicated only from the pressure constraint and then it is eliminated from the optimization problem, also the width must be fixed due to topological problems, D=8m deduced from the previous results.

The main properties of the GA are as follows:

Individual length =480, $\rho = (\rho_1, ..., \rho_{480})$
Population type: Bit String
Crossover fraction: 0.5
Mutation: Adaptive feasible
Crossover: Scattered

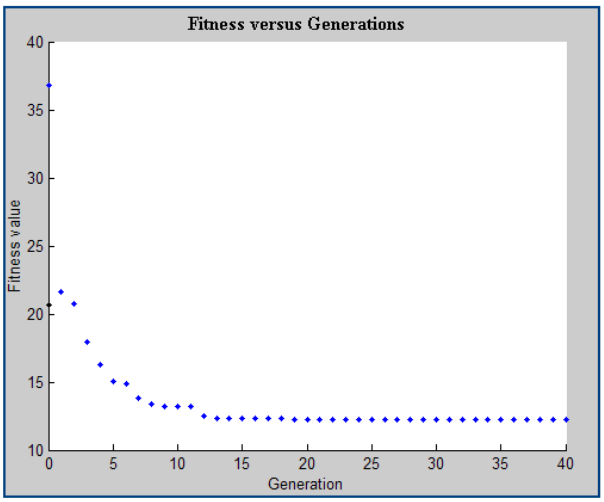

Fig. 8 Fitness function versus number of generations

By this formulation we can reproduce half of the individuals by mutation and half by scattering in each population. This constitutes a reasonable setup in the GA since scattering or mutation alone is ineffective at all; and by specifying the population type to Bit String, each density element will conserve its binary representation during mutation. Once again, in optimization problems the initial population plays an important role in drawing a general view for the final solution and speeding its convergence (Fig.8). In our method, we can control the initial population or solution; that is we define the latter through an algorithm that generates density vectors representing an extracted or void group of triangles that can be accumulated in a void domain. By this way, we avoid falling in trivial solutions when the initial population is representing only arbitrary void triangles. Finally, we obtain the following solution or mass representation for our floating breakwater regarding its conserved external dimensions (rectangle 8*6).

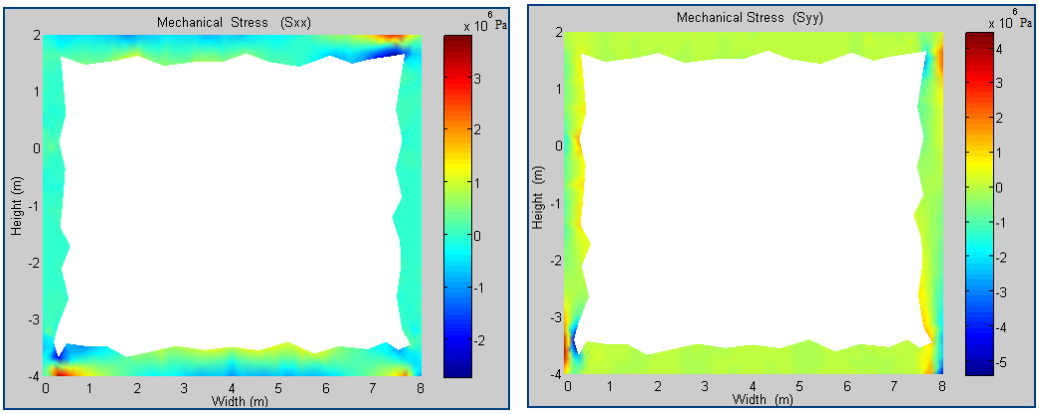

Fig. 9 Mechanical stresses σ_x (upper) and σ_y (lower)

We can notice (Fig. 8) the respected limits of the mechanical stresses due to the imposed structural constraints. Finally, it is important to note that the obtained

results, with such complicated section and with sharp edges, is certainly not so good than a smooth section. But, the importance of this method of density distribution lies in two important actualities. The first being a step on the road in topology optimization of marine structures and more particularly opens a gap for its applications to complicated external shapes used in this domain; where it will be very helpful in drawing an initial structural design which will be latterly followed by a shape optimization to smooth such sharp edges. The second fact is that any success of this method on practical applications will open up a new methodology to be benefited from it in inclusion of different materials inside the structure. For example, new applications can be implemented for floating breakwaters made up from concrete and polystyrene by detecting the distribution of these layers inside it based on the density distribution methodology.

4.2.3 Optimization with variable points

This method constitutes a new idea mainly relating topology and shape optimization under a single algorithm by using a variable number of points which create an arbitrary initial valid domain; where the coordinates of these points represent the variables for the optimization problem. The novelty of this work appears in two subjects: the first in combining the shape and topology optimization in one algorithm and the other by widening the usage of points in the optimization domain; where previous methods (Zienkiewicz and Campbell 1973, Cappello and Mancuso 2002) select key points from existing geometries or some nodal points deduced from the meshing procedure of this existing geometry to constitute the design variables of the optimization.

Usually, the changeable geometry is represented by the nodal coordinates of the discrete finite element model or by choosing a set of key points or master nodes to define the geometry entities. This method allow us to go thoroughly in shape and topology optimization; where the topology is detected by an initial number of points, and then their increase will assure the shape optimization or in other words smooth the rough boundaries and minimize the objective function until no improvements are achieved. Then, these points are not selected from the meshed domain, but they themselves create this new domain. In optimization it is very important to initialize with a significant initial solution since it plays an important role in drawing a general view for the final solution and yielding to speed its convergence toward the optimal solution; therefore the *n* points must create an initial valid domain and not just a set of arbitrary points in a domain.

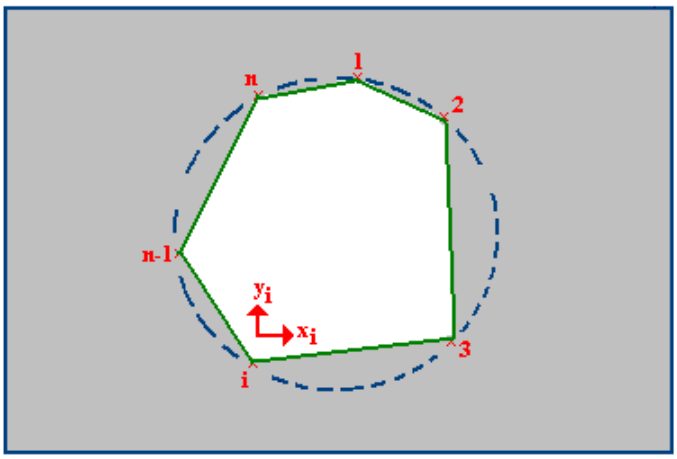

Figure 10 Initialization of a valid domain

There are two different ways to treat this problem: the first one is based on initialization of the geometric domain for every new number of points *n*, where the other is based on benefiting from the previous results and proceeding ahead by introducing new points to the obtained shape for the new value of *n*. For the first one, in order to guarantee the existence of analyzable structures in the initial solution, and especially when considering high values of *n*, a mathematical trick is implemented. It is based on selecting the *n* points on a fictitious circle (Fig.10), where each point holds a value between [0,2π]. $l = f(0,2\pi)$, where f represents a function giving spaced points in this interval consequently, $\Rightarrow$ $l_{i-1} < l_i < l_{i+1}$, then

$x_i = r \times \cos(l)$

$y_i = r \times \sin(l)$

$i = 1,\ldots\ldots\ldots\ldots\ldots n$

Moreover, these points are connected by straight lines in an ordered manner:

$1 \to 2 \to \ldots\ldots\ldots \to i \ldots\ldots\ldots \to n-1 \to n \to 1$

After, assembling the polygon of *n* sides, the problem is treated in a similar manner to other optimization problems; but in this method the shape is not predefined like the first method. Therefore, by introducing a polygonal shape there is a wide range of shape variation due to the location of the moving points. Finally, the geometry of the structure is varying for a determined number of points during the iterations of the optimization problem, and it is also varying in correspondence with the number of points. In such problems it is very useful to build a numerical work benefiting from the meshing process in order to perform the mathematical computations, so we commence by meshing the geometrical valid domain and then calculate the centre of gravity and the area of each triangle in this meshing process. (Fig. 13). It is important to note that the mesh used in the numerical calculations id totally different from another refined mesh applied for the stresses calculation.

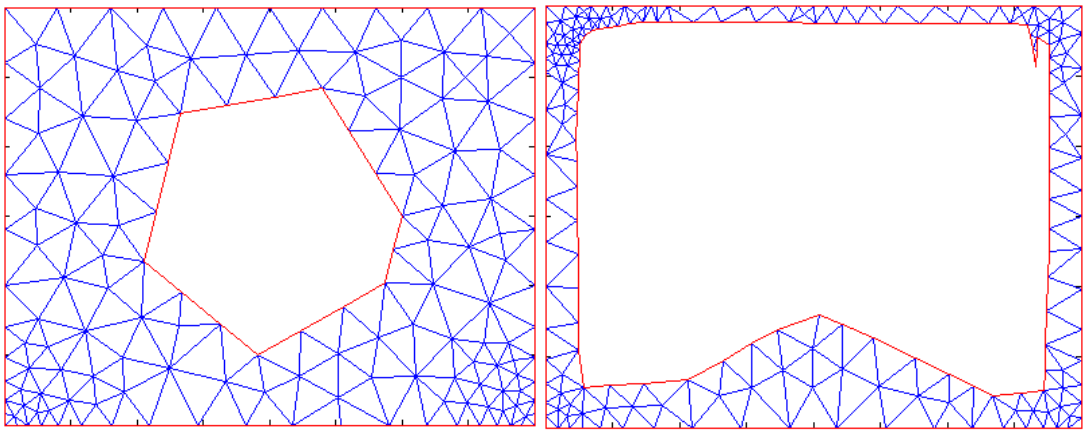

Figure 13 Calculation of geometrical properties

Then, the objective function and the constraints are defined in terms of the meshing triangles:

Objective function

The objective function can be directly expressed in terms of the numerical method as follows:

$$f_{ob}(x_i, y_i) = \rho_m \sum_{it=1}^{nt} A_{it}$$

where A_{it} corresponds to the area of each triangle in the meshed domain; and the index it corresponds to the number of the triangle, where it varies from 1 till the total number of triangles nt.

Floating constraint

The occupied volume of the breakwater can be simply expressed in terms of the areas of the meshing triangles (transform the volume notations into surface notations per 1m length).

$$C_1(x_i, y_i) = \Sigma A_{it} - S_T \frac{\rho_e}{\rho_m} \leq 0$$

Stability constraint

Similarly to the objective function, the coordinates of the centre of gravity are expressed in terms of the centres of gravity of the meshing triangles:

$$x_g = \frac{\sum_{it=1}^{nt} A_{it} \times x_{it}}{\sum_{it=1}^{nt} A_{it}} \quad \text{and} \quad y_g = \frac{\sum_{it=1}^{nt} A_{it} \times y_{it}}{\sum_{it=1}^{nt} A_{it}}$$

where x_{it} and y_{it} are the coordinates of the centre of gravity of each triangle. Then, the relevant horizontal stability constraint $(x_g = D/2)$ is written as follows:

$$G_1(x_i, y_i) = \frac{\sum_{it=1}^{nt} A_{it} \times x_{it}}{\sum_{it=1}^{nt} A_{it}} - \frac{D}{2} = 0$$

Application and results

The objective function will vary directly with any change in the number of points. Considering different values for the variable *n*, it is very logical to terminate with such results (Fig.11); that is the increase in the number of points representing the geometrical domain will yield to a decrease in the objective function until a certain limiting value where no improvement can be achieved after it. Moreover, introducing additional points to the obtained results from a previous *n* (benefit from the results of each *n*), have ameliorated the values of the objective function in comparison to those obtained by re-initializing the problem for each *n* (Fig.11).

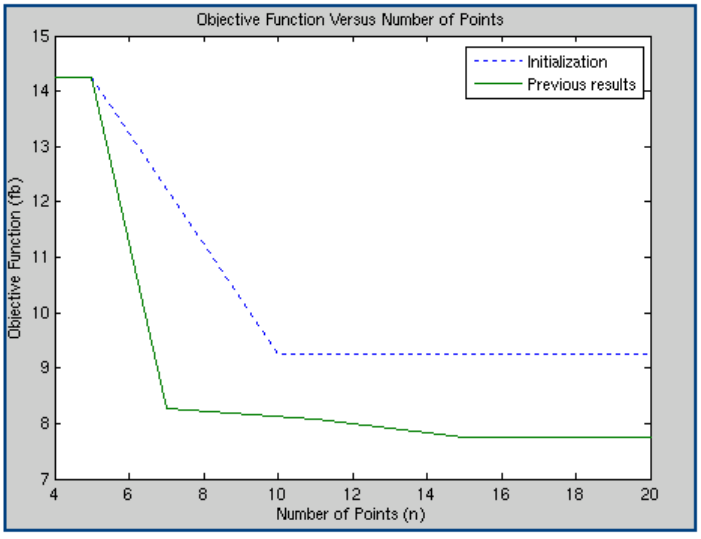

Figure 11 Variation of objective function versus

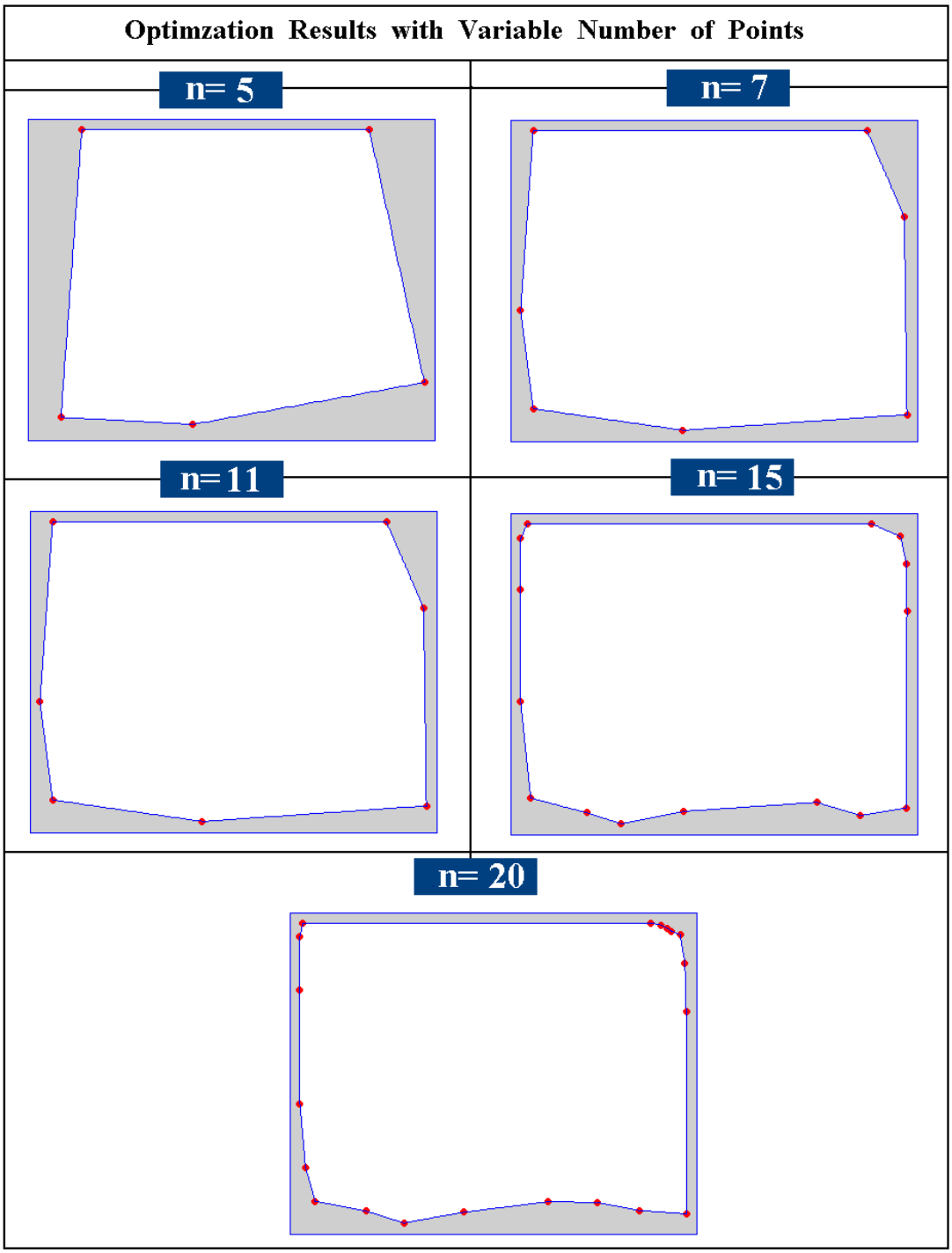

Figure 12 Optimization with variable number of points

Considering the optimization results based on the profit of the value of previous design variables (Fig.12), it is obvious to start with the 4 or 5 points solution and then to go forward until no shape improvement is noticed or obtained. In consequence, when moving from 5 points to 7,11,15,20 (Fig.12) there is a visible amelioration in the shape and the weight, where the locations of these points are also plotted on the same figures in order to understand the behaviour or the movement of these variables during the optimization process. But, this optimization method does not comprise an infinite number of solutions for the shape improvement; it is a deterministic optimization where after a certain number of points no shape improvement can be achieved and hence we can say that an optimal solution is found.

Finally, it is good to expose the optimal shape $(n=20)$ and its relevant mechanical stresses distribution on each point inside the studied domain (Fig.13).

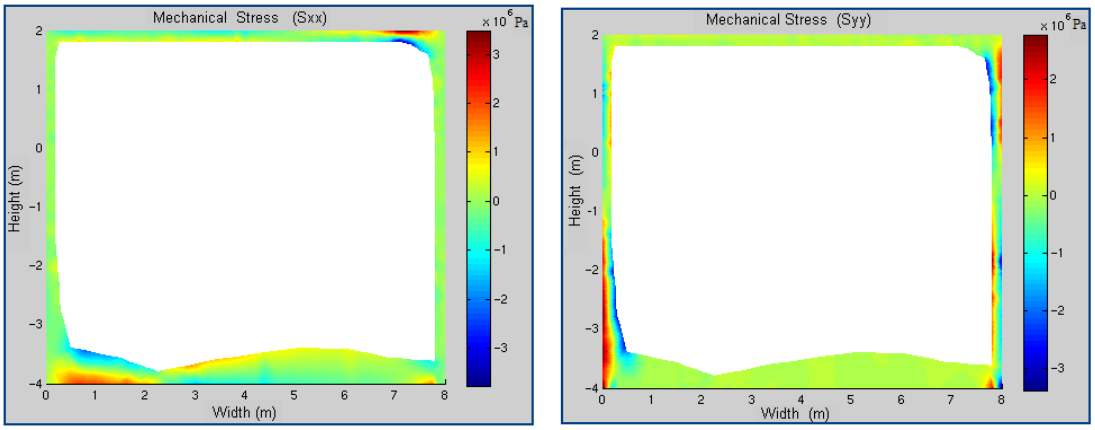

Figure 13 Mechanical stresses σ_x (left) and σ_y (right)

In order to compare these various methods, an additional application will be considered to the same structure considered here. It lies in applying the shape optimization using a predefined geometrical form. It constitutes a direct approach in optimization where it can be applied only if the type of the problem permits to create a prospective image for the final shape. Hence the problem is initialized by a specific geometrical form (rectangle, square, circle,….) and finally the optimal form will reserve the same shape but with different dimensions and location inside the outward boundary of the floating breakwater; where the variables are reduced to x_1, x_2, x_3, x_4 (Fig.5). The height of the breakwater is divided into two parts (with respect to the calm water level): a lower part, L, deduced from the dynamic pressure constraint, and an upper part, h, equals to the height of a strong wave (H=2m). Because, the optimization problem is dealing with a predefined geometry, then all physical and mechanical constraints can be directly expressed in terms of the geometrical dimensions of the breakwater in form of mathematical equations and then they are assembled in a sophisticated program leading to the optimization algorithm.

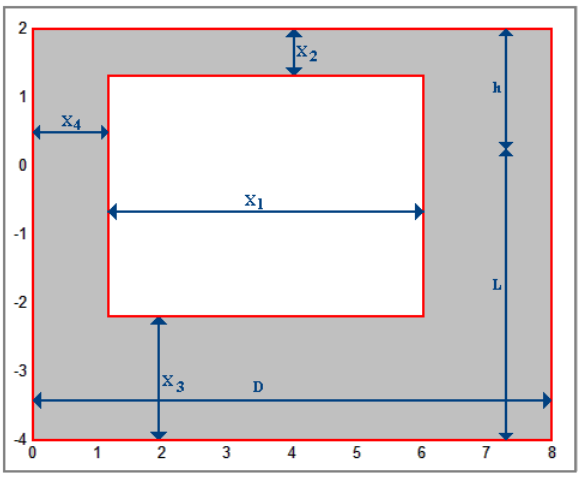

Fig.5 Predefined shape inside the floating breakwater

The numerical application yields to the following results:

$$\begin{cases} x_1 = 7.4m & x_2 = 0.367m \\ x_3 = 0.67m & x_4 = 0.3m \end{cases}$$

Replacing the variables by their corresponding values, it is capable to draw the optimized shape and its mechanical stresses distribution.

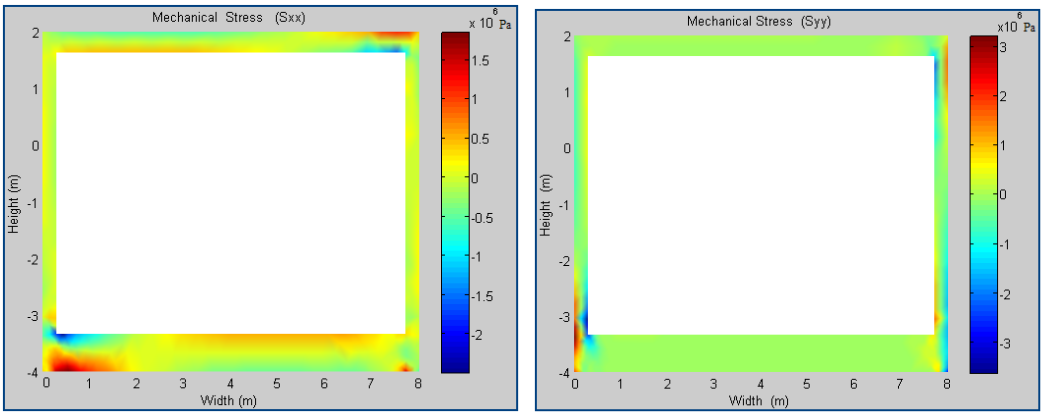

Fig.6 Mechanical stresses σ_x (upper) and σ_y (lower)

Discussions and conclusions

As a conclusion, the second method proved its robustness in combining the two previous methods and probably it will prove high capability of solving problems of irregular shapes. Moreover, another type of comparison between these methods is introduced and based on the numerical values of the objective function and the cost calculation of these methods (Table 1).

Table 1	**Method 1**	**Method 2**	**Method 3**
f_{ob}/ρ_m	12.1 m^2	7.76 m^2	11.278 m^2
f-count	11800	819	173

Surely, the second method will produce the best objective function since the *n* points can freely move in the domain without any restrictions. The third method produce a larger objective function when compared with the previous due to its predefined geometry that cannot be altered but only vary in dimensions. On the other side, method 1 as we have commented on it earlier cannot be compared to values of shape optimization rather than it is very effective in problems with irregular geometries and domain helping to draw an initial image on the mass distribution in this structure to be passed later to a shape optimization problem to ameliorate its shape and weight. But, what is interesting in this method is the new type of control and representation in topology problems summarized by the triangular mesh. Moreover, topology optimization is a much more flexible design tool than classical structural shape optimization, where in the latter only a selected part of the boundary is varied without any chance to generate a lightness hole, for example. Also, in topology all the domain is under optimization, and hence a wide range of solutions can be expected.

Moreover, it is very logical to obtain higher mechanical stresses in the second method (Fig.16) when compared to those compared in the third one (Fig.7) and this is

due to difference in the obtained volume for the two cases; where surely the structure with less material volume will hold up higher mechanical stresses. But in the first one (Fig.12), high mechanical stresses are caused by the rough surfaces related to the applied method in triangular elements extraction. Finally, the second method seems to have an accepted computational cost (Tab.1) in comparison with the others and also due to the optimal shapes and results derived from it.

4.3- Optimization including dynamical behaviour

The performance of a floating breakwater is primarily characterized by the transmission coefficient, which is the ratio of transmitted to incident wave height. Other aspects of a floating breakwater's design include a consideration of the breakwater motions and the possibilities of structural failure of the breakwater and its restraint or mooring system. Possible difficulties that a satisfactory design should overcome include a breakwater's inability to provide adequate wave protection, excessive breakwater motions, and damage or failure. The dimensions and the mass of the rectangular structure however are important parameters that are used to optimize the floating breakwater performance. The influences of the following structural dimensions are investigated during the numerical calculations:

- Structural width
- Draft of the floating section
- Mass of the structure (m)
- Mooring system

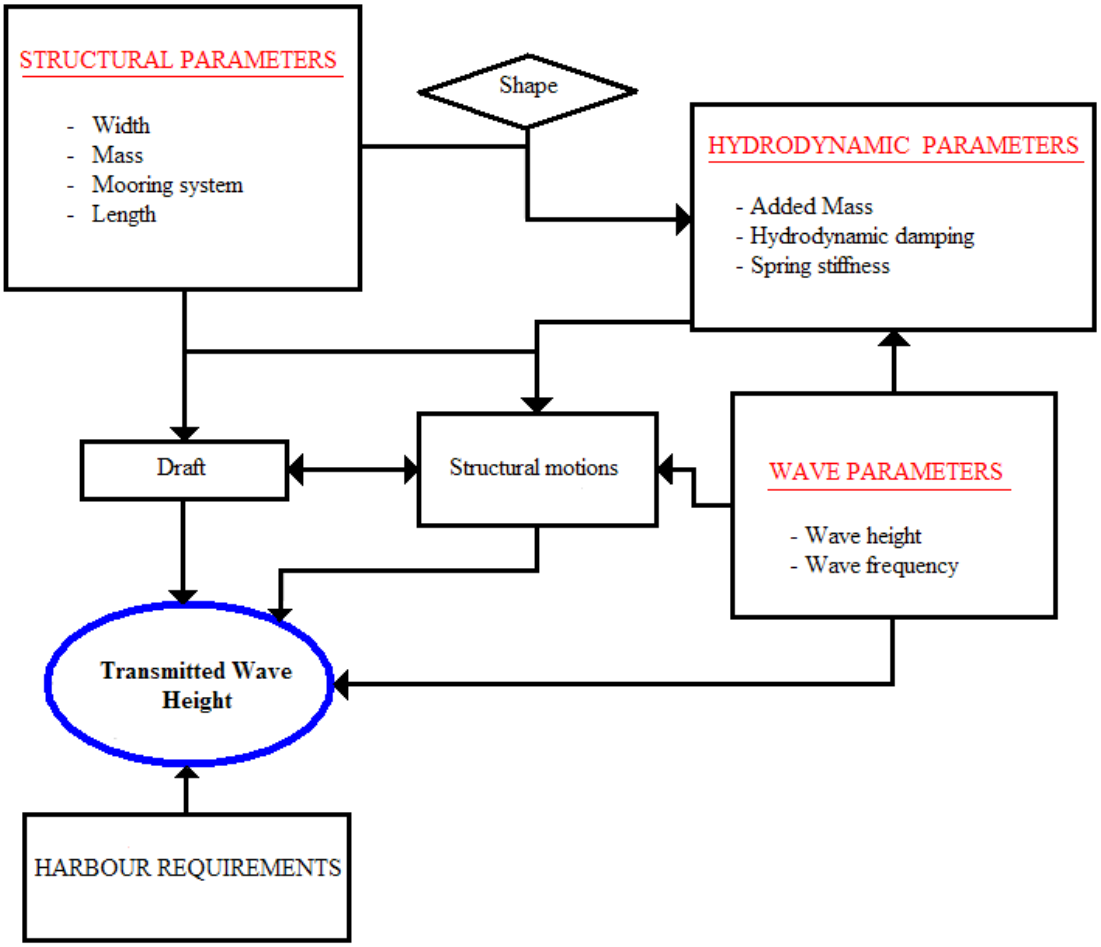

Figure 4.10 Factors and relations in the wave transmission calculation process

The influence of the structural variables on the hydrodynamic behaviour as well as the attenuating capacity has been discussed in the parametrical analysis section (section 3.3). The relations of the parameters and requirements and their influence on the wave transmission is presented in Fig 4.10. In addition, the motions

of the breakwater itself generate waves that propagate outward, contributing to the transmitted wave height. Under certain wave conditions, the breakwater may undergo resonance and become less effective at attenuating waves. Moreover, the resonance phenomenon plays an important role in such problems, where a structure oscillating in presence of an incoming wave that has its own periodic frequency may enter the resonance bands, and destructive results appear. Finally, it must be clear that we are facing two sources of resonance, one being represented by any coincidence between the oscillating frequency of the structure and that of the wave; where the other kind is the wave itself inside the port region. In presence of the sidewall, that really describes a real port problem, it seems to create a bounded domain from the port side or simply an enclosed area. Thus, any wave may be forced to resonance in port side due to specific value of the clearance distance between the sidewall and the breakwater. This implies that knowledge not only of expected design wave conditions is required but also an understanding of the response of the floating body under that sea state.

In order to take into account wave interaction with floating breakwaters we formulate a multidisciplinary problem, where a combination of fluid mechanics, dynamic behaviour of mechanical systems, the vibration theory, and the structural mechanics (mechanical resistance) are introduced to perform a complete analysis capable to develop a representative design of the structure. The interference of these phenomena together with resonance bands occurring in the port side due to the reflective sidewall, and the influence of the structural parameters on the performance of breakwaters causing mass variation and hence affecting the natural frequencies; demonstrate the complexity of a floating breakwater design, and yields to orient the problem towards an optimization approach that can consider all the relevant consequences together.

First, the hydrodynamic behaviour of the floating breakwater is solved. It constitutes from a numerical modelling of the diffraction – radiation problem combined with an analytical modelling for the dynamical behaviour of the vibrating breakwater. This composes a comprehensive study of the sea waves-breakwater interaction, and is capable to implicate the wave height in the fluid domain and especially inside the port region. Second, the optimization problem is introduced by an objective function and its relevant imposed constraints. These latter are enumerated by the floating condition, stability, minimum wave height in the port, and the mechanical resistance. The last constraint demands a finite element formulation to compute the mechanical constraints; while, the wave height constraint is derived from the hydrodynamic problem in the first part. All these constraints are expressed in terms of the geometrical parameters of the design shape, in order to be introduced into the optimization problem. Therefore, we have to solve three main models for each iteration of the optimization procedure:

1-Fluid Mechanics 2-Dynamic Motion 3- Mechanical Resistance

Due to the complexity of such optimization problem, it is sufficient to consider the predefined shape geometrical shape. (The breakwater height above the calm water level (h) is taken to be a constant value equal to 2m).

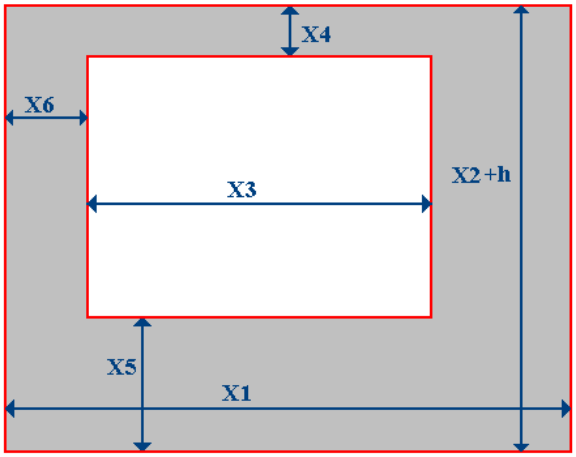

Fig.3 Defining the geometrical parameters of the floating breakwater

Objective function

It is expressed in terms of the geometrical dimensions as:

$$f_{ob}(x_1,x_2,x_3,x_4,x_5,x_6)=\rho_m\left[(x_2+h)x_1-x_3(x_2+h-x_4-x_5)\right] \quad (34)$$

Floating constraint

In fact, for a moored structure the floating condition can be expressed in an inequality in order to minimize the weight, where the difference between the buoyancy force and the weight can be equilibrated by the tension in the mooring lines.

$C_1=-\rho_m V_m g+\rho V_T g\le 0$

It can be expressed in terms of the geometrical dimensions as follows:

$$C_1(x_1,x_2,x_3,x_4,x_5,x_6)=\frac{\rho_m}{\rho}\left[(x_2+h)x_1-x_3(x_2+h-x_4-x_5)\right]-x_1\cdot x_2<0 \quad (35)$$

Stability constraint

The initial horizontal equilibrium and the stability of the floating breakwater depend on the calculation of the centre of gravity. This is performed by dividing the breakwater into 4 rectangles and calculating the new position of the centre of gravity x_G (Fig. 4) in terms of the variables and then aligning it with the centre of buoyancy for the floating breakwater which lies at the geometric centre of volume of the displaced water $(x_1/2)$.

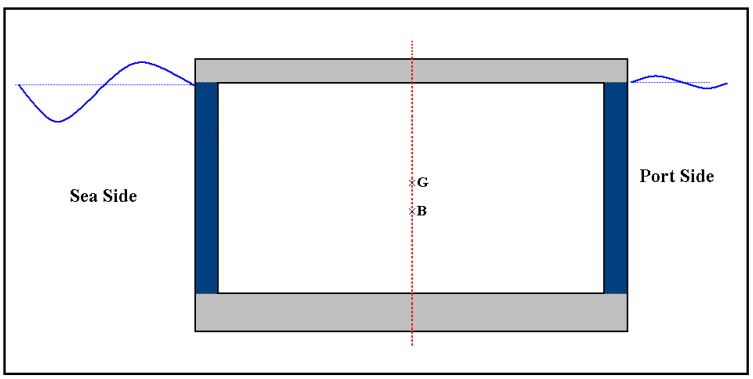

Fig.4 Centre of Gravity and centre of buoyancy

$$x_G = \frac{(x_2 + h - x_4 - x_5)\left[\frac{(x_1 - x_3 - x_6)^2}{2} + \left(x_1 - \frac{x_6}{2}\right)x_6\right] + \frac{x_1^2}{2}[x_4 + x_5]}{x_1 \times x_4 + x_1 \times x_5 + (x_2 + h - x_4 - x_5)(x_1 - x_3)}$$

The horizontal equilibrium constraint is defined by

$$C_2(x_1, x_2, x_3, x_4, x_5, x_6) = x_G - \frac{x_1}{2} = 0 \qquad (36)$$

Minimum wave height in the port side

The floating breakwater will loose its efficiency when the wave conditions transmitted to the harbour area reach a maximum. This transmitted energy to the leeward side is mainly deduced from the underflow (wave energy not influenced by the floating breakwater presence) and the radiated waves created by the oscillating structure. Moreover, handling containers in a harbour is not possible when ship motions get too large. Also, in a floating harbour, motions will cause even more problems, since both ship and floating harbour will react on the waves. To guarantee optimal harbour efficiency, the mutual motions of vessel and harbour may not exceed a certain maximum.

This is the heaviest constraint in the optimization process, where the structural parameters and mainly the draft and width must vary in order to attenuate most of the incoming wave energy. Also these parameters must deviate the structure from resonance bands deduced from the clearance distance (distance between the breakwater and the reflective sidewall in the port) or from any coincidence between the structure natural frequency and the wave frequency. Hence, this demands a complete resolution of the hydrodynamic problem of the floating breakwater. The maximum wave allowable height in the port side is limited to 20cm and can be expressed as:

$$C_3(x_1, x_2, x_3, x_4, x_5, x_6) = \eta(x,t) - 0.2 < 0 \qquad \forall\ x > a/2 \qquad (37)$$

Structural constraints

This constraint reserves its form also in this formulation:

$$C_4(x_1, x_2, x_3, x_4, x_5, x_6) = (\sigma_1 - \sigma_2)^2 - (\sigma_t + \sigma_c)(\sigma_1 + \sigma_2) - \sigma_t\sigma_c \le 0 \qquad (38)$$

Application and results

The essential characteristics of the waves, anchoring system, and port characteristics are defined by the following:

$$\begin{cases} H = 2m \\ T = 10\sec \\ d = 40m \end{cases} \qquad \begin{cases} k = 5\times10^6\ N/m \\ \alpha = 30^\circ \\ k_r = 0.3 \end{cases} \qquad \begin{cases} D = 180m \\ \rho_m = 2300kg/m^3 \\ \rho_e = 1025kg/m3 \end{cases}$$

The optimisation procedure above was applied for a floating breakwater constructed from concrete. The most important is the consistency between the

hydrodynamic performance and the structural resistance of the breakwater. Thus, a floating breakwater meeting the structural requirements will have the best attenuating performance. For strong waves (H=2m), it is difficult to design an optimal shape capable of totally attenuating the waves (allowable wave height=0.2) and respecting the resistance criteria at the same time. This reverts to the large width preferred by the hydrodynamic constraint and the inability of achieving resistive structure with such width especially when considering the floating constraint. This latter constraint plays an important role in resistance failure due to the small thickness given to the horizontal beams of the structure. Hence, we have two possibilities to surpass such a problem:

1- Designing a dual pontoon floating breakwater
2- Changing the material type

The first solution seems to be an interesting idea in the case of very strong waves. A dual pontoon floating breakwater consisting of a pair of floating cylinders of rectangular sections connected by a rigid deck or totally separated, attenuates the waves on two stages (Fig.6). Thus, the concrete choice is still valid, and the optimisation problem is reintroduced again but with a small variation in Eq. 37 which becomes: (maximum allowable wave elevation is 0.5 instead of 0.2)

$$C_3(x_1, x_2, x_3, x_4, x_5, x_6) = \eta(x,t) - 0.5 < 0$$

This yield to determine an optimal design of a concrete floating breakwater that is widespread utilised in moderate wave conditions and then introduces a second similar one to constitute the dual pontoon. The first one can totally protect the ports from normal waves or simply it can attenuate half of the strong waves. Thus, the remaining energy in such strong waves is totally arrested by the second stage of the dual floating breakwater.

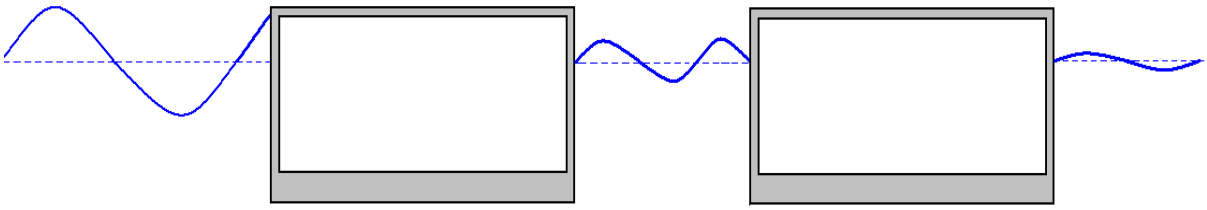

Fig 6 Dual pontoon floating breakwater

The numerical application for concrete and with a relatively high allowable wave height at the leeward side yields to the following results:

$$\begin{cases} x_1 = 11.95m & x_2 = 2.3m & x_3 = 11.35m \\ x_4 = 0.3m & x_5 = 0.3m & x_6 = 0.3m \end{cases}$$

Replacing the variables by their corresponding values, it is capable to draw the optimized shape and its mechanical stresses distribution (Fig.7).

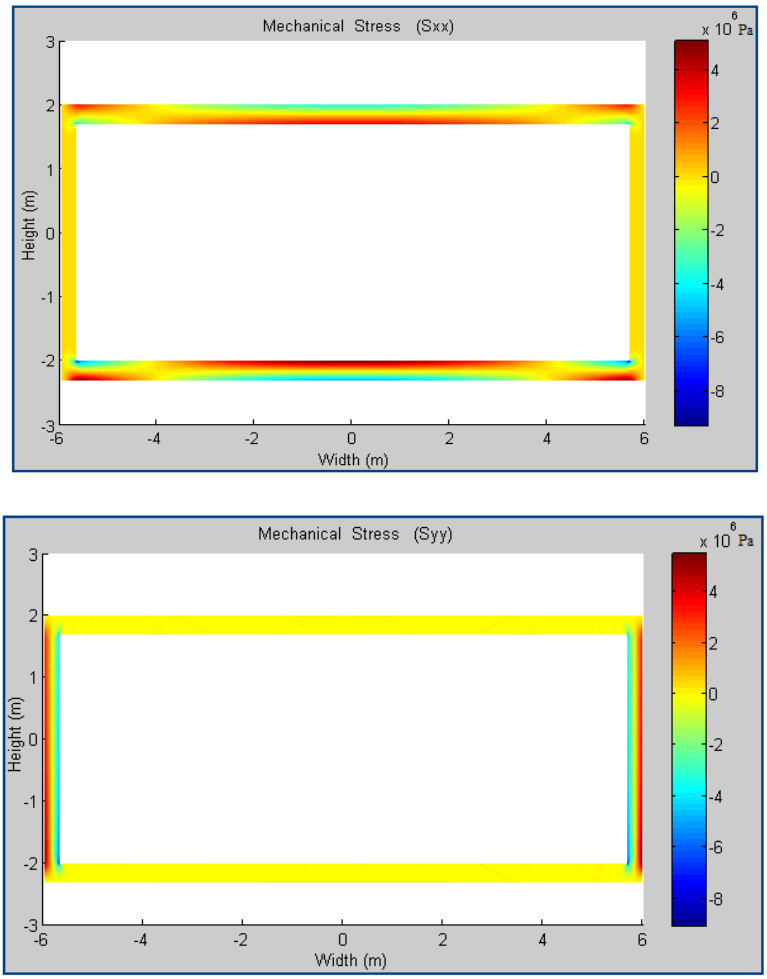

Fig. 7 Mechanical Stress Distribution for concrete σ_x (upper) σ_y (lower)

Another possibility to overcome the failure of the resistance constraint with large width is to orient the interest towards a more effective and lighter material than the concrete. Then, it will be conceivable to design a single floating breakwater surviving with strong waves. This opens up a large choice between various types of materials. But, the accumulated experience proved that the employing of composite materials permit, with equal performance, a gain of mass varying from 10 % to 50 % over the same component in concrete, and with a cost of 10% to 20% less. Moreover, they are widely applied in the ocean field, mainly in hull ships superstructure construction, due to the demand for lighter materials to improve the floating condition and to ensure the mechanical resistance in structures. The following properties are given for a composite material fabricated from glass/epoxy:

$$\begin{cases} \text{Density } \rho = 1700 \ \ Kg/m^3 \\ \text{Elasticity Module } \ E = 12.4 \times 10^3 \ MPa \\ \text{Tensile strength } \ \sigma = 90 \ MPa \end{cases}$$

The numerical application for composite materials that is capable of totally attenuating the waves in the port side yields to the following results:

$$\begin{cases} x_1 = 19.2m & x_2 = 2m & x_3 = 18.5m \\ x_4 = 0.35m & x_5 = 0.35m & x_6 = 0.35m \end{cases}$$

Through the optimization process of the two cases, we can clearly observe the priority for enlarging the width over the draft due to several advantages. When the

structural width in increased, the mass will increase too. Although the horizontal wave force on the structure will not change (for a determined draft), the increase of the mass is the reason why the sway motion amplitude decreases. Also, a wide and heavy structure is hard to put into rotation. Moreover, a wide structure is not able to move along the relative short period waves. Therefore, the wider the structure, the longer the wave period on which the structure will resonate. Finally, the increase in the width will enlarge the hydrodynamic damping.

Due to these facts, a wide structure is en effective solution to be applied in the case of ports influenced by strong waves. In Fig.8, a simulation of the wave propagation, in the same vertical plane of the breakwater, is applied to exhibit the performance of such structures. The fluid domain is taken from a 500m in the ocean side and 180m in the port side and with a water depth of -40m, where the floating breakwater constitutes a relatively small white domain in the upper boundary. The diffraction of waves due to wide structure is more effective due to the increasing contact surface or the intersection domain of fluid-structure. Then, almost a great part of the wave energy is being attenuated by the reflected waves. Also, the sway and roll radiations, due to the oscillation or dynamic behavior of the floating breakwater, are small due to cited reasons above. The last type of radiation caused by the heave motion maybe will be valuable in comparison with the other two, but it is playing a positive roll in attenuating totally the sea waves in the port domain (Fig.8). This vertical oscillation of the breakwater is producing waves out of phase from the diffraction, sway, and roll, thus yielding to a high protection of the port side. Therefore, it is easy to observe the small waves in the port side, which are under the allowable wave height value (0.2m). This also confirms the main purpose of floating breakwater which seeks to minimize the wave height in the port side in the contrary to the fixed breakwaters that are capable of completely annulling the waves.

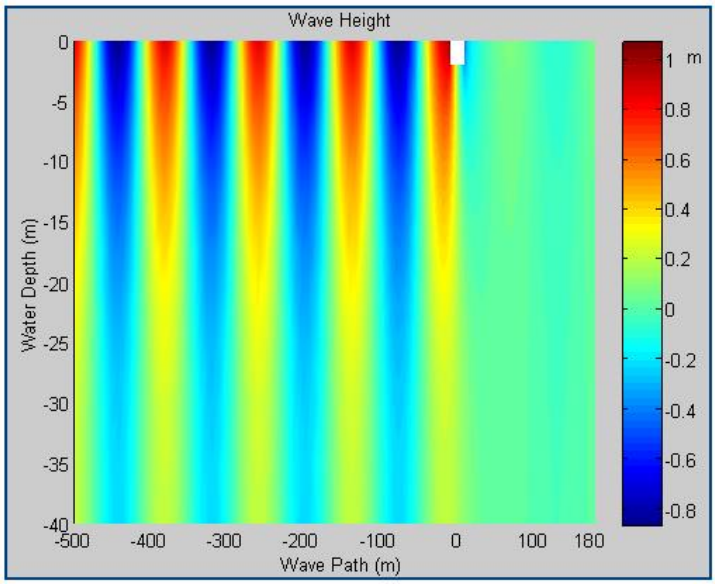

Fig.8 Wave elevation inside and outside (ocean) the port

Concerning the structure resistance, it is clear that the optimization iterations for the two types of materials are following the same methodology, which enlarges the width over the draft. The two problems yield to a similar design (enlarging width over draft with the remaining variables mainly not varying) and for two different wave height limitations inside the port (transmission coefficient=0.2 for composite

and 0.5 for concrete). These results support or demonstrate the robustness of the problem methodology producing similar answers to two different problems. For the case of concrete, the resistance constraint failed to insure a width bigger than 12m; this is the main problem causing the incapability of designing a single concrete floating breakwater that can go forward toward a larger width and therefore a higher port protection. Where, we can figure out an analogous structure with a larger width computed for the composite materials. These materials have a large band to overpass the high mechanical constraints reverting from small thickness of the beams. The two horizontal beams (upper and lower) for the two materials are mainly subjected to bending stresses. The two deflections are opposite in sense and are oriented towards the core of the breakwater. The upper deflection is due to the weight of the material, while the lower one is resulting from the water pressure acting on the bottom. (Fig.9)

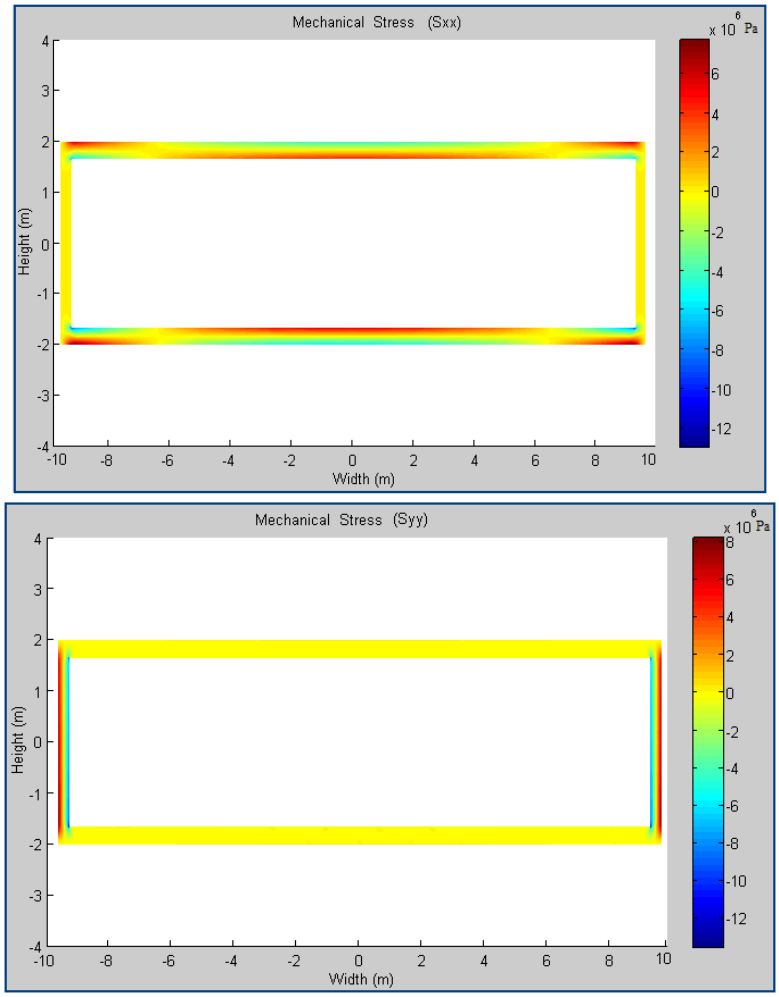

Fig. 9 Mechanical Stress Distribution for composite materials σ_x (left) σ_y (right)

We can clearly notice (Fig.7 and 9) the respected limits of the mechanical stresses due to the imposed structural constraints. (Traction and compression limits for concrete and composite materials). Twin-pontoon breakwaters may be particularly advantageous with respect to breakwater motions and lower transmission coefficients compared to single-pontoon breakwaters (Fig. 1.3). Moreover, they generally have a relatively high stiffness with respect to roll motions. Each unit may be relatively small and light compared to other single unit breakwaters and this allows flexibility relating to fabrication and installation procedures. This may open up multiple choices for future designs of floating breakwaters orienting it towards the twin pontoons.

REFERENCES

- Adee, B. H. 1975. Analysis of floating breakwater performance. In *Proceedings of Symposium on Modelling Techniques, ASCE,* pp. 1585-1602.

- Akagi, S. & Ito, K. (1984. Optimal design of semi-submersible form by minimizing its motion in random seas. J. *Mechanism, Transmissions & Automation in Design, Trans ASME,* 106: pp 23-30.

- Allaire G., Jouve F., Toader A.-M. 2002. A level-set method for shape optimization. *C.R. Acad. Sci. Paris, Ser. I 334,* pp 1–6.

- Allaire, G., Jouve, F. and Toader, A.M., 2004. Structural optimization using sensitivity analysis and a level-set method. *Journal of computational physics*, *194*(1), pp.363-393.

- Annicchiarico. W, Cerrolaza. M. 1999. Finite elements, genetic algorithms and b-splines: a combined technique for shape optimization. *Finite Element in Analysis and Design 33*(2), pp 125–141.

- Belegundu. A.D, Rajan. S.D. 1988. A shape optimization approach based on natural design variables and shape functions. *Computer Methods in Applied Mechanics and Engineering. 66*(1), pp 87–106.

- Belytschko T, Xiao S.P, Parimi C. 2003. Topology optimization with implicit functions and regularization. *International Journal of Numerical Methods in Engineering 57*(8), pp 1177–1196.

- Bendsøe M.P, Kikuchi N. 1988. Generating optimal topologies in structural design using a homogenization method. *Computer Methods in Applied Mechanical Engineering. 71*(2), pp 197–224.

- Bendsøe M.P. 1989. Optimal shape design as a material distribution problem. *Structural Optimization 1*(4), pp 193–202.

- Biggs, M.C. (1975. Constrained Minimization Using Recursive Quadratic Programming. *Towards Global Optimization*, North-Holland, pp 341-349.

- Broyden, C.G. 1970. The Convergence of a Class of Double-rank Minimization Algorithms. *J. Inst. Maths. Applics*., Vol. 6, pp 76-90.

- Cammaert. A. B., B. Morey. L. Lesley, and Warren T. 1994. *The development of a design manual for floating breakwaters in the Atlantic environment.* Including appendices. Technical Report, TR-FIS-94002. Ocean Engineering Research Centre. Memorial University of Newfoundland, St. John's. NF.

- Cappello. F, and Mancuso A. 2002. A genetic algorithm for combined topology and shape optimisations. *Computer-Aided Design, 35*(8), pp 761-769.

- Carver, R. D. 1979. *Floating breakwater wave-attenuation tests for East bay marina Olympia harbour, Washington.* Technical report HL-79-13, US Army Engineer Waterways Experiment Station, Vicksburg, Miss.

- Castillo. C, Mınguez. R., Castillo. E, Losada M.A. 2006. An optimal engineering design method with failure rate constraints and sensitivity analysis. Application to composite breakwaters. *Coastal Engineering Journal, 35*(1), pp 1 – 25.

- Cerrolazaa. M, Annicchiarico. W, Martinez. M. 2000. Optimization of 2D boundary element models using b-splines and genetic algorithms. *Engineering Analysis with Boundary Elements 25*(4), pp 427–440.

- Chakrabarti. S. K. 1987. *Hydrodynamics of offshore structures.* Elsevier Science Publishing Company, **Inc..** New York. NY.

- Chapman D., Saitou K., Jakiela M.J. 1994. Genetic Algorithms as an approach to configuration and topology design. *Journal of Mechanical Design 116*(4), pp 1005–1012.

- Chapman C., Jakiela M. 1996. Genetic algorithm-based structural topology design with compliance and topology simplification considerations. *ASME Journal of Mechanical Design 118*(1), pp 89–98.

- Chang. K.H, Choi. K.K 1992. A geometry-based parameterization method for shape design of elastic solids. *Mech. Struct. Mach. 20*(2), pp 215–252.

- Cheong, H.-F., Shankar, J., Nallayarasu, S. 1996. Analysis of submerged platform breakwater by eigen function expansion method. *Ocean Engineering 23*(8), pp 649–666.

- Chou, F.S. (1997: A minimization scheme for the motions and forces of an ocean platform in random seas. SNAME Trans, *85*, pp 32-50.

- Clauss, G.F. & Birk. L. 1996. Hydrodynamic shape optimization of large offshore structures. *Applied Ocean Research 18*(4), pp 157-171

- Cox. J. C. 1989. Design of a floating breakwater for Charleston Harbour. South Carolina. *Proceedings of Ports' 89, ASCE. Boston. MA.* pp 411 - 420.

- d'Angremond, K. and Tutuarima, W.H. 1998. Cost Comparison of Breakwater Types. *Coastal Engineering, Vol. 2, Conference proceedings*, pp 1934-1944.

- Davidon, W.C. 1959. Variable Metric Method for Minimization. *A.E.C. Research and Development Report*, ANL-5990.

- Drimer, N., Agnon, Y., Stiassnie, M. 1992. A simplified analytical model for a floating breakwater in water of finite depth. *Applied Ocean Research 14*(1), pp 33–41.

- Elchahal, Ghassan, Younes, Rafic. And Lafon, Pascal, 2006. Shape and material optimization of a 2D vertical floating breakwater. *WSEAS Transaction on Fluid Mechanics, 1*(5), pp.355-363.

- Elchahal, G., Younes, R. and Lafon, P., (Accepted paper). The effects of reflection coefficient of the harbour sidewall on the performance of floating breakwaters. *Ocean Engineering*.

- Elchahal, G., Younes, R. and Lafon, P., 2006, May. Modelling Wave Induced Pressure on Breakwaters. In *Modelling and Simulation: 17 th IASTED International Conference Proceedings. Montreal, Canada, May 24 - 26*, pp 308-312.

- Elchahal, G., Younes, R. and Lafon, P., 2006, January. Wave Interaction with Fixed and Floating Vertical Breakwater Based on Analytical Modelling. In *ASME 2006 2nd Joint US-European Fluids Engineering Summer Meeting Collocated with the 14th International Conference on Nuclear Engineering* (Vol. 1, pp. 463-472).

- Elchahal, G., Younes, R. and Lafon, P., 2007, June. Numerical modelling of floating breakwaters and shape optimization using a nonlinear programming method. In *Proceedings of the 26th International Conference on Offshore Mechanics and Engineering, OMAE2007-29116,(American Society of Mechanical Engineers, San Diego*.

- ElChahal, G., Lafon, P. and Younes, R., 2007, January. Modelling and optimizing floating breakwaters using density distribution. In *The Seventeenth International Offshore and Polar Engineering Conference*. International Society of Offshore and Polar Engineers.

- Faltinsen, O. M. 1990. *Sea loads on ships and offshore structures*. Cambridge University Press. Cambridge, UK.

- Fanjoy D.W., Crossley W.A. 2002. Topology design of planar cross-sections with a genetic algorithm: Part 1–Overcoming the obstacles, *Engineering Optimisation 34*(1), pp 1–12.

- Fletcher, R. 1970. A New Approach to Variable Metric Algorithms. *Computer Journal, 13*(3), pp 317-322.

- Fletcher, R. and Powell, M.J.D. 1963. A Rapidly Convergent Descent Method for Minimization. *The Computer Journal, 6*(2), pp 163-168.

- Fletcher, R. 1987. *Practical Methods of Optimization*. John Wiley and Sons.

- Gesraha. M, 2006. Analysis of ∏ shaped floating breakwater in oblique waves: Impervious rigid wave boards. *Applied Ocean Research, 28*(5), pp 327-338.

- Gill, P.E., Murray, W. and Wright, M.H. 1991. *Practical Optimization*. London, Academic Press.

- Gill, P.E., Murray, W. and Wright, M.H. 1991. *Numerical Linear Algebra and Optimization*. Vol. 1, AddisonWesley.

- Goda Y., *Random seas and design of maritime structures*. (University of Tokyo Press, Tokyo 1985)

- Goldfarb, D. 1970. A Family of Variable Metric Updates Derived by Variational Means. *Mathematics of Computing, 24*(109), pp 23-26.

- Goldberg D.E. 1989. Genetic Algorithms in Search, Optimization and Machine Learning, *Reading: Addison-Wesley Publishing*.

- Hamda H., Jouve F., Lutton E., Schoenauer M., Sebag M. 2002 Compact unstructured representations for evolutionary design. *Appl. Intell. 16*(2), pp 139–155.

- Han, S.P. 1977. A Globally Convergent Method for Nonlinear Programming. *J. Optimization Theory and Applications, 22*(3), pp 297, 1977.

- Heymann, E. 2006. Container shipping. Overcapacity inevitable despite increasing demand. *Deutsche Bank Research,* pp 1-10.

- Herskovits. J, Dias. G, Santos. G, Mota. C.M 2000. Shape structural optimization with an interior point nonlinear programming algorithm, *Structural Multidisciplinary Optimisation. 20*(2), pp 107–115.

- Holzleitner. L, Mahmoud. K.G. 1999. Structural shape optimization using MSC/NASTRAN and sequential quadratic programming. *Computers and Structures, 70*(5), pp 487–514.

- Holland J. 1975. *Adaptation in Natural and Artificial Systems*. University of Michigan Press, Ann Arbor, MI.

- Hock, W. And Schittkowski, K. 1983. A Comparative Performance Evaluation of 27 Nonlinear Programming Codes. *Computing, 30*(4), pp 335-358.

- Hsu, H.-H. And Wu, Y.C. 1997. The hydrodynamic coefficients for an oscillating rectangular structure on a free surface with sidewall. *Ocean Engineering 24*(2), pp 177–199.

- Isaacson. M. 1991. Measurement of regular wave reflection. *Journal of Waterway. Port. Coastal and Ocean Engineering, 117*(6), pp. 553-569.

- Isaacson. M. 1993a. Wave effects on floating breakwaters. *Proceedings of the 1993 Canadian Coastal Conference. Vancouver, BC. Vol. 1.* pp. 53-65.

- Isaacson. M. 1993b. Hydrodynamic coefficients of floating breakwaters. *Proceedings of the 11th Canadian Hydro mechanical Conference. CSCE. Fredericton. NB. Vol. 1.* pp. 485 -494.

- Isaacson, LM., and Baldwin, J. 1996. Moored structures in waves and currents. *Canadian Journal of Civil Engineering, 23*(2), pp. 418 - 430.

- Isaacson, M. and Nwogu, O. 1987. Directional wave effects on long structures. *Journal of Offshore Mechanics and Arctic Engineering. ASME, 109*(3). pp 126-132.

- Isaacson, M. N. Whiteside. R. Gardiner and Hay, D. 1994. Modelling of a circular section floating breakwater. *Proceedings of the international Symposium: Waves - Physical and Numerical Modelling, LAHR, Vancouver, BC. Vol. III.* pp. 1344-1353.

- Jakiela M.J., Chapman C., Duda J., Adewuya A., Saitou K. 2000. Continuum structural topology design with genetic algorithms. *Computer Methods for Applied Mechanics and Engineering 186*(2–4), pp 339–356.

- Jenkins W.M. 1991. Structural optimization with the genetic algorithm, *The Structural Enginering 69*(24), pp 418–422.

- Jensen E. 1992 *Topological structural design using genetic algorithms* Ph.D. dissertation, Purdue University.

- Jones. D. B. 1971. *Transportable breakwaters - a survey of concep*t. Technical Report R-727. Naval Civil Engineering Laboratory, U.S. Navy. Port Huneme. CA.

- Johansson, M. 1989. *Barrier-type breakwaters-Transmission, Reflection and Forces*. PhD, School of Civil Engineering, Chalmers University of Technology, Sweden.

- Kagemoto, H. 1992. Minimization of wave forces on an array of floating bodies. *Applied Ocean Research, 14*(2), pp 83-92

- Kane C., Schoenauer M. 1996. Topological optimum design using Genetic Algorithms, *Control Cyber. 25*(5), pp 1059–1088.

- Gaythwaite. J. W. 1990. *Design of marine facilities for berthing. Mooring and repair of vessels*. Van Nostrand Reinhold, New York.

- Lee, J.F., 1995. On the heave radiation of a rectangular structure. *Ocean Engineering 22*(1), pp 19–34.

- Lee J. and Cho W. 2003. Hydrodynamic analysis of wave interactions with a moored floating breakwater using the element galerkin method. *Canadian Journal of Civil Engineering 30*(4), pp 720-733.

- Lenting, F.V. 2003. *Een alternatief voor een verticale wand golfbreker*. Msc thesis, Delft University of Technology.

- Leonard, I. W. 1988. *Tension structures - behaviour and analysis*. McGraw Hill Book Company. New York.

- Loukogeorgaki E. and Angelides D. 2005. Stiffness of mooring lines and performance of floating breakwater in three dimensions. *Applied Ocean Research, 27*(4), pp 187-208.

- Mackerle J. 2003. Topology and shape optimization of structures using FEM and BEM a bibliography (1999–2001). *Finite Element Analysis Design, 39*(3), pp 243–253.

- McCartney, B. L. 1985. Floating breakwater design. *Journal of Watenvay. Port. Coastal and Ocean Engineering, 111*(2), pp 304-317.

- McLaren. R. W. 1981. Preparation of' floating breakwater manual. *Proceedings of the 2nd Conference on Floating Breakwaters, University of Washington. Seattle*, pp. 22 – 47.

- Molin B. 2004. Les effets non-linéaires en interaction houle-structure et leur modélisation, *Journées AUM AFM, Brest*.

- Nelder, J.A. and Mead, R. 1965. A Simplex Method for Function Minimization. *Computer Journal, 7*(4), pp 308-313.

- Newman, J. N. 1977. *Marine hydrodynamics*. M.X.T. Press. Cambridge.

- Patel, M. H. 1989. *Dynamics of offshore structures*. Butterworths. London. UK.

- Powell, M.J.D. 1978. The Convergence of Variable Metric Methods for Nonlinearly Constrained Optimization Calculations. *Nonlinear Programming 3*, Academic Press.

- Powell, M.J.D. 1978. A Fast Algorithm for Nonlinearly Constrained Optimization Calculations. *Numerical Analysis*, (pp 144-157) Springer Verlag, Vol. 630, heidelberg.

- Powell, M.J.D. 1983. Variable Metric Methods for Constrained Optimization. *Mathematical Programming: The State of the Art*, Springer Verlag, pp 288-311.

- Proceedings of the International Conference(s) on Offshore Mechanics and Arctic Engineering (OMAE), annual, http://www.omae.org.

- Proceedings of the International Offshore and Polar Engineering Conference(s) (ISOPE), annual, http://www.isope.org.

- Proceedings of the International Workshop(s) on Water Waves and Floating Bodies (IWWWFB), annual http://www.rina.org.uk.

- Rahman. M. 1994. *Water waves: relating modem theory to advanced engineering applications.* The institute of Mathematics and **its** Applications. Monogram Series. Clarendon Press, Oxford, **UK.**

- Rozvany G.I.N. 2001. Aims, scope, methods, history and unified terminology of computer-aided topology optimization in structural mechanics. *Structural Multidisciplinary Optimization 21*(2), pp 90–108.

- Ryu. Y.S, Park. K.B, Kim. T.B., and Na W.B. 2005. Optimum Design of Composite Breakwater with Metropolis GA. *6th World Congresses of Structural and Multidisciplinary Optimization - Rio de Janeiro, Brazil*

- Sannasiraj, S.A., Sundar, V., Sundarravadivelu, R. 1998. Mooring forces and motion responses of pontoon- type floating breakwaters. *Ocean Engineering 25*(1), pp 27–48.

- Sannasiraj, S.A., Sundaravadivelu, R., Sundar, V. 2000. Diffraction–radiation of multiple floating structures in directional waves. *Ocean Engineering, 28*(2), pp 201–234.

- Schepers, M.R. 1998. *Kosten beschouwing van conventionele golfbrekers met betonelementen*. Msc thesis, Delft University of Technology.

- Schleupen, A. Maute, K. Ramm, E. 2000. Adaptive FE-procedures in shape optimization. *Structural Multidisciplinary Optimization, 19*(4), pp 282–302.

- Schoenauer M. 1995. Shape representation for evolutionary optimization and identification in structural mechanics. *Genetic Algorithms in Engineering and Computer Science, 22*, pp. 443–464.

- Schoenauer M. 1996. Shape representations and evolutionary schemes. *Evolutionary Programming: Proceedings of the Fifth Annual Conference on Evolutionary Programming, San Diego, USA*, pp. 121–129.

- Schittkowski, K. 1986. NLQPL: A FORTRAN-Subroutine Solving Constrained Nonlinear Programming Problems. *Annals of Operations Research, 5*(1), pp 485-500.

- Sarpkaya, T., and Isaacson, M. 1981. *Mechanics of wave forces on offshore structures.* Van Nostrand Reinhold, New York.

- Shanno, D.F. 1970. Conditioning of Quasi-Newton Methods for Function Minimization. *Mathematics of Computing, 24*(111), pp 647-656.

- Sigmund, O. 2001. A99 line topology optimization code written in MATLAB. *Structural Multidisciplinary Optimization 21*(2), pp 120–127.

- Skop, R. A. 1988. Mooring systems: A state-of-the-art review. *Journal of Offshore Mechanics and Arctic Engineering, 110*(1), pp. 365 - 372.

- Tadjbkhsh I., Keller J. 1960. Standing surface waves of finite amplitude. *Journal of Fluid Mechanics, 8*(3), pp 442-451.

- Tai K., Cui G.Y., Ray T. 2002. Design synthesis of path generating compliant mechanisms by evolutionary optimization of topology and shape, *ASME Journal of Mechanical Design 124*(3), pp 492–500.

- Tai K, Chee TH. 2000. Design of structures and compliant mechanisms by evolutionary optimization of morphological representations of topology. *ASME Journal of Mechanical Design, 122*(4), pp 560–6.

- Tortorelli, D.A., 1993. A geometric representation scheme suitable for shape optimization. *Journal of Structural Mechanics, 21*(1), pp.95-121.

- Tsinker. G. P. 1995. *Marine structures engineering. Specialized applications*. Chapman and Hall, New York.

- Trianiafyllou, M. S. 1994. Table mechanics for moored floating systems. *Proceedings of the 7th international Conference on Behaviour of Offshore Structures. Cambridge, MA. Vol. 2.* pp. 57 - 78.

- Wang, S.Y. And Tai, K. 2005. Structural topology design optimization using Genetic Algorithms with a bit array representation. *Computer Methods in Applied Mechanics and Engineering, 194*(36), pp 3749-3770.

- Wang, S.Y. and Tai, K. 2004. Graph representation for structural topology optimization using genetic algorithms. *Computers and Structures 82*(20), pp 1609–1622.

- Watanabe E., Utsunomiya, T. and Wang, C.M. 2004. Hydroelastic Analysis of Pontoon-Type VLFS: a Literature Survey. *Engineering Structures, 26*(2), pp 245-256.

- Watanabe, E., Wang, C.M., Utsunomiya, T. and Moan T. 2004. Very Large Floating Structures: Applications, Analysis and Design. *CORE Report, 02, Singapore*, pp 104-109.

- Wehausen. J. V. 1971. The motion of floating bodies. *Annual Review of Fluid Mechanics, 3*(1), pp. 237 - *168.*

- Williams, A.N. 1994. Froude–Krylov force coefficients for bodies of rectangular section in the vicinity of the free-surface and sea-bed. *Ocean Engineering 21*(7), pp 663–682.

- Williams, A.N., and Abul-Azm A.G, 1997. Dual Pontoon Floating Breakwater. *Ocean Engineering 24*(5), pp 465-478.

- Williams, A.N., Lee, H.S., Huang, Z., 2000. Floating pontoon breakwaters. *Ocean Engineering 27*(3), pp 221–240.

- Woon, S.Y, Querin, O.M, Steven, G.P. 2001. Structural application of a shape optimization method based on a genetic algorithm. *Structural Multidisciplinary Optimization 22*(1), pp 57–64.

- Wu, C., Watanabe, E., Utsunomiya, T., 1995. An eigen function expansion–matching method for analyzing the wave-induced responses of an elastic floating plate. *Applied Ocean Research 17*(5), pp 301–310.

- Xie, Y.M., Steven, G.P., A. 1993. Simple evolutionary procedure for structural optimization. *Computers and Structures 49*(5), pp 885–896.

- Yang. R.J., Dewhirst. D.L., Lee. A. 1992. Shape optimization of connecting rod pin end using a generic model. *Finite Element in Analysis and Design 11*(3), pp 257–264.

- Yang, H.T.O., Huang, L.H., Hwang, W.S., 1997. The interference of a semi-submerged obstacle on the porous breakwater. *Applied Ocean Research 19*(5-6), pp 263–273.

- Yamamoto, T. and Takahashi S. 1974. Effects of cross-sectional shape and mooring on performance of floating breakwater. *Proceedings of the floating Breakwater Conference. University of Rhode Island, RI.* pp. 149 - 162.

- Yamamoto, T., Yoshida, A. and Ijima, T. 1980. Dynamics of elastically moored floating objects. *Applied Ocean Research, 2*(2), pp 85-92.

- Zheng, Y.H., You, Y.G., Shen, Y.M. 2004. On the radiation and diffraction of water waves by a rectangular buoy. *Ocean Engineering 31*(8), pp 1063–1082.

- Zienkiewicz, O.C, Campbell, J.C. 1973. Shape optimization and sequential linear programming. *Optimum Structural Design – Theory and Applications*, pp 109-126.

- Zhou, M., Rozvany, G.I.N. 2001. On the validity of ESO type methods in topology optimization, *Structural Multidisciplinary Optimisation 21*(1), pp 80–83.